Maturation of Human Pluripotent Stem Cell-Derived Engineered Cardiac Tissues

Jia-Ling Ruan

A dissertation

submitted in partial fulfillment of the

requirements for the degree of

Doctor of Philosophy

University of Washington

2014

Reading Committee:

Michael Regnier, Chair

Charles E. Murry

Nathan J Sniadecki

Program Authorized to Offer Degree:

Bioengineering

Abstract

Maturation of Human Pluripotent Stem Cell-Derived Engineered Cardiac Tissues

Jia-Ling Ruan

Chair of the Supervisory Committee:

Charles E. Murry, MD, PhD

Departments of Pathology, Bioengineering, and Medicine

Cardiac tissue engineering enables the generation of functional human cardiac tissue using cells derived *in vitro* in combination with biocompatible materials. Human pluripotent stem cell (hPSC)-derived cardiomyocytes provide a cell source for cardiac tissue engineering; however, their immaturity limits their potential applications. Here we sought to study the effect of mechanical conditioning and electrical pacing on the maturation of hPSC-derived cardiac tissues.

In the first part of the study, cardiomyocytes derived from human induced pluripotent stem cells (hiPSCs) were used to generate collagen-based bioengineered human cardiac tissue. Engineered tissue constructs were subject to different stress and electrical pacing conditions. This engineered human myocardium exhibits Frank-Starling curve-type force-length relationships. After 2 weeks of static stress conditioning, the engineered myocardium demonstrated at least 10-fold increase in contractility and tensile stiffness, greater cell alignment, and a 1.5-fold increase in cell size and cell volume fraction within the constructs. Stress conditioning also increased sarco-endoplasmic reticulum calcium transport ATPase 2 (SERCA2) expression. When electrical pacing was combined with static stress conditioning, the tissues showed an additional 2-fold increase in force production, tensile stiffness, and contractility, with no change in cell alignment or cell size, suggesting maturation of excitation-contraction coupling. Supporting this notion, we found expression of RYR2 and SERCA2 further increased by combined static stress and electrical stimulation. These studies demonstrate that electrical pacing and mechanical stimulation promote both the structural and functional maturation of hiPSC-derived cardiac tissues.

In the second part of the study, cardiovascular progenitors (CVPs) derived from hPSC were used as the input cell population to generate engineered tissues. The effects of a 3-D microenvironment and mechanical stress on differentiation and maturation of human cardiovascular progenitors into myocardial tissue were evaluated. Compared to 2-D culture, the unstressed 3-D environment increased cardiomyocyte numbers and decreased smooth muscle cell numbers. Additionally, 3-D culture suppressed smooth muscle cell maturation. Mechanical stress conditioning further improved cardiomyocyte maturation. Cyclic stress-conditioning increased expression of several cardiac markers, like β-myosin and cTnT, and the tissue showed enhanced force production. This 3-D system has facilitated understanding of the effect of mechanical stress on the differentiation and morphogenesis of distinct cardiovascular cell populations into organized, functional human cardiovascular tissues.

In conclusion, we were able to create a complex engineered human cardiac tissue with both stem cell-derived cardiomyocytes and CVPs. We showed that how environmental stimulations like mechanical stress, electrical pacing, and 3-D culturing can affect the maturation and specification of cells within the engineered cardiac tissues. The study paves our way to further apply these engineered cardiac tissues to other *in vitro* and *in vivo* usages like drug testing, clinical translation, and disease modeling.

Acknowledgements

In writing a thesis, I always found the most difficult part to write is not the discussion, nor the conclusions. The most difficult part is always the acknowledgments, because these few paragraphs are the only place I can express my gratitude toward people that really have impact on my past, my present, and undoubtedly my future. This is especially true for a PhD thesis that required years of works and tons of help from people.

I would first and foremost like to thank my advisor, Chuck Murry, who has been an outstanding and generous mentor, providing resource and assistance to help me go through all the ups and downs during my graduate studies. Without the help from Chuck and the two senior scientists, Hans Reinecke and Lil Pabon, I would not have been able to complete my PhD study. I would also like to show my highest gratitude to all my supervisory committees, Mike Regnier, Wendy Thomas, Nathan Sniadecki, Miqin Zhang, Deok-Ho Kim, and Chris Liu, who have taken extra time and patience to guide me to the right track.

I am grateful to all the former and present members in the Murry lab. I want to express my special appreciation to Nate Tulloch, who is the predecessor of this work and has always been supportive. I want to thank the Murry lab staffs: James Fugate, Mark Saiget, Veronica Muskheli, Melissa Walzer, Isa Werny, and Martha Lee for their help in tissue culture, histology, and lab organization. I would also like to recognize many of the Murry lab trainees and student helpers: Sarah Fernandes, James Chong, Kareen Coulombe, Daniel Yang, Xiulan Yang, Akiko Tsuchida, Hiroshi Tsuchida, Yen-Wen Liu, Nathan Palpant, Kaytlyn Beres, Jill Weyers, Meredith Roberts, Emily Shih, Shiv Bhandari, and Sonal Jain for making every day in the lab fun with their passionate and easygoing personalities.

A great portion of work in this thesis would not have been done without the help and support from the members from the Regnier lab, especially Maria Razumova and Farid Moussavi-Harami. I want to express my special thanks to Masha, who is always willing to assist me in technical difficulties and shares both the words of wisdom and the same date for birthday with me. I want to also thank the staffs from the ISCRM core: Ron Seifert, Chris Cavanaugh, Jenn Hesson, Savannah Cook, and Luz Linares for providing superb technical support in imaging, tissue culture, and histology sectioning that are the basis of current thesis. I would like to thank Kelvin Chan Tung and Gordon Keller for the kind offer to use their IBJ-derived progenitors. I also thank Wei-Zhong Zhu and Michael Laflamme for kindly sharing the antibodies for immunohistology and Western blotting.

Finally, I would love to express my thankfulness to many people outside the south lake union campus. I appreciate the help and friendship from the Vascular Research Program in the UW Department of Surgery. I want to also recognize Matt O'Donnell and people from the O'Donnell lab. Matt, though no longer in my supervisory committee, has always provided insightful advices throughout my PhD study, and no matter where I was, the O'Donnell lab is always like a second home for me. I would like to thank people from the Center for Industrial and Medical Ultrasound (CIMU) for their help and guidance in making me survive through the first few years of my PhD study. Lastly, I am also grateful to our departmental counselor, Dorian Varga, for all her help and support in making me finish my PhD.

With the help from all these people, I had a really exciting and unforgettable PhD journey.

Jia-Ling Ruan

December 10th, 2014

Dedication

I would like to dedicate this work to my parents, who made me understand the true meaning of love is not by “constraining” but by “setting it free”. I would also like to dedicate this work to my dear nanny, Carl, who taught me how to dance in the rain, instead of waiting for storm to pass by.

Table of Content

List of Figures

Lists of Table

I. Introduction

A. Cardiovascular Diseases and Cardiac Tissue Engineering

For the past century, there is a drastic progression of cardiovascular diseases (CVDs) from less than 10% of all death throughout the world to the leading cause of death in the developed countries and about 25% in the developing world.[1] By 2030, it is estimated that the global cardiovascular deaths will be 23.3 million[2] and 40.5% of the US population will be affected by CVDs.[3] Based on the WHO database, about 17 million people died from CVDs in 2012, accounting of about one in every three deaths.[4] CVD has become a major economic burden to the health care system. In 2010, the total estimated cost of CVDs was about $450 billion, about 3.6-fold of the economic cost of cancer at the same year.[3,5] As the extension of life span and the change of lifestyle, the incidence of this disease will also increase. Thus, there is a pressing need to develop advanced therapies, especially for myocardial infarction or coronary artery diseases. Acute myocardial infarction causes an irreversible damage to the heart where cardiomyocytes are replaced by non-contractile scar tissues. Unlike skin or liver, the heart has really limited regenerative ability through stem cell recruitment and the self-renewal rate is way lower than the loss rate of cardiomyocytes. Congestive heart failure emerges when the contractile function of myocardium is loss below a critical threshold.[6] Traditional treatment includes heart transplantation and assisted device therapy. About 5000 heart transplants have been performed each year as the only curative treatment for end-stage heart failure, but it is still less than one tenth of the number of demand.[7] Assisted devices like man-made artificial hearts are also less successful alternative to biological transplants due to the risk of foreign-body rejection and the need of external battery maintenance. A promising approach is to reverse or prevent heart failure by growing myocardium in diseased hearts. Several cell types including skeletal myoblasts, multipotent adult stem cells, progenitor cells, and PSCs, have been applied in the cell-based cardiac repair and showed promising but modest results with limited functional improvement and cardiac remodling.[8,9] Delivery of cells into the hostile

infarct environment results in low retention and survival rate. More than 50% of injected cells either die or are been washed out upon injection.[10,11] Thus, supporting biomaterials have been applied to increase the retention and survival of injected cells. Cardiac tissue engineering using both cells and biomaterials aims to reproduce the structure and function of complicate myocardium tissues. In addition to their potential clinical usage, cardiac tissue engineering may replace current non-human recombinant cell lines expressing cardiac ion channels for *in vitro* cardiotoxicity screening and enables generation of patient-specific engineered cardiac muscles for disease modeling. As the development of cell technology and biomaterials make possible the generation of contractile engineered cardiac tissues from autologous source, more questions regarding promoting the functional maturation of engineered tissues to appropriated benchmark (fetal, neonatal, or adult) stage are still pending to be answered. This is especially important for stem cell-based engineered myocardium since stem cell-derived cardiomyocytes functionally resemble fetal cardiomyocytes. Toward clinical translation, it is crucial that we are able to promote both the molecular and functional maturation of engineered myocardium toward its native counterpart. This chapter briefly reviews the state of the art in current cardiac tissue engineering, including the cells, biomaterials, and stimuli for cardiac tissue engineering.

B. Cells for Cardiac Tissue Engineering

Structured with both delicate and robust design that is able to precisely circulate blood from a 3-inch hummingbird to an 18-foot tall giraffe, the heart is the most efficient electro-mechanical pump that nature has bestowed to us. It governs the nutrition and oxygen supply to our body restlessly. The delicacy in mechanical structure also reflects their capability in force generation and pressure maintenance. In birds and mammals, the heart has four chamber/double pump design - right atrium (RA), right ventricle (RV), left atrium (LA), and left ventricle (LV). LV is generally twice as thick (about 1.5 cm) as RV to generate enough pumping force through the entire body. The excitable and contractile muscular tissue in the heart, myocardium, consists of both cardiomyocytes (CMs) and nonmyocytes. The

latter includes fibroblasts, endothelial cells (ECs), smooth muscle cells, nerves, mast cells and others. While the number of CMs is in constant level (about 1-2 billion) from a healthy hearts of children and adults, the non-myocyte portion varies from 1 billion just after birth to 5 billion in healthy adult.[12] After myocardial infarction, billions of CMs died and the contractile function of the heart is loss.[13] Several cell sources have been proposed to compensate the loss of cardiomyocytes in myocardial infarction (Table 1); however, each cell line has its own strength and limitation that further improvement is required to optimize the therapeutic capability. Overall, optimal cells for cardiac tissue engineering should be able to 1) be obtained in large scale, 2) form a muscle tissue with electromechanical capability to restore the contractile function, and 3) engraft with host tissues. In the following sections, I review some commonly used cell types for cardiac tissue engineering.

Table 1 Potential cell sources for cardiac tissue engineering

Cell Type	Autologous	Advantage	Limitation
Fetal CMs	No	Form contractile muscle tissues[14] Electrically couple to host[15] and improve left ventricular function[14,16] after transplantation	Limited sources; ethical issues
Skeletal myoblasts	Yes	Form contractile muscle tissues[17] Highly resistance to ischemia Improve left ventricular function[16]	Poor coupling with host tissue[18] (risk of arrhythmia)
Mesenchymal stem cells (MSCs)	Yes	Easily isolated and expandable Improve cardiac function by paracrine effect[19–21]	Age-dependent cardiac differentiation[22] and low integration efficiency[23]
Bone marrow mononuclear cells	Yes	Available at large quantity and easily isolated Mixed cell populations (HSCs, MSCs, EPCs)[24] Mostly extensive studied in clinical study[24] Modest improve in cardiac function and reduce infarct size[25]	Low differentiation efficiency
Cardiac progenitor cells/CVPs	Yes	Form contractile muscles[26] Able to differentiate into CMs, SMCs, and ECs Improve cardiac function by both paracrine factors[27] and myocardial regeneration[28] No tumorgenesis reported	Low isolation yield Biomarkers not well-defined yet
ESC-derived CMs	No	Similar to fetal CMs but expandable Coupled with host tissues[29–31] Improve cardiac function[32]	Limited sources; ethical issues Immunosuppression required[33]

IPSC-derived CMs	Yes	Similar feature to ESC-derived CMs[34] but no ethical or isolation difficulty Can make patient specific lines Demonstrate improvement in cardiac function after CM patch transplantation[35]	Potential epigenetic difference from different sources[36]
Stem cell-derived CVPs	Yes/No	Able to differentiate into CMs, SMCs, and ECs[37,38] Form contractile tissues[39] Integrate with human fetal heart tissues[40]	Purification/isolation required[41]

Abbreviation: HSCs, hematopoietic stem cells; EPCs, endothelial progenitor cells; CVPs, cardiovascular progenitors; SMCs, smooth muscle cells; ESC, embryonic stem cell; IPSC, induced pluripotent stem cell

1. Skeletal myoblasts

Skeletal myoblasts, or satellite cells, can be derived autologously at a large amount from skeletal muscles.[42] It has been showed that they have beneficial effect on post-infarct cardiac function.[16] Though these cells are able to form a muscle tissue,[17] they have poor coupling with the host tissues, which posts the risk of arrhythmia. Also, previous studies have showed that myoblast-seeded scaffold is able to prevent progression of post-myocardial infarction in a transient manner. Methods like mechanical preconditioning,[43] overexpression of gap junctional protein, connexin 43,[44] and delivery by cell-sheet technique,[45] have been used to improve the electromechanical coupling and reduce arrthymogenicity. Additionally, genetically modified myoblasts have also been adopted to regenerate ischemic heart function.[46,47] Overall, the application of skeletal myoblasts on cardiac repair still has a long way to go for heart regeneration and limited usage for other applications of cardiac tissue engineering due to the distinction in electrophysiology between skeletal muscles and cardiac muscles. On the other hand, *in vitro* myoblast-based engineered tissues can generate twitch specific force as high as 5.5±0.6 kPa and demonstrate force-length and force-frequency relationship similar to native tissues.[48] Since the active twitch force produced by these engineered tissues are still 10-100 times less than values measured from adult tissues, techniques such as mechanical stimulation, electrical stimulation, and innervation, have been used to increase the muscle maturation and force production.[49] This can pave the way for maturing actual stem cell-based cardiac engineered tissues.

2. Fetal/Neonatal cardiomyocytes

Cardiac tissue engineering using neonatal rat/embryonic chicken cardiomyocytes has been demonstrated in the late 1990s by multiple groups using different scaffolds like polyglycolic acid (PGA),[50–52] and collagen.[53] Constructs are able to synchronously and spontaneous contract, showing Starling mechanism, positive force frequency relation, and responses to different calcium concentration similar to native tissues.[53,54] Though engineered cardiac tissues with fetal/neonatal CMs have been showed to improve cardiac function in animal models, they are not clinically practical due to the limited availability/ethical issues for human usage. On the other hand, engineered cardiac tissues from neonatal rat cardiomyocytes have maximum active stresses from 2-5 mN/mm^2, which is more than 10 times less than the active force generated by adult rat myocardium.[55] Thus, multiple stimuli like chronic stretch, electrical pacing, and addition of regulatory factors have been used to increase functionality of these engineered cardiac tissues.[56–59]

3. Cardiac progenitor cells

Cardiac progenitor cells can be isolated from the adult heart muscles by different surface markers. They are known for their capability in differentiating into important cardiac lineage in the heart—cardiomyocytes, smooth muscle cells, and endothelial cells. However, due to their scarce, their application in cardiac tissue engineering is limited. On the other hand, cardiac progenitor cells derived from PSCs offer an alternative source.[60–63] Cardiac progenitor cells from stem cells has been showed to be able to expand *in vitro*.[38] Cardiac progenitor cells has been seeded in different scaffolds including collagen,[64] alginate,[65] gelatin,[64] PGA,[66,67] hyaluronic acid,[68] and cardiac extracellular matrix (ECM).[69,70] Most of these studies are focused on producing cardiac marker expressing tissues or inducing both cardiac and endothelial differentiation, while little is known about their electromechanical functions.

4. Stem cell-derived cardiomyocytes

PSC-derived cardiomyocytes are so far the cell lines with the most potential for cardiac tissue engineering. The technique for obtaining pure human cardiomyocytes has been significantly improved since the early demonstration of cardiogenesis from ESCs and PSCs and more than 90% cTnT+ cardiac population can be generated from the directed cardiac differentiation and further purification.[71–73] Upon differentiation, stem cell-derived cardiomyocytes structurally and functionally resemble fetal tissues.[74,75] Guo *et al.* generate the first functional 3-D PSC-based heart tissues from murine ESCs with a maximum contractile force of 0.48 mN.[76] In 2007, Caspi *et al.* first described using human embryonic stem cell-derived cardiomyocytes and endothelial cells to generate PLLA/PLGA-based vascularized cardiac tissues.[77] The most advanced contractile properties were demonstrated by Zhang *et al.* using fibrin/Matrigel scaffolds and hESC-derived cardiomyocytes, which exhibited high maximum active stress of 11.8 mN/mm^2, still less than the 20-40 mN/mm^2 generated by native human myocardium.[55] While the potential therapeutic usage of hESCs is hampered by ethical issues, hiPSCs provide the possibility of creating patient-matched cells for disease modeling and drug pharmacogenomics.

C. Materials for Cardiac Tissue Engineering

An ideal biomaterial for cardiac tissue engineering should meet the following requirements:[78] the materials should 1) not be immunogenic; 2) have a degradation time coinciding with their function; 3) produce biocompatible degradation byproducts; 4) possess mechanical properties such as nonlinear elasticity and anisotropy that could match those of the native myocardium; and 5) provide structural/biological information to guide cardiomyocyte attachment and promote maturation. According to the nature of the matrices, three groups of biomaterials can be distinguished: synthetic polymers, natural materials, and decellularized matrix.

1. Synthetic polymers

The advantage of using synthetic polymers is their controllable mechanical property. Based on the mechanical properties, synthetic polymers can be classified as polyesters and elastomers. Polyesters such as poly(ε-capronlacton) (PCL), poly(lactic acid) (PLA), and poly(glycolic acid) (PGA) have controllable degradation properties and are simple to manufacture, but they are also less flexible than the myocardium. In addition, the acid degradation byproducts may cause inflammatory effect.[79] On the other hand, the mechanical properties of elastomers like polyurethane (PU) are closer to those of the heart tissues, with high elasticity that can withstand strong deformation. However, the byproducts of PU are toxic substances. Non-biodegradable hydrogels like poly(*N*-isopropylacrylamide) (PNIPAAm) and poly(ethylene glycol) (PEG) are also applied in the generation of 2-D cell sheet or 3-D constructs as well.

2. Natural materials

Natural biomaterials have inherent biocompatibility and are commonly used for *in vivo* implantation. However, they are also mechanically weak and degrade rapidly by local proteases. Fibrin and collagen are the most common used natural materials for engineered cardiac tissues (Table 2). In nature, fibrin is the final step product of coagulation cascade and is a FDA-approved product. The properties of fibrin gel can be easily controlled by the concentration of thrombin for the clotting rate, by the fibrinogen concentration for the elastic modulus, and by the concentration of serine protease inhibitors for degradation rate.[80,81]

Collagen is the main constitute of ECM and it makes up 25-30% of the whole body protein content. In myocardium, type I, III, IV, and V are expressed, while type I collagen encompasses 80% of the total.[82] Type I collagen can also be found in the scar tissue as the end product of wound healing. In the process of wound healing, the more elastic type III collagen is firstly produced by young fibroblasts, and then the type III collagen is replaced by type I and the tougher scar tissue is formed. Type IV and V are the basic

components of basement membrane. The total collagen amount increases with age. The human neonatal heart has higher type I collagen, which later stabilizes by type III production postnatally.[83] Collagens generally form heterogeneous fibers under physiological condition. Fibrillar collagens, especially type I collagen, are important in tissue engineering. The formation of collagen gel using heat and neutral pH can be dated back to 1958. Gross and Kirk had showed that acidic collagen solution adjusted to physiological ionic strength and pH in the cold condition, could form a translucent collagen gel after warming up to 30-34 ^{o}C for an hour.[84] Later in 1962, Grillo and Gross proposed its use as medical implants.[85] The mechanism of collagen gelation is highly related to its molecular structure. Self-assembly of collagen begins with three helical peptide chains winding around one another to form a superhelical trimer, also known as collagen triple helix or tropocollagen. Packing with one another, the helices then form collagen fibrils in a quasihexagonal and staggered fashion. The nanofibrils then linearly and laterally self-assemble, giving rise to collagen fibers.[86]

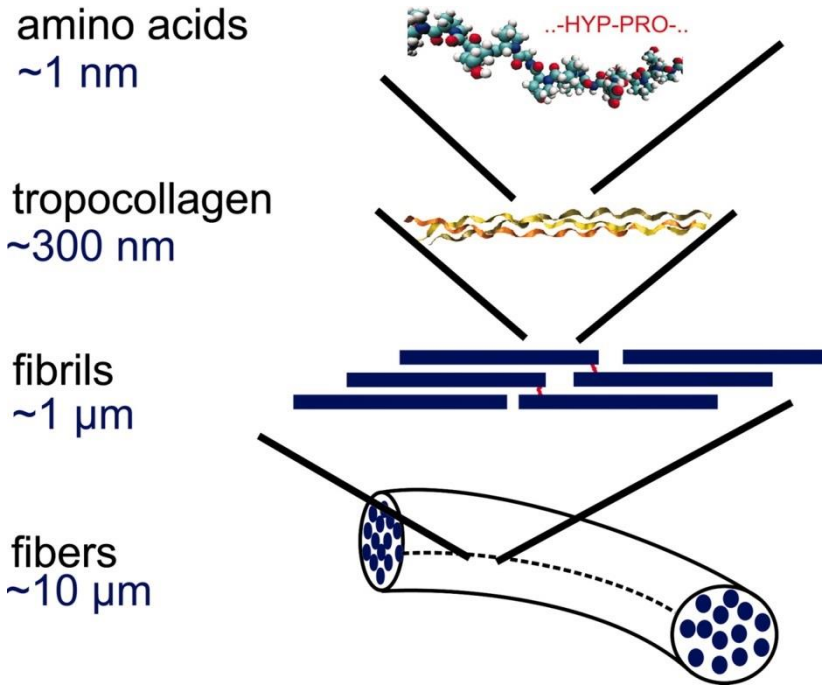

Figure I-1. Hierarchy structure of collagen fibers. [87]

Figure 1 shows a schematic view of the collagen structure hierarchy from amino acid to collagen fiber level.[87] In the primary level, collagen molecules are made up of three α chains, each of which consist of repeating Gly-X-Y triplets and is rich in glycine, praline, alanine, and hydroxyproline (X and Y are mostly proline and hydroxyproline, respectively. The existence of these amino acids limits the rotation of the polypeptide chain). The triple helix domains contribute significantly to interchain hydrogen bondings to form tropocollagen, the secondary structure (about 300 nm in length and 1.5 nm in diameter).[88] Tropocollagens then aligned in D staggered fashion (D = 64-67 nm) and form cross-striated collagen fibrils.[89] Further self-assembly of collagen fibrils gives rise to collagen fibers and hydrogel network using non-covalent (hydrophobic or electrostatic) bondings.

Upon solubilizing in an acidic solution (acetic acid), the collagen fibrils and fibers becomes positive by overprotonation, resulting in breaking up of the non-covalent bondings. PH neutralization deprotonates collagen monomers and reforms their secondary bondings. Overall, the collagen polymerization can be stated in two phases; a nucleation phase is characterized by the molecular self-assembly and a rapid

growth phase with further intermolecular crosslinking. The physical properties of collagen are often influenced by pH, temperature, ionic strength and polymerization rate during these two phases. The size of collagen fibers can be enhanced by prolonging the nucleation phase using lower pH and lower curing temperature.[90] The kinetics of collagen fibrillogenesis further affects the structure and mechanical properties of the matrix. Since the polymerization is not driven by covalent bonding and the hydrated collagen gel contains more than 99% fluid, the collagen gel exhibits viscoelastic properties, such as creep, stress relaxation, hysteresis, and strain rate dependence. The pore size (around 10 μm for 2 mg/ml @ 37 ^{o}C) of collagen gels can also be controlled by both concentration and curing temperature.[91] Overall, the mechanical integrity of collagens depends on collagen fiber content, thickness, length, and orientation, all of which are strongly influenced by the gelation condition.

In the lab, we have made a thread-like collagen constructs for our cardiac tissue engineering as demonstrated in Tulloch et al.[92]. To reduce the handling complexity in the cell embedding, the adopted protocol implied three experimental conditions: preparation of the gel solution with culture medium with calibrated ionic strength, gelation at room temperature and neutral input pH.

Table 2 Physical and structure properties of fibrin and collagen gels[93]

Materials	Crosslinking mechanism	Average pore diameter (μm)*	Young's modulus (kPa)**
Fibrin	Covalent	0.6±0.1	~80[81]
Collagen	Covalent and physical	7.4±1.1	0.5-12[94]

* For concentration of 2 mg/mL

**neonatal rat myocardium ~40 kPa; adult rat myocardium ~280 kPa[95]

3. Decellularized scaffold or extracellular matrix

Cardiac ECM contains a unique combination of structural components (e.g. collagen type I and IV, laminin, fibronectin, elastin) and functional components (e.g. growth factors and cytokine). This

composition changes dynamically to mediate the basic cardiac functionality according to the developmental and pathological stages of the heart.[96] To maintain the ECM information from original tissues, either tissues can be decellularized and use as a native 3-D scaffold or the decellularized tissues can be dissociated and further gel via self-assembly. Beating heart has been demonstrated by injecting neonatal cardiomyocytes and endothelial to decellularized rat heart.[97] However, the application of this technique to human is limited due to the distinctive sizes between human and rat heart. Also, the source of proper decellularized ECM matrix casts another problem while most of the current studies use tissues from animal models.

4. Methods of Cell Seeding

To generate an *in vitro* engineered cardiac tissue, the cells and the scaffolds must be combined to form functional constructs capable of force generation. Multiple cell seeding approaches have been applied, including seeding cells into porous materials, entrapping cells directly into gels, forming 2-D cell sheets,[98] and creating cell patches by suspension culture.[99] Porous scaffolds provide large surface area and high porosity for cell attachment and capillary growth.[100] However, since the cells are generally seeded from the top of the porous scaffolds, the distribution of cells is not uniformly and may affect the functionality.[51] Cell entrapment in hydrogels, on the other hand, provides a uniform cell distribution but the microstructure within the constructs is hard to control. Both cell sheets and cardiac patches are considered to be non-scaffold approach to generate cardiac constructs. These engineered constructs are assembled by ECM secreting by cells but they are also limited by their thickness and size.

D. Enhance Maturation of Cells in Scaffolds

To enhance the quality of cells and scaffolds in cardiac tissue engineering, several physical or chemical stimulation methods has been applied. This is especially important for stem cell-derived engineered cardiac tissues since stem cell-derived cardiomyocytes have relatively immature phenotype similar to

fetal cardiomyocytes. Here we briefly review the native cardiac development and its implication to cardiac directed differentiation from stem cells, properties of stem cell-derived cardiomyocytes, and the current efforts on maturation of stem cell-derived cardiomyocytes.

1. Native cardiac development and directed differentiation

Contracting as early as day 21 post-fertilization, the human heart is the first to be functional during embryogenesis. Despite the timing varies based on different species, heart development can generally be distinguished into several stages. Several days within gastrulation, three germ layers (endoderm, mesoderm, and ectoderm) are formed. Mesodermal cells then migrate and start to express cardiac progenitor markers, such as Mesp1/2 and Fgf8.[101] The bilaterally located cardiac progenitors within the cardiac crescent migrate medially and form a linear heart tube, which loops rightwardly and eventually compartmentalizes into the four chambers. Early stage development of heart provides a template for designing hPSC cardiac differentiation. In general, the heart is derived from mesoderm. However, the inductive activity originates from the anterior endoderm and some evidences have showed ectodermal influences on cardiac induction by mediating TGFβ (BMP4, Nodal) and Wnt signaling.[102] The ability to direct differentiate hPSCs generally involve stage-specific activation and inhibition of four key signaling pathways in early cardiac development- TGFβ superfamily (NODAL/activin A and BMP), Wnt, and FGF.[103] In this thesis, two directed differentiation methods were used to generate CVPs and cardiomyocytes, respectively. These two methods cover the basic format of cardiac differentiation widely in use.

For CVP generation, suspending hPSC colonies are used to generate embryoid bodies (EBs), which enable differentiation toward three germ lineages. The protocol further uses activin A and BMP4 to simulate the NODAL signaling and BMP expression during mesoderm induction. Later, Wnt signaling inhibitors like DKK1 and NODAL antagonists (e.g. SB431542) are used to promote cardiac progenitor specification while VEGF promote the CVP expansion and maturation. Further optimization can be

achieved by mediating BMP and Wnt signaling during mesoderm induction and CVP specification stages.[104] Using this protocol, CVPs can generally be monitored one day after Wnt signaling inhibition by coexpression of KDR and PDGFRα from flow cytometry. KDR, also known as VEGFR-2 or Flk, is generally used as a cardiac mesoderm marker though it also expresses on different mesoderm population. Previous studies showed that KDR^{high} population contains hematopoietic progenitors while KDR^{low} population contains cardiac progenitors.[105] PDGFRα, though is not a specific marker for the mesodermal population, has been identified in human heart and multiple stages during cardiogenesis.[106,107] Here it is used as a marker to segregate populations at mesoderm stage. The CVP population has showed to be able to differentiate into cardiomyocytes, vascular smooth muscle, fibroblast, and endothelium in the later stage of differentiation.[104] The other method to generate hPSC-derived cardiomyocytes is to culture hPSCs into high density monolayer with high cell density.[108] A high dose of activin A, followed by BMP4, are used to induce mesodermal development. Due to its biphasic role in cardiac specification, mediation of WNT signaling can be applied to improve the differentiation efficiency.[109,110] Epithelial-to-mesenchymal transition (EMT) can be further promote by Matrigel overlay for some stem cell lines.[71] Beating cardiomyocytes can generally be observed from day 7-14. Both nodal and working type cells can be generated from this protocol and the portion of each population is cell line dependent.[111]

2. Properties of stem cell-derived cardiomyocytes

Previous studies demonstrated no difference in the ultrastructure from embryonic stem cell (ESC) and induced pluripotent stem cell (iPSC)-derived cardiomyocytes,[34] although their epigenetic status might be different.[112,113] The function and structure of hPSC-derived cardiomyocytes have been reported by many groups (Table 3). In general, these cardiomyocytes are considered less mature than adult cardiomyocytes, and more similar to fetal phenotype or failing heart.

Table 3 Comparison of hPSC-CMs and adult CMs

	hPSC-CMs	Adult CMs
Morphology	Circular shape	Rod shape
Size	Width ~7μm Length ~10 μm	Width ~25 μm Length ~100 μm
Sarcomere Length	~1.5 μm[34]	1.6-2.2 μm
Percentage of cell capable of proliferation	60 % in early stage (10-21 days)[114]* 40 % intermediate (21-35 days) <1 % in late stage (>35 days)	<1 % at age of 25[115]**
Ultrastructure	Mononucleated No T tubule development[116] Disarrayed sarcomere Circumferential gap junction Low myofibril content Mitochondria located perinuclearly	~25 % multinucleated Aligned sarcomere and polarized gap junction Myofibrils occupied 40-52% of cell volume[117] Mitochondria aligned with myofibrils
Bioenergetic source	Low number and volume fraction of mitochondria Glycolysis + oxidative phosphorylation	Mitochondria occupied 15-25 % of cell volume[117] Fatty acid oxidation
Action potential[118]	Resting membrane potential ~-35 mV(early); -70 mV (late) Upstroke velocity 2-200 V/s Less Kir2.1 expression	Resting membrane potential ~-85 mV Upstroke velocity ~200 V/s More Kir2.1 expression
Calcium handling	Trans-sarcolemmal influx of calcium Limited SR function More NCX expression Lack of junctin and tradin for RyR function; lack of calsequestrin for SR calcium buffering (express calreticulin instead); lack of phospholamban for SERCA modulation	CICR Mature SR (account for 70% of total calcium release) Less NCX expression
Contractile function	~ nN range/cell Frank-Starling mechanism Negative force-frequency relationship No post-rest potentiation	~μN range/cell Frank-Starling mechanism Positive force frequency relationship Post-rest potentiation
Other functional responses	ISO: rate↑, calcium trace amplitude↑, relaxation time↓ but no inotropic response[119]	ISO: positive chronotropic, lusitropic and inotropic responses

* Percentage of cells labeled with [^{3}H] thymidine after 17 hr incubation

**C14-based birth dating

Abbreviation: NCX, sodium calcium ion exchanger; ISO, isoproterenol

Adult ventricular cells are generally 17-25 um in diameter and 60-140 um in length. Myofibrils (50-60%) with the interspaced mitochondria (~20 %) occupied about half of their volumes and the nucleus only accounts for 5% of the cell volume. For hPSC-derived cardiomyocytes, the morphology is more circular and the overall size is smaller. Like embryonic or fetal cardiomyocytes, hPSC-derived cardiomyocytes have high proliferation rate in early stage and the capability of proliferation is lost during prolonged culturing. While T-tubule can be identified at 32 weeks of gestation in human,[120] no robust evidence of T-tubules has been observed in hPSC-derived cardiomyocyte so far. From genetic expression profile, there is a big difference in cardiac ion channels and calcium handling genes between hPSC-derived and adult cardiomyocytes.[121,122] hPSC-derived cardiomyocytes contract spontaneously and shows a less negative resting potential, slower depolarization speed, and slower conduction velocity (human adult heart is about 46 cm/s).[123]

For hPSC-derived cardiomyocytes, calcium transient shows smaller amplitude and slower kinetics due to immature SR and poor electrical coordination. In many cases, though there is a chronotropic response, the inotropic and lusitropic response to beta-receptor agonist is small or sometimes missed due to lack of PLB, the protein mediating SERCA.[124] On the other hand, NCX, the protein peaks around 20-week of gestation in human heart development, is abundantly expressed in hPSC-CMs and also contributes to calcium influx.[125,126] Missing of RyR regulated protein, JCTN and TRDN has been reported in hPSC-CMs.[127] hPSC-CMs, like fetal cardiomyocytes, use CARL as its primary calcium regulator inside SR. Developmentally, CARL will be replaced by CSQ after birth via post-translational modification.[127,128] Previous study has reported that CSQ expression in hPSC-CMs can increase the SR calcium content and facilitate calcium handling maturation.[129] Alternatively, IP3-mediated calcium signaling is also showed to be involved in contractility in hPSC-CMs.[130]

Other molecular level maturation includes switching from ssTnI to cTnI,[131] shifting titin isoform from N2BA to N2B,[132] and increasing the β-MHC to α-MHC ratio.

E. Maturation of Stem Cell-derived Cardiomyocytes

Multiple methods have been applied to mature cardiomyocytes. Biochemical signals, like cytokine or small molecules, are the most intensively used applications. In addition, physical stimulations like electrical pacing and mechanical force have also been studied closely. This section briefly reviewed some common techniques used in maturing hPSC-derived cardiomyocytes. The detailed introduction for electrical stimulation and mechanical stimulation will be included in Chapter II.

Long term culture: While neonatal or adult cardiomyocytes dedifferentiate in *in vitro* culture within several weeks, human stem cell-derived cardiomyocytes have showed improved ultrastructure and functionality in long term culture. Studies showed that cardiomyocytes after 80-120 days of *in vitro* culture have increased cell size and anisotropy, greater myofibril density, increased calcium release and reuptake rate, faster upstroke velocity, and increased contractile performance.[133] Ultrastructural analysis of 180 day-old cardiomyocytes also showed that more packed myofibrils and the appearance of Z-, A-, H-, and I-band compared to early stage cardiomyocytes. Fully developed M-band can also be observed in 1-year old cardiomyocytes.[134] It has also been shown that replating or temporal culture under 3-D condition during long term 2-D culture can further promote cardiac electrophysiology.[135]

Thyroid hormones: In human, tri-iodothyronine (T3) are low during first 30 weeks of gestation and then increases by over 3-fold at term. Treating hiPSC-CMs with T3 for one week promotes cardiac hypertrophy, anisotropy, sarcomere length, and contractile kinetics.[136]

MicroRNA: MicroRNAs play important role in normal heart development and cardiac pathogenesis. Studies comparing microRNA profiles of hESC-derived, fetal and adult ventricular cardiomyocytes

showed that miR-499 promoted ventricular specification and miR-1 facilitated maturation of cardiac electrophysiology.[137]

Other methods such as force expression of Kir2.1[138] and calsequestrin,[139] govern primarily on promoting the electrophysiological function of stem cell-derived cardiomyocytes. Finding the optimal degree of maturation is important for further application of stem cell-derived cardiomyocytes.

F. Scope of this thesis

Bearing in mind that unique environmental cues is needed to sustain cardiomyocyte culture and promote their functional maturation, I hypothesize that biophysical factors like mechanical stress and electrical pacing are essential for functional maturation of engineered cardiac tissues. Thus, the objective of the present study is to demonstrate the functional maturation of engineered cardiac constructs under combinative mechanical and electrical stimulation mechanical stress conditioning using both stem cell-derived cardiomyocytes and stem cell-derived cardiovascular progenitors. The second chapter of this thesis demonstrates the functional maturation in both force production and calcium handling level using iPSC-derived engineered cardiac tissues under combinatory mechanical and electrical stimulation. The third chapter concerns the effect of mechanical stress conditioning on stem cell-derived cardiovascular progenitors. The thesis ends by providing conclusions and the future perspectives in cardiac tissue engineering presented in Chapter IV.

II. Combinatory Electrical and Mechanical Conditioning Promotes Physiological Maturation of Human Engineered Cardiac Tissues

During development, mechanical loading and electrical activity are major determinants of cardiomyocyte growth and maturation.[58,140,141] These stimuli help ensure that the heart's size and performance are matched to the growing body's need for blood flow. This present study is aimed at examining the effects of mechanical and electrical stimulation of engineered heart tissues from hiPSCs.[142] We report that these combined stimuli are able to promote contractility, calcium handling dynamics, and passive mechanics of the engineered human cardiac tissue.

A. Mechanical Force

Mechanical force is a very crucial factor in regulating growth and remodeling of cardiovascular tissues during both development and adulthood. It generally works as a feedback loop in modifying both the cellular architecture and heart function to maintain homeostatic condition. During early stage of development, the heart experiences both mechanical deformation (tension and strain) and fluid flow (shear stress and pressure).[143,144] The mechanical function (contraction) of the heart can be dated back as early as the heart tube fusion (the fourth week in vertebrate). Cyclic pulsatile flow is generated from the heart beat and mechanically stimulates the cardiovascular cells. Later, a sequence of mechanical deformation events, such as cardiac looping and cardiac separation, further change the force experienced by the cells and stimulate them by secreting matrix or continuing change the heart shape to acquire adaptive functions. In diseased state, increased workload generally accompanies myocardial hypertrophy and fibrosis. Overall, sensing of force by cardiac muscles involves activation of multiple cellular signaling pathways (e.g. Src, FAK, JNK, and ERK), integrin/ECM interaction, and stretch-activated ion channels, leading to final function remodeling like modulating the electrical activity or calcium handling.[143] Using strain imaging from either MRI or ultrasound, deformation of the heart can be

quantified.[143] In general, 5-20% shortening can be detected in the heart, depending on the stage and location of the myocardium.[145,146]

In vitro application of mechanical conditioning generally includes applying stretch or strain on the engineered constructs. Physically, stretch is an imprecise term used to describe the behavior of applying stress to a body. Summation of stress across an area is force. Strain is the proportional deformation induced by the applied stress. However, the terms are used interchangeably in most of the literatures. Since the major components in the engineered cardiac tissues are cells and collagen, the following session describe the effect of mechanical strain on the collagen and cells individually.

1. Effect of mechanical stimulation on collagen gels

Previous studies have showed that constraining collagen gel contraction can improve the mechanical properties of collagen gels.[147] When collagen/cell mixture is casted into troughs with anchors in both ends, the presence of anchors directs the gel contracting along the anchor direction and in the direction perpendicular to the troughs, the gel is able to contract freely. The contraction of collagen/cell mixture is related to tissue remodeling and mediated primarily by integrin.[148] Therefore, the constraint stress is considered to be cell dependent. The distance between the anchors also affects the fibril alignment. Longer gels tend to have better fibril alignment, but the gel will break by the increased constraint force if it is too long. [147] This gel contraction effect can not only align the cells and collagen fibrils along the constraint axis but also increase the density of collagen fibrils, and the same effect can also be observed by applying dynamic loading on the thread like collagen gel.[149] In addition, the frequency and amplitude of dynamic loading such as cyclic stress also has been showed to affect the stiffness of collagen gels, while the mechanical properties at different time intervals are more conservative.[150]

2. Effect of mechanical stimulation on cardiomyocytes

The mechanosensing of cardiomyocytes is really common in adapting increase pressure or cardiac workload during normal or pathologic condition. Cardiomyocytes generally respond to different mechanical changes through hypertrophy (increase myocyte size) or hyperplasia (increase cell number/proliferation) depending on the age of cardiomyocytes.[151–153] The loss of hyperplasia function in young cardiomyocytes during development is generally compensated by the hypertrophic growth, result in a 30 to 40-fold volume increase.[154] Cardiac hypertrophy encompasses two phenotypes; under exercise training or developmental hemodynamic overload, cardiomyocytes enlarge to meet the functional need to produce more force and resistance. Conversely, pathologic hypertrophy caused by change in either mechanical workload or neurohumoral activation in diseased states (e.g. hypertension, valve disease, and myocardial infarction) generally results in less force production, prolonged calcium transient, and blunted β-adrenergic response. The mechanoresponse of cardiomyocytes can be depicted into a feedback loop that intercellular, intracellular, and extracellular loads are sensed by multiple protein structures related to cytoskeletons and induced functional response.[143] *In vitro* application of stretch can be used to simulate diastolic stretch in cardiac cycle. The amplitude of stretch can simulate as the preload and the frequency of stretch as heart rate. Many studies have demonstrated the bioeffect of mechanical stretch on cultured cardiomyocytes (Table 4). The earliest studies of mechanical stretch on cardiomyocytes can be dated back to late 80s/early 90s using mostly 2-D culture and non-human cardiomyocytes. Mechanical stretch is showed to enhance hyperplasia, promote RNA and protein expression, and involve in multiple signaling transduction pathways belonging to either MAPK or JAK/STAT pathway.[140] However, little is known about the mechanoresponse of hPSC-derived cardiomyocytes.

Table 4 Mechanical stretch on cardiomyocytes.

Species/Cell line	Age	Mechanical parameter	Effects	Ref
3-D				
Rat	neonatal	2 Hz, 10% strain, 7 day static and 7 day cyclic; 0.45-0.95 mg/ml type I collagen gel (rat tail)	Function like highly differentiated cardiac tissue	[57]
Rat	neonatal	Static (110% of slack length), phasic (2Hz, 10% strain), auxotonic; 0.88 mg/ml type I collagen (rat tail)	Electrical coupled to host myocardium, prevent further dilation and improve cardiac function	[155]
Human ESC- and iPSC-derived		Static, cyclic (5-10%, 1 Hz) or progressive static (6.5% increments at day 7, 10, 14 and 17); 1.2-1.25 mg/ml type I collagen-based materials	Improve alignment and cardiac hypertrophy	[156,157]
Human ESC-derived (40-50% cTnT+ cells)		Static(control) or 1.25 Hz, 12 % for 72 h Gelatin sponges	Increase cTnT and CNX43 expression; faster calcium cycle; increase expression of MYH7 gene and MLC2v protein	[158]
Murine J1 ESC-derived	17 days	1-3 Hz, 10 %, 7 day static and 3 day cyclic; 0.4 mg/ml type I collagen gel with 10 μg/ml fibronectin	Frequency dependent on cardiac gene expression. Neonatal phenotype (histology).	[159]
Chicken and rat	embryonic and neonatal	1.5 Hz, 20%, 4 day static and 6 day cyclic; 0.12-1.32 mg/ml type I collagen gel (rat tail)	Increase force production	[56]
Chicken	embryonic	0.5 Hz, 5%, for 48 h; 0.67 mg/ml type I collagen gel (rat tail)	Increase proliferation by p38MAPK phosphorylation	[160]
2-D				
Mouse ESC-derived	-	1 Hz, 10 % for 2 week; On PLCL (elastic) and PLGA (non-elastic) scaffold	Elevate cardiac gene expression and reduce fibrotic tissue formation *in vivo*.	[161]
Human ESC-derived	Day 25-40 post differentiation	0.5 Hz, 10-25 % stretch for 24 hour on Bioflex plates	Increase in cell size; promote sarcomere organization; αMHC, βMHC, ANF expression↑	[162]
Mouse D3 ESC-derived	-	1 Hz, 5 or 10 % for 1 h	Increase ROS generation; activate a5b1 integrin and subsequent PI3K/Akt;	[163]

			induce Wnt/ -catenin signaling	
Rat	adult	1-4 Hz; 3-15 %; for a few min Duty cycle (diastolic: systolic): 1.5	Elevate ROS production and calcium spark rate by increasing strain and frequency	[164]
Rat	neonatal	Single stretch, 10-20 %; for a few min	Increase RNA content and protein synthesis; enhance proto-oncogenes and fetal-type contractile protein gene expression; activate PKC; involved in autocrine or paracrine mechanism	[165–167]
Rat	neonatal	1 Hz; 10 or 20 % for 0-48 h	Increase connexin 43 expression and polarization; promote self-organization	[168]

B. Electrical Stimulation

In native heart, mechanical stretch is induced by electrical signal. This coupling is known as excitation contraction coupling, which is crucial for both development and function of myocardium. During development, the heart starts to beat as early as five weeks after the last normal menstrual period. The embryonic heart begins to beat at a rate similar to maternal heartbeats, about 1 Hz, and then linearly accelerates to 3 Hz in the ninth week. It then starts to decelerate to about 2-2.5 Hz.[169] The dynamic change in heart rate might be compensation to the limited cardiac performance during development. Fetal heart, operating close to the top of the ascending limb of Frank Starling curve, has been shown to have limited capacity to increase stroke volume by increasing diastolic filling pressure,[170,171] and thus, increase in heart rate can help improving cardiac output in some senses. Cardiomyocytes are said to be autorhythmic with their own electrical system and capable of working independently to the nervous system. The heartbeat is coordinated by a cardiac conduction system composed of modified cardiomyocytes able to trigger action potential at different rates. The action potential in cardiomyocytes

is generated by a sequential change in the sarcolemmal permeability to sodium, calcium, and potassium ions by voltage gated ion channels. This action potential can be triggered by electrical current and is consisted of several different phases. In the depolarization phase, the rapid depolarization is due to rapid inward current of sodium ion (I_{Na}) from the fast sodium channel. The activation status of the fast sodium channel is membrane potential dependent. A more positive membrane potential will cause the fast sodium channel to be less sensitive to open. This sodium channel is also time dependent; the inactivation process is automatically occurs a millisecond after its activation and this leads to phase 1 of action potential, a small early repolarization spike from the net outward current causing by potassium (I_{to1}) and chloride ions (I_{to2}). Phase 2, or the plateau phase is unique to cardiomyocytes. L-type calcium channel opens in this phase, causing an inward movement of calcium ion (I_{Ca}). The opening generally lasts for 200-400 ms. The delayed rectifier potassium channels (I_{KS}) still move the potassium outward and thus counterbalances the inward positive charge. During phase 3, L-type calcium channel closes and only the slow delayed rectifier potassium channels keep move ion outward, reducing the membrane potential. The reduction in membrane potential further promotes the opening of rapid delayed rectifier potassium channels (I_{Kr}) and the inward rectifier potassium channel (I_{k1}), causing the cell to repolarize. The inward rectifier potassium channels keep functioning and keep the resting membrane potential. For automatic cells like pacemaker cells, hyperpolarization-activated cyclic nucleotide-gated (HCN) channels open immediately after the end of previous action potential, causing the membrane potential to slowly become more positive by conducting sodium and potassium ions (I_f). HCN-1,-2, and -4 have been showed to be expressed in undifferentiated stem cells and stem cell-derived cardiomyocytes,[172] and the missing of inward rectifier potassium channel and highly expression of the fast sodium channel Nav1.5 has also contributed to initiate spontaneous excitability.[173]

Multiple literatures have showed positive effects of electrical pacing on cardiomyocytes. Electrical pacing of rat neonatal cardiomyocytes has been showed to induce drastic hypertrophic effects, such as

increasing in cellular size, NPPA mRNA transcript, and myofibrillar organization.[174] Xia et al. demonstrate that electrical stimulation of neonatal cardiomyocytes activates the calcineurin/NFKT3 and GATA4 pathway, mediates cardiac gene expression, and increase mitochondrial content and activity.[175,176] Other studies have showed that rapidly paced cardiomyocytes change the behavior of cardiac fibroblasts, driving them toward an active myofibroblast phenotype.[177] Electrical stimulation of adult cardiomyocyte culture showed improvement in both contractile properties and calcium handling.[178] Electrical stimulation has also been used to promote functional assembly of cardiomyocytes on collagen sponge.[179] Previous studies showed that electrical stimulated engineered cardiac tissue demonstrated markedly improvement in the electrophysiological properties.[180] Enhance connexin 43 mRNA transcript level has been demonstrated from cardiomyocytes subject to 6h combinative electrical and mechanical stimulation.[181] However, little is known about the effect of combinative mechanical and electrical stimulation on 3-D engineered cardiac tissues. In this chapter, electrical pacing was used to further promote cardiomyocyte maturation in engineered cardiac tissues.

C. Methods

1. Directed differentiation of hPSC into cardiomyocytes

Undifferentiated human IMR90-iPSCs[142] (James A. Thomson, U. Wisconsin-Madison) were cultured as described previously.[156] Cells were routinely passaged with Dispase (Invitrogen) on irradiated mouse embryonic fibroblasts (MEFs) on 0.1% gelatin-coated 10cm tissue culture plates. Standard Human Pluripotent Cell Medium (DMEM/F12 with 20% Knockout Serum Replacer, 1% MEM non-essential amino acids, 1% sodium pyruvate solution, 100 U/mL penicillin G, 100 mg/mL streptomycin, and 120 μM β-mercaptoethanol) supplemented with 5 ng/mL basic FGF (Stemgent) were used in maintaining and expanding the cultures.

Cardiomyocytes were generated using a modified version of the monolayer-based differentiation protocol described by Laflamme et al.[182] To prepare for cardiac differentiation, hiPSCs were passaged off from MEFs and maintained 2-4 passages on Matrigel (BD Biosciences) in MEF-conditioned medium with 5 ng/mL basic FGF. To prepare differentiation set up, cells were incubated with Versene solution (0.5 mM EDTA and 1.1 mM glucose in PBS) and scrapped with a cell lifter (Corning). The cell solution was mildly triturated with a P1000 pipette to attain a mostly single cell suspension for even replating. Cells were then plated at a density of 300,000 cells per well into 24-well plates (Corning) coated with Matrigel and fed with 1 mL of MEF-conditioned medium with 5 ng/mL basic FGF. Medium was changed daily for another 24-48 hour until the plates had attained confluence. One day before the initiation of differentiation, the cells were incubated with medium supplemented with 1 μM Chiron 9902 (a Wnt agonist, Cayman). The differentiation was initiated with feeding the cells with 0.5 mL of RPMI medium (Invitrogen) with B27 supplement without insulin (Invitrogen), 100 U/mL penicillin G, 100 mg/mL streptomycin, and 100 ng/mL activin A (R&D Systems). After 24 hours, medium was carefully changed to 1mL of the same medium containing no activin A and supplemented with 5 ng/mL BMP4 (R&D Systems) and 1 μM Chiron 9902. At day 3 of differentiation, plates were fed with 1mL of the same medium supplemented with 1 μM Xav 939 (a Wnt antagonist, Tocris Bioscience). Plates were then fed every other day with 1mL of the same medium without Xav 939 after day 5. Spontaneously contracting cardiomyocytes were observed on day 8 - 12 from the onset of differentiation. Cardiomyocyte preparations used for generation of cardiac constructs were between day 14 and day 21 from onset of differentiation, and at the time of construct generation, moved into RPMI medium made with standard B27 supplement containing insulin (Invitrogen).

2. Generation of cardiac constructs

To make engineered heart tissue constructs, hiPSC-derived cardiomyocytes were trypsinized into single cells from Matrigel plates and then encapsulated in a collagen-based 3-D scaffold.[156] The ingredients of

our cardiac constructs were collagen type I (final concentration 1.25 mg/mL, neutralized with NaOH; Invitrogen), 11% vol/vol mouse basement membrane extract (Geltrex, Invitrogen), and 57% medium (RPMI). The gel and media were mixed together on ice and cells gently added. Bioengineered tissue constructs were cast in troughs (20 mm*3 mm*3 mm) in Tissue Train 6-well plates (Flexcell) at a density of 2 million cells per 100 µL of gel mixture. These troughs were formed by mounting Tissue Train 6-well plates (Flexcell) over Trough Loader posts set in a Bioflex base-plate under vacuum (Flexcell) (Figure II-1). Two nylon mesh tabs were affixed to the periphery of the well at opposing ends. The cell-gel mixture impregnated those nylon meshes, which secure the construct at a fixed length and transmit uniaxial tension to the construct as described in the introduction section. The cell-gel mixtures were incubated for 1 hour at room temperature for matrix solidification. The base-plate vacuum was then released and RPMI medium with standard B27 supplement containing insulin was used to feed the resulting cardiac tissue constructs. One day after construct generation, cell viability was analyzed by LIVE/DEAD staining kit (Life Technology) with 30-minute incubation with dyes and then imaging under a fluorescent microscope. No stress conditions were achieved by cutting one end of the construct free from the nylon tab, while static stress conditioning was maintained by spanning constructs at a fixed static length between the two nylon tabs. Constructs were cultured in a mechanical regimen of no stress or static stress for 2 weeks before further analysis. For combined mechanical and electrical stimulation, 1-week static stress conditioned constructs were subjected to a second week of electrical stimulation with 2 Hz, 5 V, 5 ms pulse (C-Pace EP Culture Pacer, IonOptix). The three stimulation conditions are referred as no stress (NS), static stress (SS), and static stress + E pacing (SE).

A subset of cells used for construct generation was quantified by flow cytometry for cardiac troponin T (cTnT) as an indicator of cardiomyocyte input purity.[92] Cells were first fixed for 10 minutes in cold 4% paraformaldehyde (PF, Sigma) and then incubated with 5% FBS/0.75% saponin (Sigma) in PBS containing cTnT antibody (mouse IgG1, Thermo Scientific Clone13-11, 1:100 dilution) for 30 minutes at room

temperature. Samples subsequently were washed twice with 5% FBS/0.75% saponin in PBS and stained with the secondary antibody (goat anti-mouse-IgG-PE, GαM-PE, 1:200 dilution) for 30 minute at room temperature in the dark. Each sample was washed 3 times with 5% FBS in PBS and re-fixed in 1.3% PF. Samples were analyzed within 7 days on a BD FACS Canto II machine (BD Biosciences). A mouse IgG1 isotype control antibody (eBioscience, 1:100 dilution), in conjunction with the same secondary, was used to gate samples with FlowJo version 9.3.1 software.

In this experiment, we used high purity of cardiomyocytes from hiPSCs (73±3 % cTnT+ cells based on flow cytometry from 9 runs; representative flow result showed as Figure II-2A). The hiPSC-derived cardiomyocytes displayed nuclear expression of the cardiomyocyte transcription factor Nkx2.5 and robust sarcomeric organization visualized by α-actinin immunostaining (Figure II-2B). Over 70% (71.2±3.6 %) of cells were still viable after 24 hour of cell seeding into collagen gels. The engineered constructs were then subjected to 2 weeks of culture under conditions of no mechanical stress (NS; one end cut free from the attachment tab), 2 weeks of static stress (SS), or 2 weeks of static stress including 1 week of electrical pacing (SE). Spontaneous contraction was generally observed 4 to 7 day post construct formation for all groups. After 2 weeks of growth and remodeling, engineered constructs subjected to SS exhibited improved cardiomyocyte density and myofibrillar alignment (visualized using α-actinin immunostaining, Figure II-2C) when compared to NS constructs (Figure II-2D)

3. Mechanical measurements

The experimental setup is shown schematically in Figure II-3. 2-mm long construct sections were suspended on stainless steel hooks attached between a force transducer (Aurora Scientific, model 400A) and a length controller (Aurora Scientific, model 312B). Slack length was determined as the length immediately preceding the stretch step before a positive amplitude twitch transient was observed on the force trace. The construct length was changed by adjusting the position of the length controller arm

and at the same time force from spontaneously contracting constructs was continuously monitored. From the initial slack length, 4% stretches were applied to the construct at intervals of 30 seconds to a final length of 125% initial slack length. For cell-free collagen matrix constructs, slack length was defined as the length from a 4% stretch step where an immediate increase occurred in the measured passive force. The recorded force and length signals were analyzed using customized LabView software. Passive tension was measured as the baseline of force traces. The active force or the amplitude of spontaneous isometric twitch force was measured on 4 consecutive transients in the plateau region after each length step. Force was normalized to the construct's cross-sectional area which was calculated by measuring the diameter at non-strained length, assuming circular cross-sectional geometry. For force frequency relation studies, constructs were paced at 2, 2.5, and 3 Hz, using pulses of 5 V with 40 ms pulse duration. An inline perfusion system (Warner Instruments) was used to keep the solution temperature at 37^{o}C and infuse drugs. The twitch force amplitudes were measured on 4 transients at each frequency. Constructs were perfused with HEPES-buffered Tyrode solution (pH 7.4; 1.8 mM calcium unless indicated otherwise). Contractile responses were determined under the following conditions: varying extracellular Ca^{2+} from 10-4000 μM, 1 μM verapamil (Tocris Bioscience), and 1 μM Bay K8644 (Tocris Bioscience), using 6-9 tissue constructs for each group.

4. Histo- and immunostaining

For staining, adhered cells were fixed on slides (Lab-Tek Chamber Slides) while constructs were fixed by immersion for 20 minutes in 4% paraformaldehyde. Cells were stained on the slides, while constructs were embedded in paraffin and cut into 5 μm sections. For measurements of cell alignment and cell volume fraction in constructs, slides were stained with Sirius Red (1%, Sigma) and counterstained with Fast Green (1%, Sigma) in saturated picric acid (1.3% in water, Sigma). For cell size measurement and bona fide muscle cross sectional area study, slides were stained overnight with MYH7 antibody (A4.951, 1:2 dilution, DSHB) and anti-α-actinin (Sigma, 1:800 dilution) , respectively. Slides were then

biotinylated goat anti-mouse secondary for an hour (Jackson Labs, 1:400), followed by thirty minute incubation in the enzyme-based ABC reagent (Vector Labs) and developed by DAB peroxidase substrate kit (Vector Labs). After dehydration, slides were counterstained with hematoxylin and coverslipped with glass covers (Corning) using Permount mounting medium (Fisher). For immunofluorescence, slides were stained with the primary antibody or a cocktail of two primary antibodies overnight at 4C, followed by one hour with Alexa fluorophore-conjugated secondary antibody or cocktail of two secondary antibodies incubation at room temperature. Hoechst (Sigma) counterstain was used to visualize the nuclei. The following primary antibodies were used: goat polyclonal anti-human Nkx2.5 (R&D Systems, 1:400 dilution), mouse monoclonal anti-SERCA2 ATPase (Sigma, 1:500 dilution), rabbit polyclonal anti-RYR2 (Sigma, 1:500 dilution), and mouse monoclonal anti-α-actinin (Sigma, 1:800 dilution); on sections the latter was used after proteinase K digestion (20 μg/mL in 0.01 M TrisHCl buffer, pH 7.3, at 37° C for 30 min, Roche). Immunofluorescent secondary antibodies included Alexa 488- or 594-conjugated goat anti-mouse, goat anti-rabbit or horse anti-goat (Invitrogen, 1:200 dilutions). Vectashield (Vector Labs) medium was used to mount glass coverslips (Corning) onto immunofluorescent slides.

5. Microscopy and histological analysis

To quantify cell alignment within the constructs, 100X Sirius Red/Fast Green stained micrographs were taken and analyzed using a custom fiber orientation analysis program as previous described.[156] Alignment is defined by the inversed of the magnitude of angle dispersion (the standard deviation of angles of cell edges). Low angle dispersion indicates high degree of alignment. For percentage cell area analysis, Sirius Red and Fast Green channels were separated by color deconvolution plugin in ImageJ (NIH)[183] and converted into grey scale images. The cell volume fraction (percentage cell area within the construct) was defined by the Fast Green positive area to the whole construct area. To quantify cell size, 400X MYH7 stained micrographs were analyzed by dividing the DAB positive area to the number of DAB positive cells in the constructs. To quantify bone fide muscle cross sectional area, 100X α-actinin stained

images were acquired. All immunofluorescent images were collected by a Nikon A1 Confocal System attached to a Nikon Ti-E inverted microscope platform with water-immersion Nikon 60x CFI Plan Apo objective lens (1.2 NA). Images were acquired using Nikon NIS Elements 3.1 software as a single scan with the pinhole adjusted to 1 Airy unit at 1024x1024 pixel density. All images were captured as 12-bit raw files and then rescaled to 8-bit images for further processing. Photoshop 7.0 (Adobe) was used for figure preparation.

6. Western blot

Constructs were cut off from the nylon mesh tabs, quickly washed in PBS, and sonicated for 10 minutes in RIPA buffer (Sigma) containing 1% protease inhibitor cocktail (Sigma). After a quick spin, samples were stored for later analysis at -80°C in sample buffer, containing 100 mM TrisHCl pH 8.0, 10 mM EDTA, 20% glycerol, 2% SDS, 2% BME and 0.05% Bromophenol Blue. Western blotting was performed following separation of proteins on 4-20% gradient SDS-PAGE. Separated proteins were transferred to a PVDF membrane and blocked 1 hour at room temperature in 5% nonfat dry milk in TBS solution with 0.1% Tween. The blocked membrane was then incubated overnight at 4°C in T-TBS with 1% milk and mouse anti-RYR2 (Abcam, dilution 1:1000), anti-SERCA2 specific antibodies (Sigma, dilution 1:1000), or rabbit anti-GAPDH (Sigma, dilution 1:1000), then washed and incubated with horseradish peroxidase–conjugated secondary antibody (Abcam, dilution 1:2000). Bands were visualized by using a Pierce ECL-plus detection kit (Thermo Scientific) and quantified by ImageJ. For sequential analysis of protein levels the blots were gently stripped with RestoreTM Western Blot Stripping Buffer (Thermo Scientific), and the membrane was blocked 1 hour and re-probed as described above. All proteins were normalized to GAPDH expression level. n=1-3 for each group from three runs of biologically independent experiments.

7. Statistical analysis

Results are given as the mean ± standard error of the mean (SEM); error bars within graphs represent SEM. Significance was determined using single factor ANOVA followed by Student's t-test with 95% or greater confidence level based on Bonferroni correction for multiple comparisons. To eliminate inter-experimental variation between western blot films, western blot data were also standardized before being subject to statistical analysis. To standardized western blot results, western blot data were first log-transformed, mean-centered, followed by autoscaling as described previously.[184]

8. Transmission electron microscopy (TEM)

Protocol for electron microscopy has been described as Tulloch et al.[156] The middle segment of constructs was fixed in half-strength Karnovsky's fixative (2.0% paraformaldehyde, 2.5% glutaraldehyde, 0.1 mol/L cacodylate buffer, 3mmol/L CaCl2, pH 7.3) overnight and washed in 0.1 mol/L cacodylate buffer for 1h. After post-fixed in 1.0% OsO4, rinsed and dehydrated through a graded series of alcohols and propylene oxide, the constructs were embedded into Eponate resin (Ted Pella). Sections for light and TEM were cut using a Reichert Ultracut E microtome. Sections were mounted on 0.25% formvar coated rhodium/copper grids and stained with uranyl acetate and lead citrate. For imaging, samples were examined using a JEM 1200EX II TEM (JEOL Ltd, Tokyo) with an accelerating voltage of 80 kV, a 300u condenser aperture, a 50u objective aperture, and a spot size setting of 3.

9. Two photon excitation microscopy and second harmonic generation

Two photon laser scanning, also called two photon excitation microscopy, uses two photons with half of the required energy to excite a molecule. When the molecule absorbs two photons with sufficient combined energy, it is excited from ground state to a high vibrational level in the excited state. The molecule then lost energy to reach the lowest vibrational level in the excited state and return to the ground state by radiationless energy loss or light emission. The emitted photon will have a lower energy compared to the energy required in excitation, and thus the fluorescent light emitted have a longer

wavelength (since E=hf=hc/**λ**, so lower energy means longer wavelength). Since the probability of two photon event occurring is relatively high at the focal plane due to high photon density, the pinhole that generally used in confocal laser scanning microscopy is not needed and less scattering occurs in surrounding tissues. Lower input energy and longer input wavelength reduce the phototoxicity and photobleaching and enhance the penetration depth. However, the overall resolution in two photon microscopy is still slightly lower than confocal microscopy. Many biological structures respond the femtosecond pulses from near-infrared laser light with second harmonic generation and two photon excited fluorescence. Second harmonic generation is resulted from a nonabsorptive, nonlinear light-collagen interaction based on the hierarchical structure of collagen. The noncentrosymmetric highly crystalline triple helix, the molecular packing and scattering in both collagen fibrils and fibers all contributed to the second harmonic generation. Construct sections were prepared as described in histostaining. The section were examine using the multiphoton microscope (Olympus FV1000 MPE BX61) employed a Mai Tai high power laser (Spectra-Physics). The pulse width, repetition rate, objective and the central wavelength are 100 fs, 76 MHz, 25 X water immersion (NA=0.65), and 860 nm, respectively. The signals were collected in the forward propagating direction with a bandpass filter at 415 nm for SHG signal. Images were acquired at 512x512 pixel density and processed in Photoshop.

D. Result

1. Structural remodeling and cardiac hypertrophy of engineered cardiac tissues

We quantified the intercellular alignment by measuring the reciprocal of the cell axis dispersion angles.[156] Both the SS and SE groups showed higher degree of alignment compared to NS group (Figure II-4A, alignment value of SS: 4.24±0.52, SE: 4.08±0.30, NS: 1.22±0.07, n=3-7 for each group, NS vs SS, $p < 0.005$; NS vs SE, $p < 0.0001$). However, pacing along with stress conditioning did not further promote cell

alignment over stress alone. To understand how conditioning affects matrix remodeling, we measured passive force from human cardiac constructs using a series of short increasing length steps while simultaneously recording tension. When compared to cell-free collagen matrix, the presence cardiomyocytes increased passive stiffness significantly (Figure II-4B), as cell free collagen matrix constructs showed a passive stiffness of 0.079±0.041 kPa, while constructs with cardiomyocytes in the NS condition demonstrated a passive stiffness of 0.47±0.22 kPa. SS conditioning further promoted the passive stiffness markedly to 11.13±1.17 kPa, while the combination with SE conditioning raised passive stiffness about 2-fold further to 21.51±4.02 kPa ($p < 0.001$ between each group). This significant change in stiffness from NS to SS conditions is correlated with a significant difference in cell volume fraction within the constructs, as histological analysis of Sirius Red/Fast Green stained slides revealed that the SS conditioning increased the cell area within the construct for more than 10 % over the NS conditioning (Figure II-4C). Collagen SHG also showed both collagen fibers from SS and SE are more aligned than those from NS (Figure II-4G). Addition of electrical pacing to SS conditioning slightly further increased the cell area within the constructs, but did not reach significance. We assessed the size of cardiomyocytes by quantifying the MYH7 area within the construct (Figure II-5). Cardiomyocytes within constructs exposed to SS (774±38 μm^2) were significantly larger than those in the NS condition (503±26 μm^2). Combination of static stress with electrical pacing did not result in a further increase in cardiomyocyte size compared to SS-conditioned group alone (795±46 μm^2). We also quantified the bona fide muscle cross sectional area by analyzing α-actinin positive area in cross section within engineered tissues and did not find any difference among different stimulation conditionings (NS: 21.0±4.63%, SS: 23.13±3.99%, SE: 28.60±7.01%).

2. Contractility of engineered cardiac tissues

The active twitch force (Figure II-6B) was recorded over an incrementally lengthening stretch routine (Figure II-6A).[92] In the force trace example showed at Figure II-6B, active twitch force transients were

undistinguishable at slack length, but their amplitudes increased over a series of 4% lengthening stretches. This is in accordance with the cellular basis of the Frank-Starling mechanism. These spontaneous contraction of these constructs were abolished upon incubation with 2,3-butanedione monoxime (BDM, 30 mM), an actin-myosin interaction inhibitor (Figure II-7A & B), but reappeared upon washout (Figure II-7C). On the other hand, incubation the constructs with the β-adrenergic agonist isoproterenol demonstrated a markedly positive chronotropic response but only a slightly inotropic response (Figure II-7D).[92] The amplitude of active force production in the engineered cardiac tissue changed with extracellular calcium concentration (Figure II-8A), demonstrating a well-functioning Ca^{2+} induced Ca^{2+} release (CICR) mechanism. The L-type calcium channel inhibitor verapamil reduced the twitch force amplitude (Figure II-8B & C) while L-type calcium channel agonist, Bay K8644, increased the contraction rate and slightly increased force amplitude (Figure II-8D & E). These experiments suggest extracellular calcium as the source in engineered cardiac tissue for driving the contractile function. We then generated the Starling curve by plotting the amplitude of twitch force, normalized to cross-sectional area, versus change in length (Figure II-6C). A comparison of the slopes of this relationship illustrates the difference in contractility of these constructs (Figure II-6D). We observed a more than 10-fold enhancement in contractility comparing NS to SS conditioning ($p < 0.001$). Adding electrical pacing further augmented contractility by additional 2-fold ($p < 0.01$).

3. Calcium handling dynamics of bioengineered cardiac tissues

We hypothesized that the enhancement in contractility results at least partially from maturation of excitation-contraction coupling of the engineered tissues. Western blots demonstrated that SERCA2 protein expression was significantly upregulated 2-fold by SS conditioning (NS vs SS, $p<0.01$). SE also exhibited a significant 2.5-fold increase from NS conditioning (NS vs SE, $p < 0.001$). However, addition of electrical pacing did not reach significance in SERCA2 expression when comparing to SS conditioning (Figure II-9B). RYR2 expression in SE group was also elevated by 1.5-fold from NS conditioning but only

slightly increased from SS conditioning (Figure II-9C). To eliminate the variability between western blot experiments, western blot data were also standardized by log-transforming, mean-centering, and autoscaling.[184] SERCA2 expression from standardized data showed similar enhancement from NS to SS and NS to SE like raw data (Figure II-10A), while a significant 1.8-fold increase of RYR2 expression when comparing SE constructs to NS constructs was revealed in the standardized dataset (Figure II-10B, NS vs SE, $p < 0.001$).

We then examined the force-frequency relationship, a well-established maturation index for excitation-contraction coupling.[185] Adult human cardiomyocytes have a positive force-frequency relationship, showing increasing force with increasing pacing frequency. On the other hand, human stem cell-derived cardiomyocytes have a negative force-frequency relationship,[186,187] likely due to immature sarcoplasmic reticulum (SR) development, such that increased pacing frequency reduces active force production. In the NS engineered heart tissues we found a prominent negative force-frequency relationship. As stimulation frequency increased from 2 to 3 Hz, twitch amplitude decreased by 43.19±0.01% ($p = 0.02$). In tissues conditioned by SS, however, twitch amplitude decreased by only 16.85±0.03% from 2 to 3 Hz ($p = 0.03$). The tissues conditioned by SE showed a 4.40±0.36% decrease in force production from 2 to 3 Hz, nearly unchanged from baseline (Figure II-11). These data demonstrate a more mature dynamic balance of calcium handling in the SS and, especially, SE conditioned constructs.

4. Ultrastructure of engineered cardiac tissues

Stress-transmitted adhering junctions, fascia adherens and desmosomes, were clearly observed in the engineered cardiac tissues with a higher density in constructs treated with static stress conditioning (Figure II-12A & B). The increase in adhering junctional structures indicates the cardiomyocytes were able to response to external mechanical conditioning and remodeled the cell-cell interaction. Compared to no stress conditioning, the sarcomeres of cardiomyocytes in the stress condition were also more aligned, which might be the response to aligned collagen fibers. We did not find any gap junctional like

structure in electron micrographs but many primitive intercalated disk-like structures exist in the constructs, suggesting that the cardiomyocytes are still maturing.

E. Discussion

In the current study we demonstrated that human myocardium can be generated using hiPSCs, and that this engineered heart tissue is highly responsive to both mechanical and electrical cues. In response to static stress, the engineered heart tissues showed increased cell alignment, cardiomyocyte hypertrophy, increased contractility and passive stiffness, increased expression of Ca^{2+} handling proteins, an enhanced force-frequency relationship. When electrical pacing was added to the conditioning regimen, we observed a further increase in passive stiffness, an additional 2-fold increase in contractility, further increased expression of Ca^{2+} handling proteins and an improved in the force-frequency relation. Previous observations have estimated the size of hESC-derived cardiomyocytes, cultured on monolayer, to be 480±32 μm^2 [133] in the early stages (day 20 to 40 post differentiation) and revealed that longer term culture (80 to 120 days post differentiation) is needed to increase the size 3-fold. Here, our input population used cardiomyocytes from day 14 to 21 post differentiation and, after the additional 14 day of tissue culture conditioning, the cardiomyocytes are still early stage (less than day 40 post differentiation). With stress conditioning in the construct, early stage hiPSC-derived cardiomyocytes demonstrated a 1.5-fold increase in size. SE conditioning showed a slight increased trend toward further cardiac hypertrophy, but not to significance. Similar cell size increases have been observed with T3-treatment of early stage hiPSC-derived cardiomyocytes in 2-D culture with a similar 1.5-fold size increase in a 1 week treatment.[136]

Compared to embryoid body or monolayer culture of cardiomyocytes, 3-D engineered heart tissue shows significant cellular maturation.[55,157,180,188–190] Our previous study showed that cyclic stress and SS demonstrate comparable effects in structural organization of PSC-derived cardiac constructs.[156] Here we showed that the SS conditioning itself is enough to promote structural organization of hiPSC-derived

cardiac tissues and furthermore, enhances the functionality of engineered myocardium, which has not been demonstrated in previous studies.[56,156,191] The presence of electrical pacing does not appear to significantly promote overt structural reorganization compared to the SS-treated group, but electrical pacing conditioning does enhance both stiffness and contractility of the engineered tissue. The difference in passive stiffness between constructs is likely due to remodeling of the extracellular matrix by cardiomyocytes and/or other cells in the tissues. We previously reported that hESC-derived cardiac tissue constructs show remodeling of the original matrix with organized collagen fiber bundles and that stress conditioning significantly increased collagen fiber alignment as well as cell alignment.[156] In these studies, we found that passive stiffness increases markedly with stress conditioning and with electrical stimulation. Overall, the passive stiffness of those constructs is still somewhat less than the passive stiffness of rat neonatal myocardium (38.5±9.1 kPa) measured using the same system.[95] This may be a result of remaining immaturity of the collagen matrix, which still demonstrates a lower alignment value in engineered cardiac tissue when compared to naïve myocardium (alignment value of rat heart is 9.08).[156,192] The immaturity of these stem cell-derived cardiomyocytes are also reflected in the low force development compared to native myocardiums, where active force from human adult ventricular strip is generally over 10 mN/mm^2.[193,194] Our engineered cardiac tissues showed force production within the range of most reported values using neonatal rat ventricular myocytes (0.4-4.6 mN/mm^2) or human stem cell-derived cardiomyocytes (0.12-4.4 mN/mm^2).[157,188,195,196] It should be noted that the methods to calculate the contractile stress amplitude is not standardized and containing non-myocyte component may also underestimate the actual force production from myocyte population. Many studies had just reported the absolute force generated by constructs, but the difference in tissue geometry makes the results incomparable. By analyzing a-actinin positive area within the cross section of our constructs, we show that there is no difference in bona fide muscle cross sectional area between three conditioning groups (NS: 21.0±4.63%, SS: 23.13±3.99%, SE: 28.60±7.01%) and, thus, it is reasonable to report the

specific force for comparing different conditional groups. From the bona fide muscle cross sectional area, we can estimated that the twitch forces at 125 % stretch for NS, SS, and SE are 0.08, 0.83, 1.30 mN/mm^2, respectively, which are close to the active force production from newborn (1.1 ±0.3 mN/mm^2 at 2 Hz pacing) and infant strip (1.7±0.9 mN/mm^2 at 2 Hz pacing).[197]

An important observation in this study was that our engineered heart tissue constructs demonstrated increasing twitch force as length increases, in accordance with the cellular basis of the Frank-Starling mechanism. This is a fundamental characteristic of native heart muscle, and its presence here suggests we are on the right track in developing realistic models of human myocardium. Several studies have demonstrated similar results anecdotally in human stem cell-derived cardiac tissue,[55,156,157,189] but in this current study, we demonstrated this effect in hiPSC-derived myocardium and, further, established that contractility can be promoted by combining electrical and mechanical conditioning. In our study, length dependent contractility (measured as average slope of twitch force over the change in length) was increased 2-fold in the SE group compared to the SS-conditioned tissues, and both groups demonstrated at least 10-fold enhancement over NS group. The increased contractility likely has several components, including greater cell alignment that would increase the resultant vector of force production, as well as cellular adaptations such as cardiomyocyte hypertrophy (including increased content in myofibril proteins), and increased expression of Ca^{2+} handling proteins such as SERCA2 and RyR2. In addition, we had previously showed an increased Ca^{2+} kinetics (upstroke velocity) in constructs subjected to stress conditioning.[92] These results indicate maturing SR with enhanced calcium handling in stress-conditioned cardiac tissue constructs. The increase in SERCA2 expression in stress-conditioned constructs is also consistent with our observation of a less negative force-frequency relationship. For normal mature cardiomyocytes, a positive force frequency relationship is important for mediating cardiac output during exercise. Increasing pacing frequency increases the opening of L-type calcium channels, resulting in more calcium getting into cells. On the other hand, the function of sodium calcium exchanger to

transport the calcium out is diminished at the same time. Thus, the overall net calcium inside the cell increases and SR is able to store more calcium for next contraction. For stem cell-derived cardiomyocytes, there is more expression of sodium calcium exchanger but less expression of SERCA2,[198] which makes the calcium outflux more than influx and the SR not able to load more calcium for next contraction. Through stress conditioning and electrical pacing, the expression of more SERCA2 enables more calcium load in SR, and thus a more blunted force frequency relationship.

It was interesting that electrical pacing had a significant additive effect on passive stiffness (>2-fold increase), contractility (>2-fold increase), and expression of calcium handling proteins (1.5- 2.5-fold increase), without having detectable effects on cardiomyocyte alignment or hypertrophy. This indicates that different features of maturation are controlled by different stimuli and suggests that multiple pathways may be needed for optimal maturation. One caveat to our experiments is that longer electrical stimulation periods or different stimulation regimes may be needed to further promote this effect. For instance, studies by Hirt et al. indicated that chronic electrical pacing for 16-18 days promoted higher cardiomyocyte to ECM ratio.[191] Additionally, Nunes et al. also showed that a gradually increasing pacing frequency from 1 Hz to 6 Hz over a week can further enhance the structure and electrophysiological function of engineered cardiac constructs compared to a low frequency ramp up regime from 1 Hz to 3 Hz.[180]

In summary, we generated cardiac tissue from hiPSC-derived cardiomyocytes and demonstrated structural and functional improvement of this bioengineered myocardium when subjected to stress conditioning and electrical stimulation. Specifically, we show that: 1) 2 week stress conditioning promotes alignment, percentage cell area, passive stiffness, cardiac hypertrophy, and contractility of engineered cardiac tissues, 2) the passive stiffness and contractility of engineered cardiac tissues can be further promoted by 1 week electrical stimulation, and 3) the enhancement in functional maturation

from these cues is correlated to the enhanced expression of SR-related proteins and the enhanced function of calcium handling dynamics.

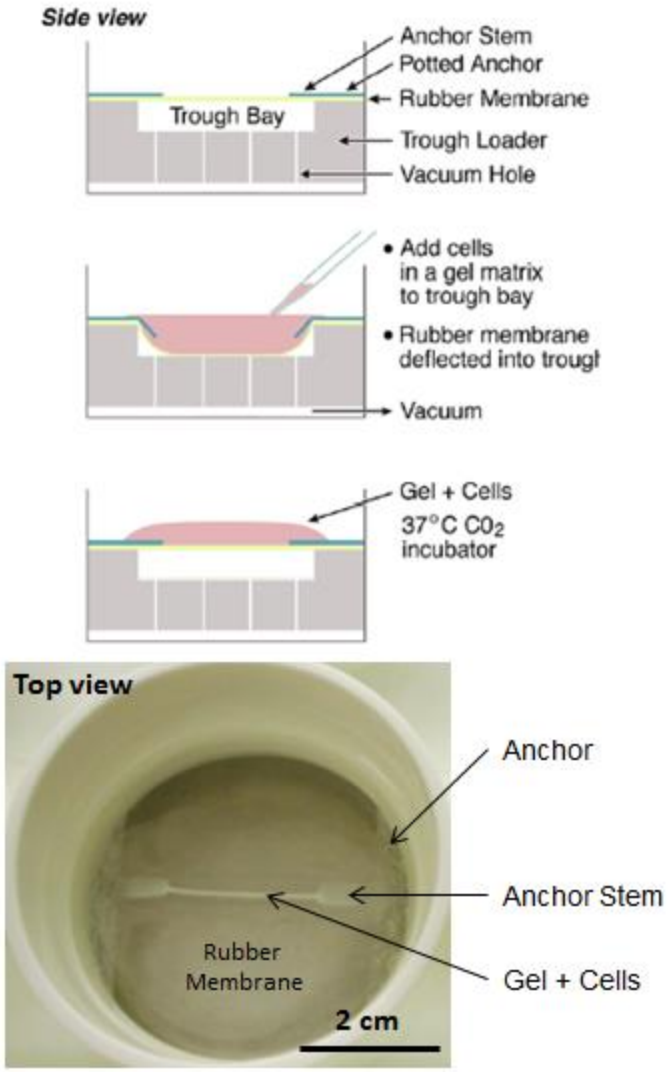

Figure II-1 Schematic protocol for construct making with Tissue Train culture system setup.

(Side view figure adopted from Flexcell Corp.)

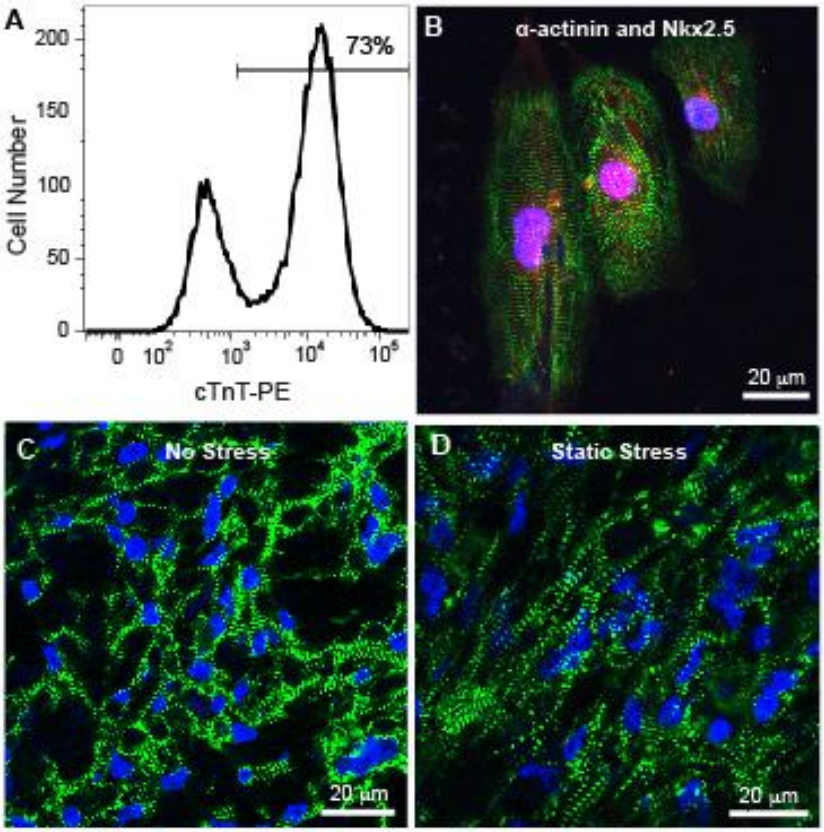

Figure II-2 Generation of high purity human iPSC-derived constructs.

A, Human cardiomyocytes were generated from the IMR90-iPSC line at a purity of over 70% by cardiac troponin T (cTnT) flow cytometric analysis. B, The cardiomyocytes displayed robust sarcomeric organization by α-actinin immunostaining (green), as well as nuclear expression of the cardiomyocyte transcription factor Nkx2.5 (red). Immunofluorescent staining for α-actinin of IPSCs-derived human bioengineered cardiac tissues under NS, C, and SS conditioning, D.

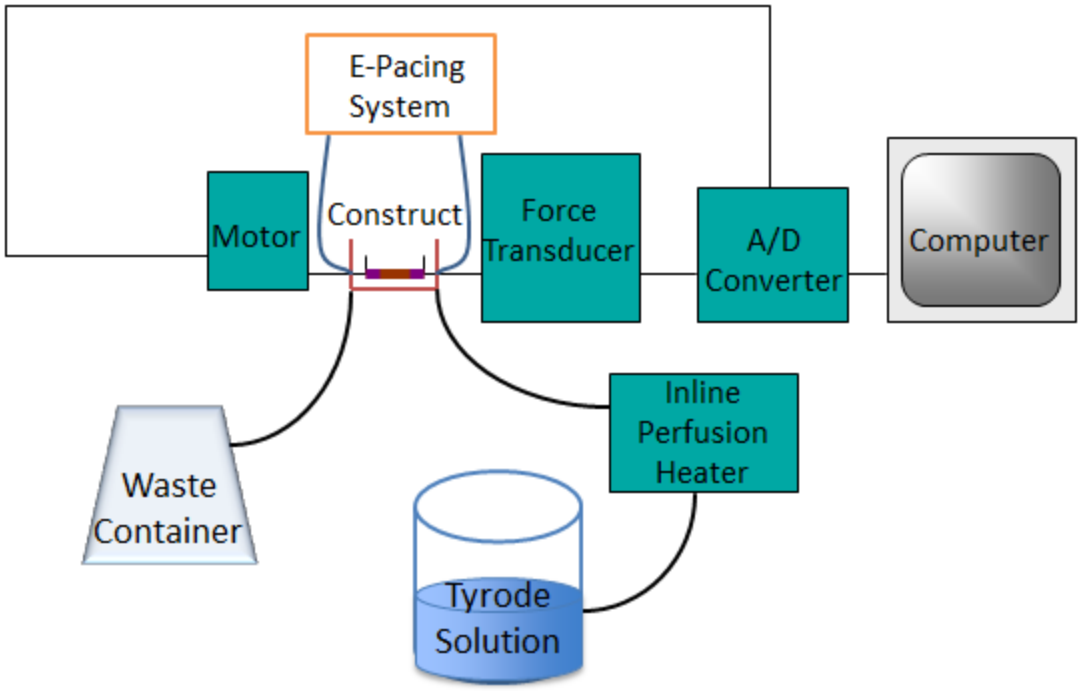

Figure II-3 Active and passive force measurement system setup.

Constructs were dissected into 2 mm sections and stretched between a length controlled motor and a force transducer in a chamber perfused with warm HEPES-buffered Tyrode solution. Both active and passive forces were recorded in the system.

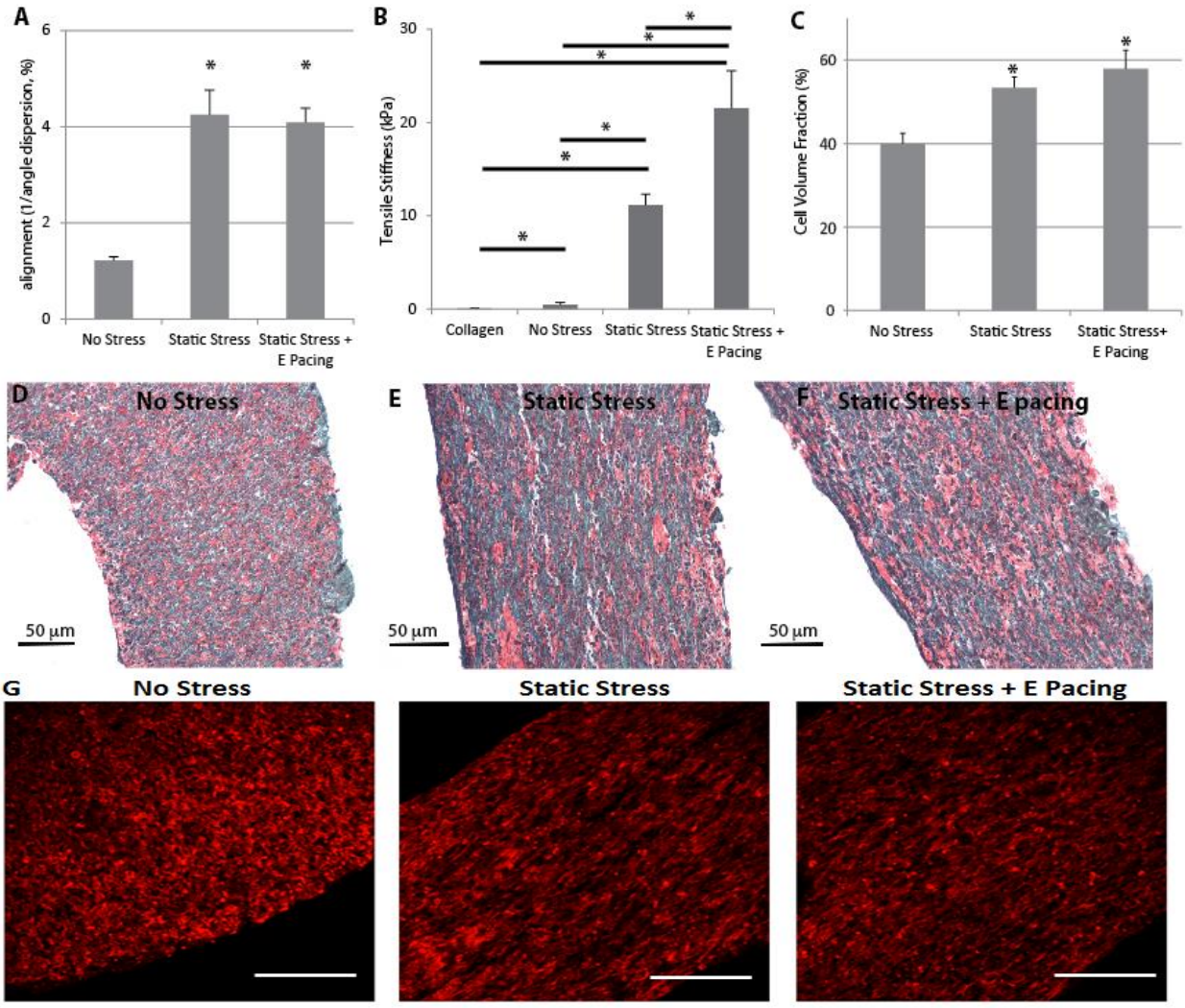

Figure II-4 Characterization of cell alignment and matrix remodeling.

A, Constructs exposed to stress conditioning demonstrated significantly increased cell alignment compared to constructs without stress conditioning (NS vs SS, * $p < 0.005$; NS vs SE, * $p < 0.0001$). Electrical pacing along with stress conditioning did not further promote the cell alignment. B, The passive stiffness of constructs was measured by stretching constructs incrementally to 125% of slack length. Tensile stiffness was estimated from the slope of passive stress-strain relationship. The tensile stiffness of cell-free collagen matrix is 0.079 ± 0.041kPa. Addition of cells increased the stiffness ~ 7-fold, stress conditioning by a further ~20-fold, and electrical pacing by an additional ~2-fold (NS: 0.47±0.22 kPa; SS: 11.13±1.17 kPa; SE: 21.51±4.02 kPa, * $p < 0.001$). C, Stress conditioning also promoted ECM

remodeling by increasing the percentage cell area within the constructs (NS vs SS, NS vs SE, *p <0.005), while 1 week of electrical stimulation offered no further benefit (SS vs SE, p=0.4). D, E, and F, are representative Sirius Red/Fast Green stains of NS, SS and SE, respectively. G, Collagen alignment from second harmonic generation of two photon microscopy. Constructs under static stress and static stress with pacing demonstrate more aligned collagen fibers compared to no stress group. The scale bar is 50 μm.

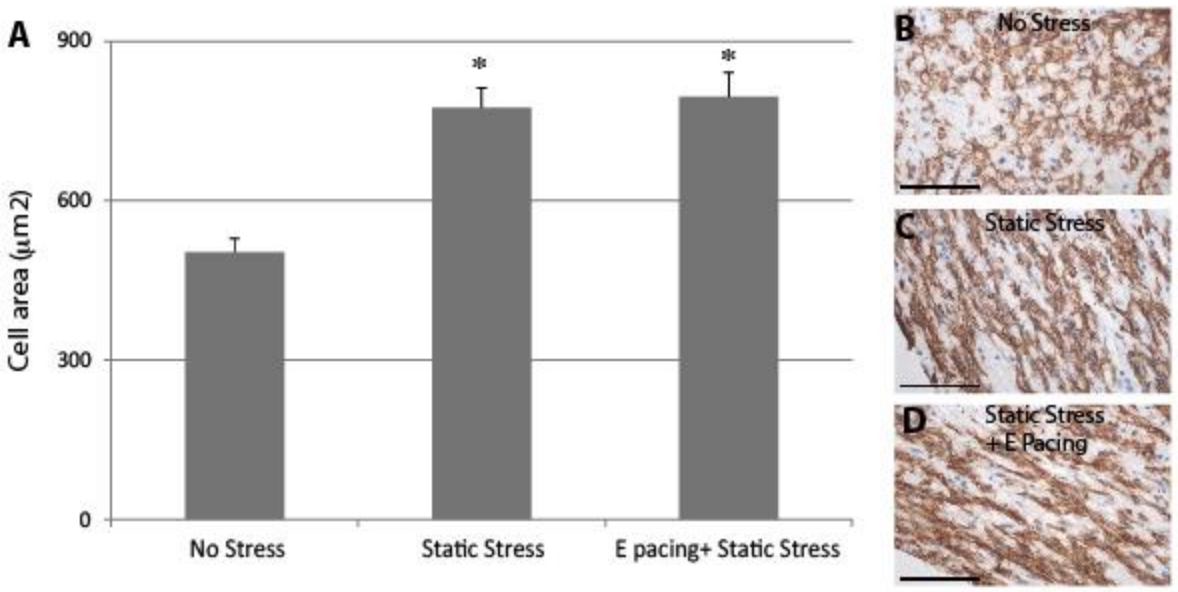

Figure II-5 Stress conditioning increases cardiomyocyte hypertrophy.

A, MYH7 positive area was measured to determine cardiomyocyte size from constructs in the different conditioning regimes. Cardiomyocyte size increased ~50% from NS vs. SS constructs, with no further increase in the ES group.(NS to SS: * $p < 0.001$; NS to SE: * $p < 0.001$) B, C, and D, shows MYH7 positive cells in constructs from NS, SS, and SE, respectively. Hematoxylin counterstain denotes nuclei. The scale bar is 50 µm.

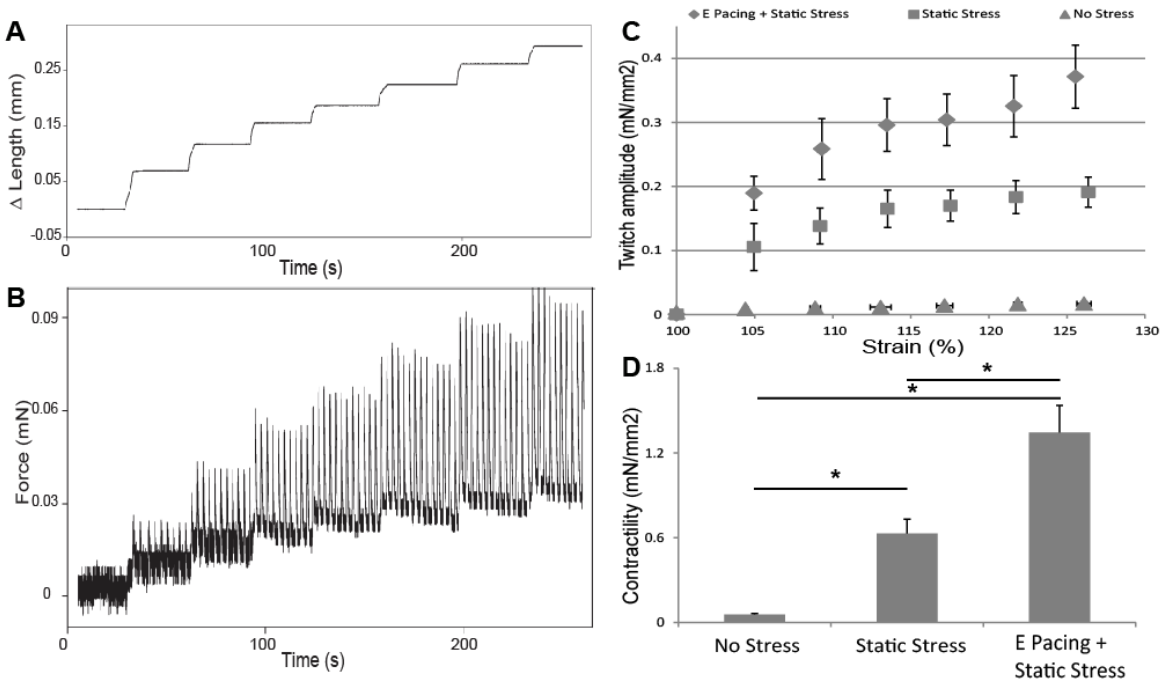

Figure II-6 Stress conditioning and electrical stimulation increase contractility.

Representative length (A) and force (B) traces demonstrate the response of a spontaneously contracting cardiac tissue construct to a series of stretches up to 125% of slack length. The amplitude of the isometric twitch force increased with increasing preparation length, in accordance with the Frank-Starling mechanism. C, Isometric twitch force amplitude measured at different preparation lengths is enhanced by 2 weeks of SS conditioning (squares) in comparison to NS conditioning (triangles). Addition of electrical stimulation (diamonds) further increased contractility as show in (D). D, Contractility of constructs from the 3 stimulation conditions. Contractility is measured from the slope of the twitch force-strain curve, which is the active force development. The contractility of no stress constructs was 0.055±0.009 mN/mm^2. Stress conditioning promoted the contractility 10-fold (0.63±0.10 mM/mm^2) and addition of electrical pacing further enhanced force development another 2-fold (1.34±0.19 mN/mm^2).NS vs SS: $p < 0.001$; SS vs SE: $p < 0.01$.

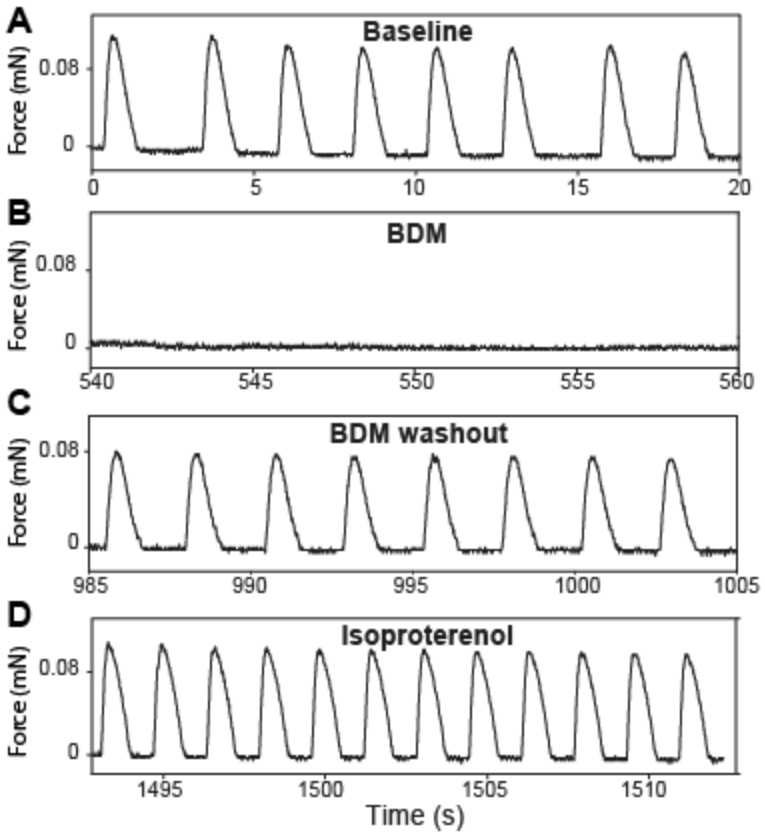

Figure II-7 Constructs showed negative inotropic response with BDM and positive chronotropic/inotropic response with isoproterenol in a stress conditioned construct.[92]

A, Representative force trace at 125% slack length with pharmacological agent perfusion. B, Incubation the constructs with 30mM BDM inhibited spontaneous contractions. C, Contractions returned within 3 minutes of BDM washout. D, Incubation with the β-adrenergic agonist isoproterenol (10 µM) increased rate markedly and slightly increases the twitch force.

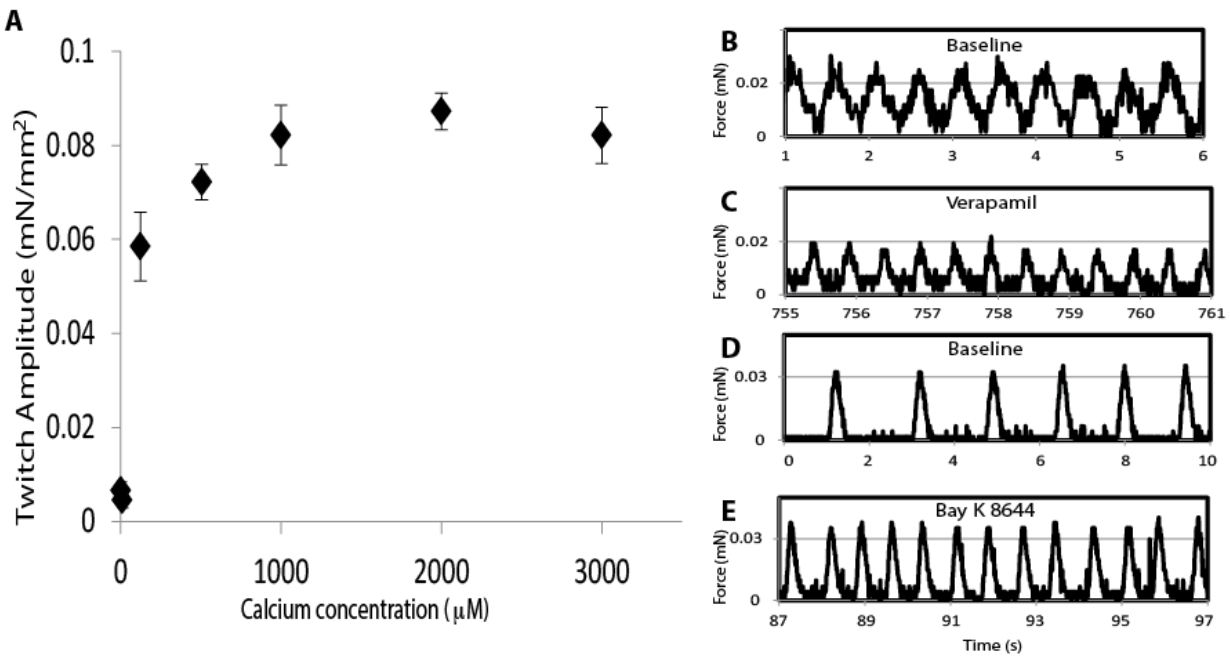

Figure II-8 Contraction of human engineered cardiac tissue is affected by extracellular calcium concentration and L-type calcium channel agents.

A, A stress-conditioned engineered cardiac tissue was perfused with Tyrode solution with varying concentrations of calcium. Twitch amplitude of engineered cardiac tissue was largely affected based on the extracellular calcium concentration. B & C, Twitch amplitude decreased after constructs were perfused with L-type calcium channel antagonist, verapamil (1 μM). D & E, L-type calcium channel agonist, Bay K 8644 (1 μM), enhanced the contractility both inotropically and chronotropically.

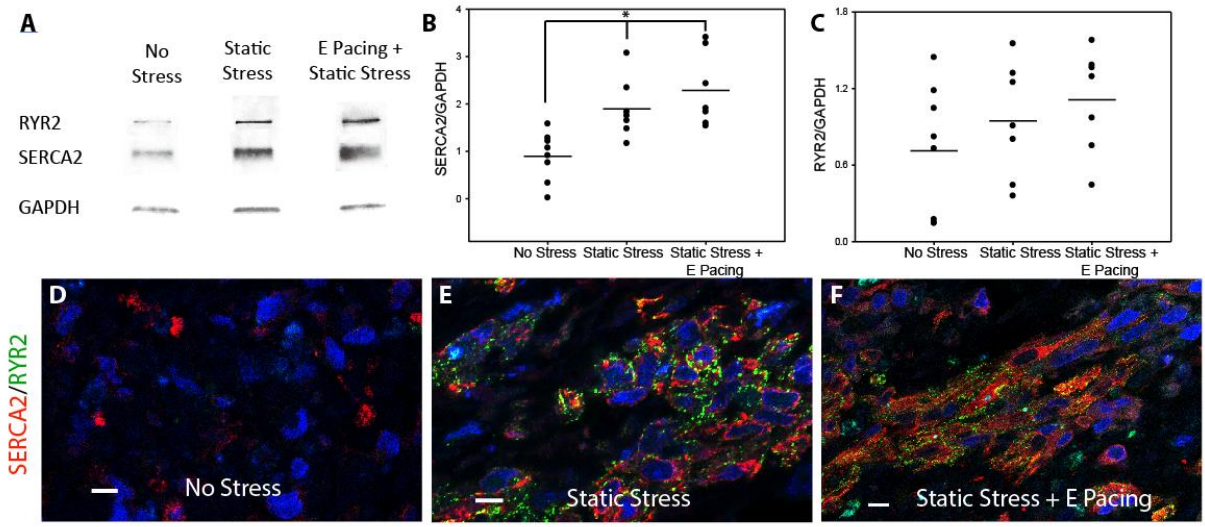

Figure II-9 Increase in calcium handling protein expression by stress conditioning and electrical stimulation.

A, Western blot of SR-related proteins, SERCA2 and RYR2, from constructs subjected to different conditioning regimes. B&C, Mean/dot plot of quantified western blot data. Data were normalized to internal control (GAPDH). B, Compared to the NS control, SS conditioned constructs increased SERCA2 expression by 2-fold (NS vs SS, * $p < 0.01$) and SE-conditioned constructs by 2.5-fold (NS vs SE, * $p < 0.001$). C, An increasing RYR2 expression trend was observed from NS to SE constructs but did not reach statistical significance. n=8 for NS, n=7 for SS, and n=7 for SE. Representative immunostaining images of engineered cardiac tissues stained with SERCA2 (red) and RYR2 (green) from NS (D), SS (E) and SE (F) conditionings. The scale bar is 10 µm.

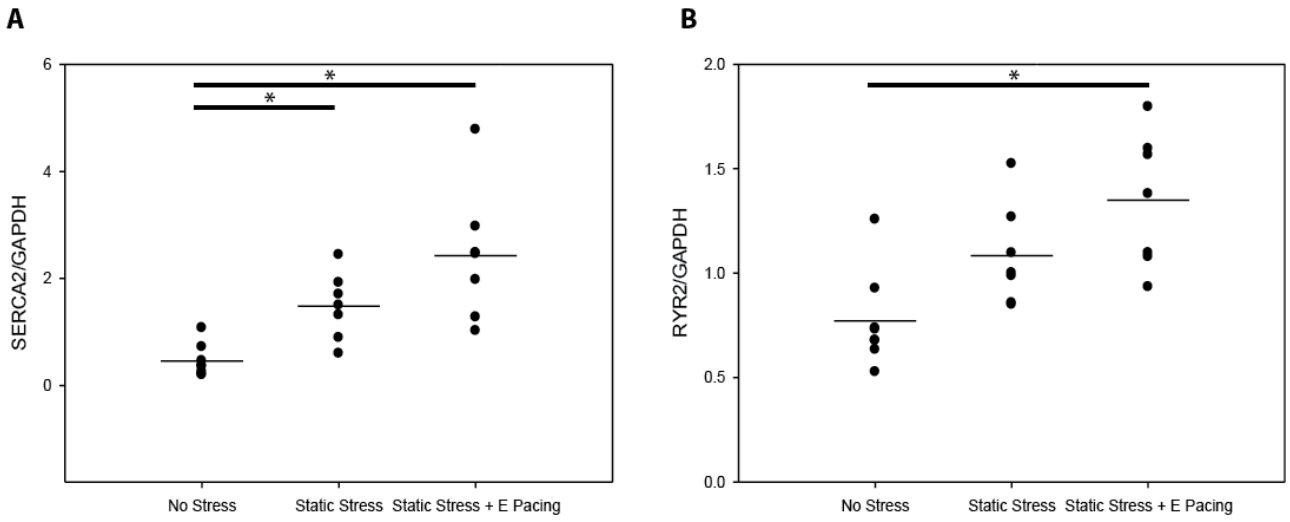

Figure II-10 Processed data from Western blot of Figure 5B and 5C.

Data are underwent log transformation, mean centering, and autoscaling as described previously.[184] A, Similar significant increase in SERCA2 expression can be observed from the SS and SE constructs to NS constructs (NS vs SS, * $p < 0.01$; NS vs SE, * $p < 0.001$), while the increase from SS to SE constructs was not significant. B, An increasing trend of RYR2 expression from SS conditioned constructs to NS constructs was also observed but did not reach significance (NS vs SS, $p = 0.02$). 1 week of electrical pacing with static stress significantly increased RYR2 by 1.8-fold (NS vs SE, * $p < 0.001$) from that of NS constructs, but it was not significantly different from SS constructs. n=8 for NS, n=7 for SS, and n=7 for SE.

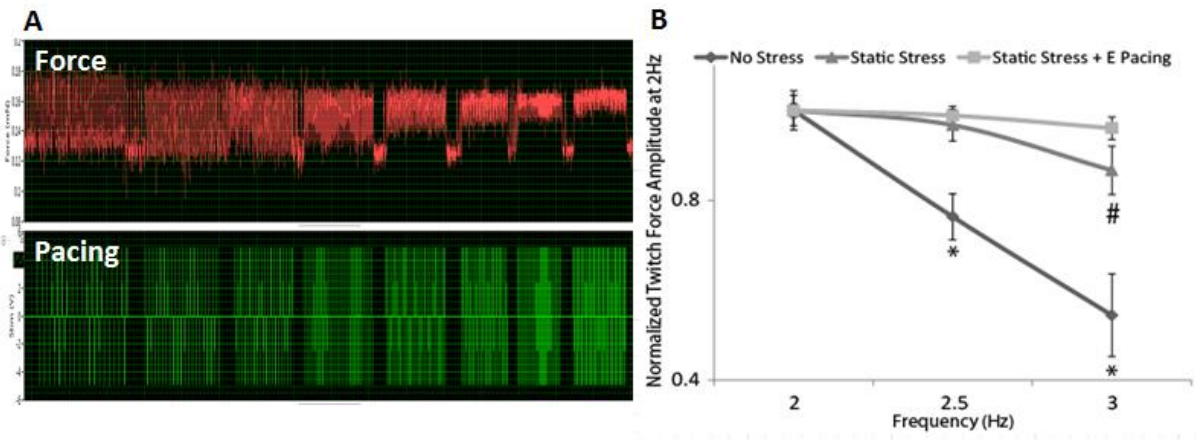

Figure II-11 Force frequency relationship of engineered cardiac tissues.

A, Engineered cardiac tissues were subjected to pacing with incremental frequency. The lower panel was the representative pacing trace while the upper panel showed the corresponding force trace. B, The twitch amplitude under 2, 2.5, and 3 Hz pacing frequency were normalized to those at 2 Hz. Due to immature development of SR, the force frequency relations of these constructs were negative, but static stress and electrical pacing pre-conditioning were able to mitigate the effect (NS p= 0.04 for 2 Hz vs 2.5 Hz, p=0.02 for 2 Hz vs 3 Hz; SS p =0.03 for 2 Hz vs 3 Hz).

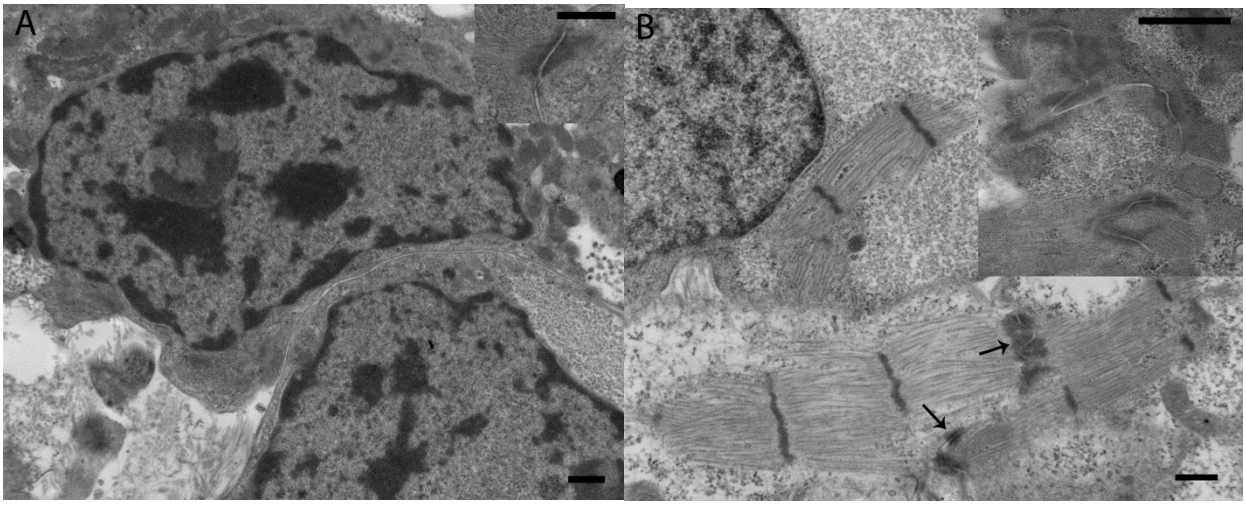

Figure II-12 Stress Condition promotes intercellular adhering junctions.

Representative electron microscopic image of engineered cardiac tissues under no stress condition (A) and static stress condition (B). The upward arrow points to a fascia adherens junction and the downward arrow indicates a desmosome. The upper right corner shows a zoom-in figure of primitive intercalated disc-like structure. Also apparent are contractile elements with A-bands of myosin interspersed with Z-lines. The scale bar is 500 nm.

III. Mechanical Conditioning Affects Cell Fate Determination and Maturation on Cardiovascular Progenitors in 3-D Collagen Engineered Tissues

A. Introduction

Direct differentiation of stem cells toward certain lineages generally involves in steps simulating its nature developmental environments. For heart development, sequential induction of mesoderm, multipotent cardiovascular progenitor cells and functional derivatives are important steps. Identification of cardiovascular cells has demonstrated identified *in vivo* with specific biomarkers expression.[38,107] It has been showed that during direct differentiation process, stem cells are also able to generate tri-potential cardiovascular progenitors like their *in vivo* counterparts and capable of differentiating into cardiomyocytes, smooth muscle, and endothelial cells.[37,199] Here we used KDR and PDGFRα-expressing to identify the input progenitor cell population to make engineered tissue and studied the effect of mechanical stress on cell fate determination and maturation.

The primordium of the heart is through the migration of mesodermal cells from the primitive streak to the splanchnic mesoderm, forming the cardiac crescent. The cardiac crescent contains two distinct pools of cardiac progenitors with origination of anterior splanchnic mesoderm and pharyngeal mesoderm, respectively. The first heart field (FHF) in the medial region of the crescent merges in the midline to form the primordial heart tube and ultimately contributes to the left ventricles and atria. The second heart field (SHF) located posteriorly and medially to the FHF and contribute to the arterial end of the heart tube initially and then to the majority of cardiomyocytes in the right ventricles and the outflow tract. The interaction of these two heart progenitors is important in many aspects of heart morphogenesis. Kinase inert domain receptor (KDR) is a type III receptor tyrosine kinase also known as VEGFR2, CD309, or Flk1. Studies have demonstrated that both endocardium and a population of myocardium are

developed from a KDR expression population that exits the primitive streak.[200] It has also been showed that the expression level of KDR during cardiac direct differentiation can identify the cardiogenic progenitor population as distinct from the hemangioblast population.[105,199] Due to other potential contribution in mesodermal lineage, the usage of KDR as the only cardiovascular progenitor marker is problematic.[201] Thus, inclusion of another cardiogenesis marker is generally required for more specific identification of desired population. Platelet-derived growth factor receptor-alpha (PDGFRα) has been shown to coexpress with KDR in cardiac mesoderm at the embryonic stage.[202] PDGFR are cell surface tyrosine kinase receptor for PDGF family that regulates many important functions like proliferation, organogenesis, and diseases. Studies have showed that PDGFRα is expressed in both developing and diseased human heart.[107] The expression of KDR/PDGFRα has been used to denote cardiac mesoderm generation in embryoid body-based cardiac direct differentiation protocol and the resulting cell population from this protocol has showed to be able to give rise to cardiomyocytes, smooth muscle/fibroblastic, and endothelial lineages.[62] The protocol generally requires the EBs to be dissociated and plated into 2 dimension culture plates after cardiac mesoderm induction for follow-up experiments. The goals in our experiment, thus, are 1) to demonstrate the creation of human cardiac tissues with a single line of PSCs, and 2) to study the effect of specific mechanical manipulation on the effect of lineage commitment and maturation.

B. Materials and Methods

1. EB-based direct differentiation for progenitor generation

Undifferentiated human ESCs (H7) and iPSCs (IMR90) were maintained as described in the previous section. Briefly, human stem cells were grew on Matrigel-coated plates in MEF-conditioned medium supplemented with 5 ng/mL basic FGF and passaged with collagenase IV (200 U/mL, Invitrogen) followed by 0.05% trypsin-EDTA (Invitrogen) or Dispase (STEMCELL). CVPs of human IBJ line were

provided by courtesy of Dr. Gorden Keller from University of Toronto, Canada. All the growing of CVPs and CVP-based constructs were occurred in a "Backbone" medium made fresh daily. The Backbone medium contains Stempro Base medium (Gibco), Supplement 34 (Invitrogen), penicillin G (100 U/mL, Cellgro), streptomycin (100 mg/mL, Cellgro); L-glutamine (1 mmol/L, Invitrogen), ascorbic acid 2-phosphate (50 µg/mL, Sigma), transferrin (150 µg/mL, Roche), and monothioglycerol (0.039 µL/mL, Sigma), with the further addition of various stage-specific cytokines as described below.[37,104,203] H7-derived cardiovascular progenitors were generated as described previously.[204] Following 1 hour pre-incubation in 10 µM ROCK inhibitor Y27632 (Tocris Bioscience), cells were gently detached using collagenase IV and trypsin and cultured as embryoid bodies (EBs) in ultra-low attachment 10-cm plates (Corning) at a density of 6 million cells per plate in relative hypoxia (5% oxygen) in low-dose BMP4 (0.5 ng/mL, R&D Systems) and ROCK inhibitor (10 µM) for 24 hours. On day 1 of differentiation, EBs were resuspended in a Mesoderm Induction medium (Backbone with 10 ng/mL BMP4, 6 ng/mL activin A, R&D, and 5 ng/mL basic FGF) and placed back into hypoxia. On day 4, the EBs were resuspended in Backbone medium supplemented with VEGF (10 ng/mL) and Dkk1 (150 ng/mL, R&D Systems) to promote cardiovascular progenitor differentiation and placed back in hypoxia. After an additional 24 hours, EBs were pre-incubated in ROCK inhibitor before digestion with trypsin, light vortexing, and disruption with a 20-gauge needle (BD Biosciences). Cells were counted and resuspended in Backbone medium, an aliquot was taken for live cell KDR/PDGFRα staining and flow cytometry, and the remaining cells were used for 3-D CVP construct generation (described below) or plated 2-dimentionally at a density of 1 million cells per well in Matrigel-coated 6-well plates. The constructs and plated progenitors were kept in Backbone medium with VEGF (10 ng/mL) and Dkk1 (150 ng/mL) in normoxic (20% oxygen) conditions until day 9 of differentiation. All subsequent feeds were Backbone supplemented solely with 10 ng/mL VEGF.

The protocol has been extended to IMR90 line with some modifications (Figure III-1). Firstly, before onset of differentiation, undifferentiated stem cells were treated overnight with 1 μM CHIR99021 (a Wnt agonist, Cayman). On the day of differentiation (T0), undifferentiated stem cells were pre-incubated in 10 μM ROCK inhibitor Y27632 (Tocris Bioscience), detached using Dispase, and cultured as EB format in ultra-low attachment 10-cm plates WITH high dose BMP (5 ng/ml), 1 μM CHIR99021, and 10 μM ROCK inhibitor. On day one of differentiation (T1), EBs were treated with a mesoderm induction medium with BMP concentration at 10 ng/ml, 1 μM CHIR99021 and without activin A. Wnt signaling is inhibited at day 3 with XAV939 (Tocris Bioscience) and at the same time the CVP population was induced by VEGF containing Backbone medium supplemented with SB-431542(5.4 μM, a Nodal inhibitor, Tocris Bioscience) and dorsomorphin (0.6 μM, a BMP inhibitor, Tocris Bioscience).

2. Generation of CVP constructs

One day after Wnt signal inhibition, the EBs were dissociated and CVPs could be identified by KDR-PDGFRα staining. Based on the intensity of KDR, two cell populations, CVP population and hematogioblast progenitor population, could generally be observed. CVP population was generally more dominant (>60 %) in this protocol. The CVPs were either encapsulated in a 3-D collagen gels at a density of 2 million cells per 100 μL of gel mixture as described in the previous Method section or plated into 2-D Matrigel-coated plates. For no stress condition, one end of the construct was cut free off the nylon tab. Static stress conditioning was achieved by spanning the constructs at a fixed static length between the two nylon tabs. For cyclic stress conditioning, one day following construct generation, Tissue Train plates were placed onto a baseplate with Arctangle loading posts. An FX-4000T system was connected to the baseplate and applied uniaxial cyclic stress at a frequency of 1 Hz, 5% elongation under a sine waveform setting. Constructs were cultured under the same mechanical regime of no stress, static stress, or cyclic stress conditioning for 2 weeks.

3. Flow cytometry

KDR / PDGFRα double staining was conducted on live input cells at time of progenitor construct generation. The flow cytometry staining protocol is similar to what described in the previous Method section. Cells were incubated with directly conjugated antibodies hKDR-PE (mouse IgG1, R&D Clone 89106, 15:100 dilution) and hPDGFRα-APC (mouse IgG1, R&D Clone PRa292, 10:100 dilution) for 30 minutes at 4 ^{0}C in the dark. Isotype control used for gating was done by replacing the abovementioned antibodies with mouse IgG1-PE (eBioscience Clone P3.6.2.8.1) and mouse IgG1-APC (eBioscience Clone P3.6.2.8.1). Samples were fixed in 1.3% PF and stored at 4 ^{0}C in the dark till further analysis.

To disrupt cardiovascular tissue constructs for flow cytometry, the 3-D constructs were dispersed to single cells using a trypsin-based technique as described previously.[92] Each construct was rinsed twice in the versene solution (0.5 mM EDTA and 1.1 mM glucose in PBS) containing 30 μM BDM (Sigma) and 10 μM ROCK inhibitor Y27632 before dissected into several pieces. The construct was then placed in a 0.05% trypsin solution with 30 μM BDM and 10 μM Rock inhibitor. After 2 rounds of 5-10 minute incubation at 37°C and light vortexing, the remaining pieces were disrupt with 20-gauge needle and a P1000 pipette until no visible clump was found. An equal volume of Stop solution (50% DMEM/F12, Invitrogen; 50% fetal bovine serum, FBS, Hyclone; Matrigel, 1:800; DNAse, 200 U/mL, Calbiochem) was added to the construct mixture to stop the enzyme reaction. The cells were then fixed for 10 minutes in cold 4% PF and kept in PBS with 5% FBS.

For analysis of CVP cell fate, cells from constructs or from Matrigel plates were incubated with 0.75% saponin/5% FBS in PBS containing cardiac troponin T (cTnT, mouse IgG1, ThermoScientific Clone13-11, 1:100 dilution), smooth muscle α-actin (SMA, rabbit IgG, Abcam Clone E184, 1:200 dilution) or hCD31-PE (mouse IgG1, eBioscience Clone WM59, 1:5 dilution) for 30 minutes at room temperature. Secondary antibodies used for cTnT and SMA staining were goat anti-mouse-IgG-PE (GαM-PE, Jackson Cat# 115-116-072, 1:200) and donkey anti-rabbit-IgG-APC (DαR-APC, Jackson Cat# 711-136-152, 1:500). For

isotype control, primary antibodies used for cTnT and SMA staining were mouse IgG1 (eBioscience Cat# 14-4714, 1:100) and rabbit IgG (Cell Signaling Cat# 2729, 1:1000). The same antibodies listed above were used as the secondary antibodies, whereas mouse IgG1-PE (eBioscience Cat# 12-4714, 1:100) was used as isotype control for CD31 staining. All samples were run on a BD FACS Canto II machine (BD Biosciences) and gated against isotype controls.

Results were analyzed using FlowJo version 9.3.1 software. Data are a summary of 3-6 biological replicates, n= 2-6 constructs for each group. For analyzing protein intensity per cell, cTnT+, SMA+, or CD31+ events were analyzed for averaged mean PE (cTnT, CD31) or APC (SMA) fluorescence and the results were normalized to the whole experiment average to diminish the inter-experimental difference.

4. Quantitative RT-PCR

Constructs were disrupted in RLT buffer containing 1% β-mercaptoethanol (Sigma) with a 20-gauge needle. Protocol of RNA isolation from whole constructs was described in the protocol for the RNeasy Fibrous Tissue Kit (Qiagen). RNA concentration is quantified by NanoDrop 1000 Spectrophotometer (Thermo Scientific). For H7-derived CVP constructs, 1 µg RNA was used to generate cDNA for further downstream cDNA generation, while 20 ng RNA was used for IBJ-derived CVP constructs. cDNA was generated using random hexamers (Promega) and Superscript II Reverse Transcriptase (Invitrogen) using the following reaction design: Step 1: 95°C, 2 min; Step 2, 42°C, 60 min; Step 3: 95°C, 5 min. For quantitative PCR, the following housekeeping genes were used to verify the normalization and the one with the smallest standard deviation (SD< 0.5) in Ct value was chosen for normalization.

hGAPDH (238 bp)	F: GAGTCAACGGATTTGGTCGT R: TTGATTTTGGAGGGATCTCG
hHPRT (94 bp)	F:TGACACTGGCAAAACAATGCA R:GGTCCTTTTCACCAGCAAGCT
hRPL27 (123 bp)	F:ATCGCCAAGAGATCAAAGATAA R:TCTGAAGACATCCTTATTGACG
hRPL13A (90 bp)	F:TTGCCTGCCCTTCCTCCATTGTTG R:CCTATGTCCCAGGGCTGCCTGT
hGUSB (101 bp)	F:GAAAATATGTGGTTGGAGAGCTCATT

	R:CCGAGTGAAGATCCCCTTTTTA
hHMBS (113 bp)	F:TGCAACGGCGGAAGAAAA R:ACGAGGCTTTCAATGTTGCC
hTBP (117 bp)	F:GAGCTGTGATGTGAAGTTTCC R:TCTGGGTTTGATCATTCTGTAG
hB2M (69 bp)	F:CTCCGTGGCCTTAGCTGTG R:TTTGGAGTACGCTGGATAGCCT
hSDHA (86 bp)	F:TGGGAACAAGAGGGCATCTG R:CCACCACTGCATCAAATTCATG
hUBC (124 bp)	F:CGGTGAACGCCGATGATTAT R:ATCTGCATTGTCAAGTGACGA

The step is important since for each cell line and each differentiation run, the resulting population might be different and changing the housekeeping gene expression level between constructs. The change of housekeeping gene from condition to condition was very obvious in iPSC-derived constructs, which might be resulted from the distinction of cell lineage between different condition and run of experiment. For H7, GAPDH was used as the housekeeping gene for normalization while HPRT was used for IBJ for normalization.

qPCR was carried out with 0.2 µM primers and 2X SensiMix SYBR reagent (Bioline). All samples were ran in at least duplicates in a 96-well plate format on a 7900 HT Fast Real Time PCR System (Applied Biosystems). The reaction design was showed as follow: Step 1: Step 1: 95°C, 15 min; Step 2: 95°C 15 sec, annealing at 60°C for 30 sec, elongation at 72°C for 30 sec (40 cycles); Step 3: cleanup at 72°C for 5 min; a melting curve (Step 4) of 95°C 15 sec, 60°C 15 sec, and a 2% ramp rate to 95°C, 15 sec was recorded in the end to check for single product formation by melting curve peak. Primer sequences are as follows: βMHC: GGGCAACAGGAAAGTTGGC, ACGGTGGTCTCTCCTTGGG; αMHC: GTCATTGCTGAAACCGAGAATG, GCAAAGTACTGGATGACACGCT; Nkx2.5: CCAAGGACCCTAGAGCCGAA, ATAGGCGGGGTAGGCGTTAT. Sample Ct were determined using SDS 2.2.1 software (Applied Biosystems).

5. Immunostaining and microscopy

For immunohistochemistry, constructs were fixed and embedded in paraffin as described in the previous Method section. The primary antibody staining was performed overnight, followed by one hour of secondary antibody incubation. For light microscopy, biotinylated secondary antibodies were used followed by a 30-minute incubation in the ABC reagent (Vector Labs) and visualized by DAB (Sigma) or Vector Red (Vector Labs). Hematoxylin was used for nuclear counterstain. For immunofluorescence, Alexa fluorophore-conjugated secondary antibodies were employed; Hoechst (Sigma) counterstain was used to visualize the nuclei.

The following primary antibodies were used: mouse monoclonal anti-cardiac troponin T (Developmental Studies Hybridoma Bank, 1:1000), rabbit polyclonal anti-RYR2 (Sigma, 1:500), mouse anti-TNNT2(Sigma, 1:500), goat polyclonal anti-human Nkx2.5 (R&D Systems, 1:400), mouse monoclonal anti-human CD31 (Dako, 1:15), and mouse monoclonal anti-SMA (DAKO, 1:200). For light microscopy, secondary antibodies were biotinylated goat anti-mouse IgG (Jackson Labs, 1:500) and biotinylated horse anti-goat IgG (Jackson Labs, 1:500), while for immunofluorescent microscopy, secondary antibodies included Alexa 488- or 594-conjugated goat anti-mouse, goat anti-rabbit or horse anti-goat (Invitrogen, 1:100). Permount (Fisher) and Vectashield (Vector Labs) media were used as the mounting medium onto light microscopy and immunofluorescent slides correspondingly.

Nikon Eclipse 80i microscope fitted with dry 10x-, 20x-, and 60x-Nikon objective and lenses of 0.30 and 0.95 NA was used for light micrographs. The images were captured by Olympus Qcolor 3MB camera and Qcapture Pro software. All immunofluorescent images were collected as described in the previous Method section. All images were exported into Photoshop 7.0 (Adobe) for further processing.

6. Western blot

Western blotting was performed following separation of proteins on 12.5% SDS-PAGE. The cTnT band was visualized using antibodies from Santa Cruz Biotechnology (primary sc-8121, 1:1000 and secondary

sc-2005, 1:5000) and ECL-plus detection kit (GE). Sequentially, after stripping antibodies with RestoreTM Western Blot Stripping Buffer (Thermo scientific, #21059), the membrane was blocked overnight in TBS with 0,1% Tween and 1% nonfat milk and re-probed using GAPDH specific antibodies (Rockland, Inc. 600-401-7625, 1:10000) and secondary HPC conjugated antibody (Southernbiotech, #4030, 1:10000). Densitometry was performed on scanned films using ImageJ (NIH). The ratio of cTnT/GAPDH intensity was normalized for each sample to the values of no stress sample on that blot.

7. Mechanical measurements

Constructs were dissected into 2 mm-long sections and suspended between a force transducer (Aurora Scientific, model 400A) and a length controller (Aurora Scientific, model 312B). Slack length was determined as the length step before a positive amplitude twitch transient appears. From the initial slack length, constructs were stretched to a final length of 125% initial length with tension recorded simultaneously. An inline perfusion system (Warner Instruments) was used to keep the solution temperature around 37 ^{o}C and infuse pharmacological agents in a HEPES-buffered Tyrode solution (1.8 mM $CaCl_2$, 1 mM $MgCl_2$, 5.4 mM KCl, 140 mM NaCl, 0.33 mM NaH_2PO_4, 10 mM HEPES, 5 mM glucose, pH 7.4). For calcium free HEPES-buffered Tyrode buffer, 5mM EGTA was added to replace $CaCl_2$. Force and length signals were digitally recorded and analyzed using custom LabView software. N=3-4 from two biological replicates.

8. Statistical analysis

Results are depicted as mean ± standard error of the mean (SEM). Significance was determined using single factor ANOVA followed by Student's t-test with 95% or greater confidence level.

C. Results

1. Bioengineered progenitor constructs mature into cardiovascular tissues

Tri-potential CVPs were derived from hPSCs using BMP4, activin A, basic FGF, VEGF, Wnt inhibitors and/or BMP inhibitor and Nodal inhibitor in 3 sequential stages as previously reported.[37,203] The lineage markers KDR and PDGFRα were co-expressed in the majority of CVPs (Figure III-2A), signifying a capability of differentiating toward cardiac and vascular fates.[37,104] While a majority of cells were identified as $KDR^{low}/PDGFR\alpha^{+}$ cardiovascular progenitors, a small population of cells were identified as KDR^{high} hemangioblasts which have endothelial and hematopoietic potential.[37,205] Since previous studies showed the cardiogenic potential of the sorted majority $KDR^{low}/PDGRF\alpha^{+}$ population versus the cardiogenic potential of the unsorted cells has been found to be virtually identical,[104] the unsorted progenitors were applied as our input population for the generation of CVP constructs.

These tri-potential CVP-derived constructs were able to mature into cardiovascular tissue over two weeks of differentiation within this 3-D matrix (Figure III-2B-F). The constructs expressed the contractile protein cardiac troponin T (cTnT), and the endothelial marker CD31 (Figure III-2C and D). The presence of smooth muscle lineage in the constructs was demonstrated using smooth muscle actin (SMA) or smooth muscle myosin heavy chain marker, SM1 (Figure III-2E and F). Several native myocardium-like structures were also observed in the CVP constructs. Endothelial cells formed lumen-containing structures adjacent to cardiomyocytes and smooth muscle cells (Figure III-2G and I). Staining of smooth muscle marker, SMA, and cardiac marker, cTnT, showed that the SMA+ cells lie in the interstitial gap between cardiomyocytes (Figure III-2H).

Spontaneous contraction can be observed within 5-7 days post construct formation. Cyclic stress-conditioned constructs showed higher contraction rate than those from plated cells or no stress conditioning (Figure III-3). Construct slides were also subject to two photon microscopy for collagen

organization (Figure III-4) and Sirius Red/Fast Green staining for cell alignment (data not shown). In contrast to stem cell-derived cardiomyocyte constructs, the progenitor constructs has more irregular collagen organization, which might be resulted from remodeling of ECM by different cell population. No sign of collagen or cell alignment was observed in the CVP constructs from three mechanical conditionings.

2. Progenitor fate-choice and maturation in 2-D versus 3-D bioengineered tissues

By flow cytometric analysis, H7-derived CVPs cultured within 3-D engineered tissue showed higher differentiation toward cardiac lineage and diminished smooth muscle commitment. Cells dissociated from the CVP constructs were differentiated into cardiomyocytes, smooth muscle cells, and endothelial cells as indicating by cTnT, SMA, and CD31 positive cell populations. CVPs from 3-D constructs demonstrated 34% higher cardiomyocyte content than progenitors plated in 2-D culture (Figure III-5A; 3-D vs 2-D: 63% vs 47%, $p<0.05$). Smooth muscle cell differentiation, on the other hand, decreased by 68% in constructs (Figure III-5A; 3-D vs 2-D: 4% vs 11%, $p=0.0001$), and endothelial cell differentiation remained unchanged (Figure III-5A). Similar effect was observed on hiPSC-derived CVP constructs. For IMR90-derived CVPs, cardiomyocyte differentiation in 3-D engineered tissue increased 42% over 2-D culture (Figure III-5B; 3-D vs 2-D: 65% vs 45%, $p<0.05$) and smooth muscle differentiation decreased 83% over 2-D culture (Figure III-5B, 3-D vs 2-D: 3% vs 14%, $p <0.005$). Again, no difference was observed in endothelial cell differentiation between 2-D and 3-D conditions (Figure III-5B). For IBJ-derived CVPs, cardiac differentiation increased by 145% in the constructs (Figure III-5C, 3-D vs 2-D: 49% vs 20%, respectively, $p<0.05$) while the smooth muscle cell differentiation decreased 56% (Figure III-5C, 3-D vs 2-D: 36% vs 82%, $p<0.005$). Endothelial cell differentiation was increased by 865% (Figure III-5C, 3-D vs 2-D: 12% vs 1%, $p<0.005$).

In addition to differences in fate choice, the expression of cardiomyocyte, smooth muscle, and endothelial markers was differentially affected by 3-D engineered versus 2-D culture conditions. H7-derived cardiomyocytes cultured in 3-D tissue demonstrated an over 2-fold increase in averaged cTnT intensity per cTnT+ cell over those cultured in 2-D conditions (Figure III-6A). Similar effect was observed in H7-derived endothelial cells, which showed a 2-fold increase in CD31 intensity per cell (Figure III-6A). Smooth muscle cells, on the contrary, had a 1.7-fold decrease in per-cell SMA intensity in 3-D conditions compared to 2-D culture (Figure III-6A). On the other hand, for both hiPSC-derived CVPs, the average cTnT intensity per cTnT+ cell has not changed among 2-D plated cells and the 3-D constructs (Figure III-6B and C). For IMR90-derived smooth muscle cells, 3-D culture had a 2.8-fold decrease in SMA intensity per SMA+ cells over those in 2-D plated cells (Figure III-6B), while a 2-fold increase was observed in 2-D IBJ-derived CVPs (Figure III-6C). CD31 intensity was not changed among between plated cells and constructs in IMR90-derived CVP constructs (Figure III-6B), while a 1.2-fold increase was observed in 3-D IBJ-derived constructs (Figure III-6C).

3. Progenitor fate-choice and maturation with mechanical stress conditioning

CVP constructs underwent 2 weeks of no stress, static stress, or cyclic stress conditionings. These constructs mostly showed no difference in fate choice except that a markedly increase in endothelial differentiation was found on cyclic stretched H7-derived CVP constructs (Figure III-7A). However, the maturation of CVPs was differently affected by the stress conditionings. Cyclic stress conditioning increased cTnT intensity per cTnT+ cell by about 1.5-fold over static or no stress conditioning in both H7 and IBJ-derived CVP constructs (Figure III-8A and Figure III-8C, $p<0.05$). Furthermore, cTnT expression was independently analyzed by Western Blot of whole construct lysates (Figure III-9). Cyclic stress-conditioned constructs had significantly higher normalized cTnT protein levels than unstressed constructs ($p<0.05$). In contrast to the apparent effect of stress conditioning on cardiomyocyte

maturation, smooth muscle maturation, as measured by per-cell SMA intensity, as well as endothelial cell maturation, as measured by per-cell CD31 intensity, were not affected by the conditioning regimes tested (Figure III-8).

4. Cell maturation and cell fate by quantitative RT-PCR

RNA was extracted from the whole constructs for qPCR analysis. The transcript expression level for each gene was first normalized to the housekeeping gene, GAPDH, and then normalized to those from no stress group (Figure III-10). Multiple cardiac contractile protein related genes (TNNT2, MYH6, and MYH7) were analyzed in the transcriptional level. Overall, MYH7 was the only increased transcript in H7-derived CVP constructs under cyclic stress condition. The effect was not observed in both IMR90-derived or IBJ-derived CVP constructs under cyclic stress conditioning (data not shown).

MYH6 and MYH7 showed dynamic change between cyclic stress and other stress conditioning.[92] MYH6 encodes the alpha heavy chain subunit (fast isoform) of cardiac myosin while MYH7 encodes the beta heavy chain subunit (slow isoform). Both genes were also expressed in skeletal muscle and smooth muscle in addition to cardiomyocytes. From our result, there is a decrease in MYH6 transcript in cyclic stress group and the MYH7 transcript level was increased. The ratio of these two isoforms varies during the stage of heart development and disease. In rodent model, a T3-mediated rapid transition from β-MHC to α-MHC occurs during early neonatal development.[206] In human fetal ventricular samples, the relative expression of α-MHC decreases with the gestation age.[207]

We also did not find any change in the genetic expression of the hypertrophic hormones, NPPA and NPPB, which are generally activated under mechanical stimulation. Atrial natriuretic peptide, encoded by NPPA, is a vasodilator hormone secreted by atrial cardiomyocytes to mediate the water and electrolyte homeostasis in response to increased afterload or injury. Brain natriuretic peptide is mainly produced in the ventricular cardiomyocytes in human in response to stretching of heart muscles. No difference in the expression level of NPPA and NPPB was found between different stress groups. For

early cardiac transcriptional factors, NKX2.5, GATA4, and GATA6, no difference was observed from all conditions. Homeobox protein Nkx2.5, encoded by NKX2.5 gene, plays critical role in heart formation. It has been showed to interact with GATA4, a zinc finger transcription factor encoded by GATA4 gene. Both GATA4 and GATA6 continually express in the adult cardiomyocytes, participating cardiac hypertrophy. They can also be found in other organs like liver and lung.

We also analyzed the transcriptional level expression of calcium handling proteins, including L-type calcium channel, SERCA2, and RYR2. CACNA1C gene encodes Cav1.2, the alpha C subunit of L-type voltage dependent calcium channel. ATP2A2 encodes SERCA2 that catalyzes the hydrolysis of ATP and mediates the translocation of calcium from the cytosol to SR. The function of SERCA2 is mediated by phospholamban encoded by PLN, which also showed no change between groups in the experiment. RYR2 encodes ryanodine receptor that controlling intracellular calcium level by releasing calcium through SR. Transcript level for SERCA2 is also not different between groups SCN5a encodes Nav1.5, a tetrodotoxin-resistant voltage-gated sodium channel subunit found primarily in cardiomyocytes. The sodium channel is responsible for the initial upstroke of action potential and can be inactivated by intracellular calcium levels. It should be noted that the expression of Cav1.2, SERCA2, PLN, RYR2, and SCN5A is not cardiac specific.

Gap junction transcript GJA1 (CNX 43), GJA 5 (CNX40) and GJA7 (CNX45) did not show significant change much between stress groups. Connexin 43 is the main cardiac connexin found in ventricular myocardium and also present in atrial myocytes and His-Purkinje system. Connexin 45 that forms voltage sensitive channels with high conductance is found in SA node, atrioventricular (AV) node and His bundles. On the contrary, connexin 40 forms voltage channels with high conductance and is generally found in fast conducting tissues like His-Purkinje system and atrial myocytes. In addition to cardiomyocytes, gap junction can also be formed between smooth muscles, endothelium, and fibroblasts.

We also analyzed smooth muscle and endothelial markers. TAGLN was used as a marker for smooth muscle/fibroblastic cell lineage and VWF and CDH5 were used for endothelial cell tracing. SM22 or TAGLN encodes transgelin, which is a transformation actin cross-linking/gelling protein found in fibroblasts and smooth muscles. VWF encodes von Willebrand factor, a blood glycoprotein produced by endothelium for blood coagulation. Transcript analysis showed no change in TAGLN and vWF expression.

5. Force production of bioengineered cardiovascular tissues

CVP constructs were subject to a series of short increasing length steps while simultaneously recording tension. The CVP constructs were able to demonstrate Frank Starling relation that increasing preload enhances the active force production (Figure III-11). A significant increase in both passive and active force magnitude was observed in constructs subject to cyclic stress (Figure III-12). Non-stressed H7-derived CVP construct had a passive stiffness of 0.22±0.04 kPa, while those subject to static stress and cyclic stress increased the passive stiffness to 0.47±0.05 kPa and 0.71±0.12 kPa, respectively ($p<0.005$ to no stress conditioning). No significant difference in passive stiffness was found between constructs subjected to static stress or cyclic stress conditionings. From the Frank-Starling curve, we can also define the contractility of these cardiovascular tissues. The contractility of these engineered tissues was also increased by stress conditionings. Static stress increased the contractility by 3-fold over non-stressed conditioning while cyclic stress further increased the contractility by 2-fold ($p<0.05$). In addition to the Frank Starling mechanism, these engineered tissues demonstrated characteristics similar to native myocardium. The constructs were responsive to extracellular calcium concentration and BDM (2,3-butanedione monixime), a non-selective reversible myosin ATPase inhibitor (Figure III-13). Increase in extracellular calcium concentration increase the force production and addition of BDM totally blocks the contractility. Addition of beta-adrenergic agonist, isoproterenol, demonstrates positive chronotropic and slightly inotropic effect, indicating the engineered tissue is functionally similar to stem cell-derived engineered cardiac tissues and native myocardium.

D. Discussion

Here we demonstrates that 1) hPSC-derived CVPs in a 3-D collagen environment are able to differentiated into human cardiovascular tissue composed of multiple cell types that organized structurally similar to real tissue, 2) the 3-D environment altered cell fate and maturation significantly compared to 2-D culture, 3) cyclic stress conditioning promote the cardiac maturation in CVP constructs, and 4) the pharmacological response of these engineered tissues is really similar to real myocardium. To our knowledge, this is the first study to examine the relative contributions to differentiation and maturation of a particular *in vitro* manipulation on cardiovascular cell types arising from a single multipotent progenitor.

Differentiation from pluripotent cells into cardiomyocytes has been established using both 2-D[156,182,203] and 3-D-based differentiation methods;[37,199] however, we examined the comparative efficiency of 2-D versus 3-D environments in a single differentiation protocol utilizing a committed cardiovascular precursor stage. From all cell lines, we found cardiac lineage was promoted by 3-D conditioning while smooth muscle differentiation was diminished in 3-D constructs. For ESC-derived cardiovascular constructs, cardiomyocytes and endothelial cells differentiated in 3-D tissue conditions had a significantly increased amount of the contractile protein cTnT or endothelial protein CD31 per cTnT+ or CD31+ cell, respectively, whereas the SMA protein content in SMA+ cells in 3-D scaffold was lower than that from cells plated in 2-D. However, in hiPSC-derived cardiovascular constructs, though the SMA protein content was decrease in 3-D scaffold, no effect of cTnT level increase was observed. It should be noted that CVPs from different cell lines had distinct lineage commitments, which may affect the behavior of cells under different conditionings.

We have showed that 3-D culture condition can promote cardiogenesis and suppress smooth muscle/fibroblastic genesis in both ESCs and iPSCs though there is discrepancy between cell lines for mechanical stress on cardiac maturation. Cyclic stress conditioning further promotes cardiac maturation

in molecular level only for H7 and IBJ lines, while no effect was observed in IMR90-derived CVPs. Previous studies in calcium transients showed increased upstroke velocity and peak height, suggesting the calcium handling mechanism is more mature in cyclic stress group.[92] Further analysis in force production revealed that the engineered cardiovascular tissue demonstrated several native myocardium-like characteristics, such as Frank-Starling mechanism, responses to calcium concentration, BDM, and β-adrenergic agent. Moreover, stress conditioning increased the passive stiffness and cyclic stress conditioning further increased the contractility of engineered cardiovascular tissues. Taken together, these changes in contractile gene expression, protein levels, calcium flux, and force production all indicated that cyclic stress conditioning increased maturation of the cardiac subset of this engineered human cardiovascular tissue.

Previous study using cultured neonatal rat ventricular myocytes shows under high cyclic stress induced cardiac hypertrophy (20 % strain), the mRNA and protein levels of SERCA2 and RYR2 would be down regulated and ANF mRNA would be promoted simultaneously but the phospholamban mRNA level was unaffected.[208] In our system, we did not observe change in most of these genes between the stress conditioning groups but were able to observe functional enhancement in cyclic stress groups. Since many of those genes are not cardiac specific, it is possible that the change was occurs in cardiomyocytes but got diluted by non-cardiomyocyte portion. Histological examination of CVP constructs demonstrates the construct has myocardium like architecture, with interstitial fibroblastic cells and lumen-forming endothelial cells. Ultrastructure examination by transmission electron microscope shows alignment of both cells and contractile protein of cardiomyocytes. However, study of collagen fibers using two photon microscopy shows the collagen fibers are not as aligned as those from cardiomyocyte only constructs but the signal intensity is higher in cyclic stress group. This suggests that non-myocyte portion might play an important role in promoting the cardiac maturation either through paracrine effect[209] or matrix component remodeling. Previous studies showed that isolation of hESC-cardiomyocytes in early

stage without further interaction of non-myocyte failed to develop electrophysiological maturation and the effect can be rescued by addition of non-myocyte portion back to the culture.[210] The non-myocyte portion from cardiac direct differentiation generally contains cells present in embryonic heart and many of the cell types, such as fibroblasts, smooth muscles, and endotheliums, have been showed to be responsive to mechanical stimulation in various degree. Future prospection of this project may include further manipulating different non-myocyte lineage by incorporating additional environmental cue.

With their capability to differentiate into cardiac related cell lines, stem cell-derived CVPs can be good indicators to show how different environmental cues affect cell specification. A study using CVPs on decellularized heart showed formation of vessel structure and endocardial surface,[39] suggesting that the basic architecture in addition to mechanical stimulation can also facilitate the lineage specification of progenitors. In addition, they have been showed to be able to structurally and functionally integrate into human fetal heart tissues in an *in vivo* model.[40] Therefore, it would also be interested to know the *in vivo* performance of the CVP constructs. In sum, this chapter proves the idea that it is possible to generate a myocardium like tissue using a single line of PSCs. Those engineered tissues demonstrate similar physiological effect and cellular response to mechanical stress.

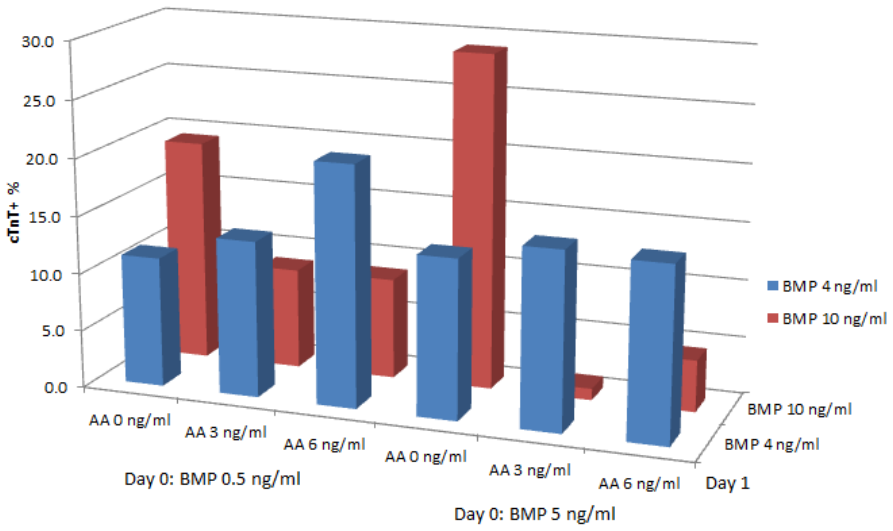

Day 1	AA 0 ng/ml	AA 3 ng/ml	AA 6 ng/ml	AA 0 ng/ml	AA 3 ng/ml	AA 6 ng/ml
BMP 4 ng/ml	11.3	13.6	20.9	13.8	15.4	15.1
BMP 10 ng/ml	19.3	8.7	8.8	29.0	1.0	4.5

Figure III-1 Optimization of BMP and activin A (AA) concentration during EB-based direct differentiation of IMR90.

The efficiency was assessed by FACS analysis of cTnT+ cell population 14 days after onset of differentiation. High BMP concentration at day 0 and day1 with low activin A concentration at day 1 seems to work best to induce cardiac differentiation in IMR90 line. Together with Wnt, Nodal, and BMP inhibitors at day 3, we were able to acquire cardiomyocytes at a purity of at least 60%.

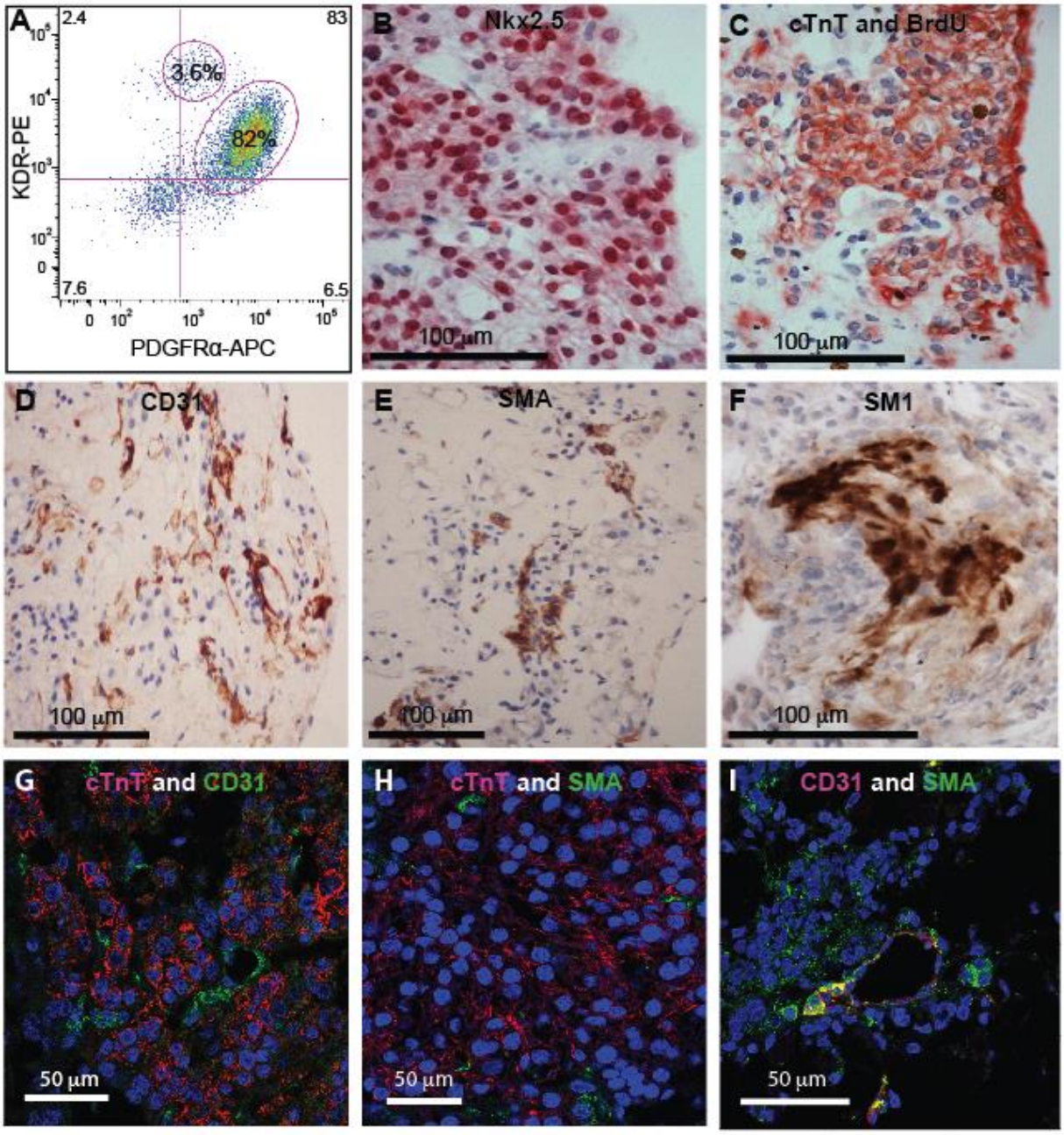

Figure III-2 Identification of different cell lineage in H7-derived CVP constructs.

A, Flow analysis showed two distinct populations of progenitors: hemangioblast, the progenitor that forms the blood islands during development, and CVP population. B, CVPs in collagen gel were able to express the cardiac transcription factor, Nkx2.5 (red). C, These progenitor cells matured over two weeks into contractile cardiac tissues. The contractile protein cardiac troponin T (cTnT) denotes the cardiac lineage in the constructs. The endothelial and smooth muscle lineages are highlighted by (D) the

endothelial marker, CD31 (red), and (E) the smooth muscle actin (SMA, brown), respectively. cTnT+ cardiomyocytes continued to proliferate as noted by 24 hour BrdU incorporation (brown). F, The construct also expressed late smooth muscle marker, smooth muscle myosin heavy chain (SM1, brown). G, Co-staining of cTnT and CD31 demonstrates the lumen structure formed by endothelial cells in the constructs. H, cTnT/SMA staining of progenitor construct demonstrates interstitial localization of smooth muscle lineage. I, Endothelial lumen can also be found surrounded by smooth muscle lineage.

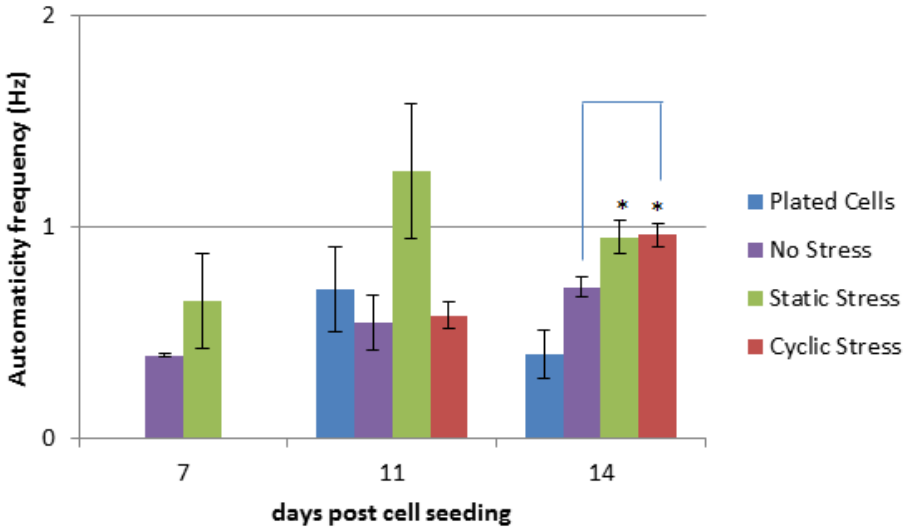

Figure III-3 Stress conditioning promotes contraction rate in IMR90-derived CVP constructs.

Two weeks after culturing under different conditionings, constructs underwent static stress and cyclic stress conditioning showed higher contraction rate compared to plated cells (* $p<0.01$). Constructs conditioned by cyclic stress also contracted faster than those from no stress conditioning ($p<0.05$).

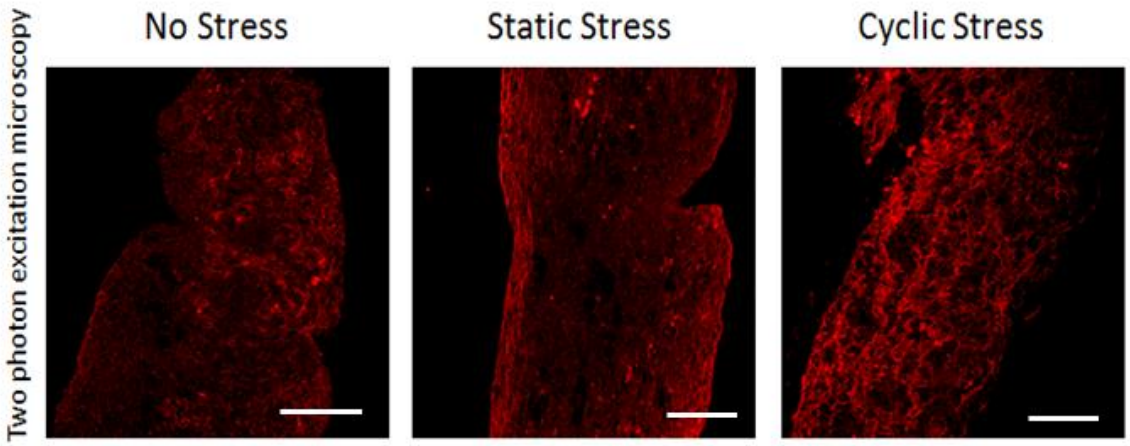

Figure III-4 Collagen organization from CVP constructs under different stress conditioning.

The collagens inside the CVP constructs were not well aligned like those in cardiomyocyte constructs.

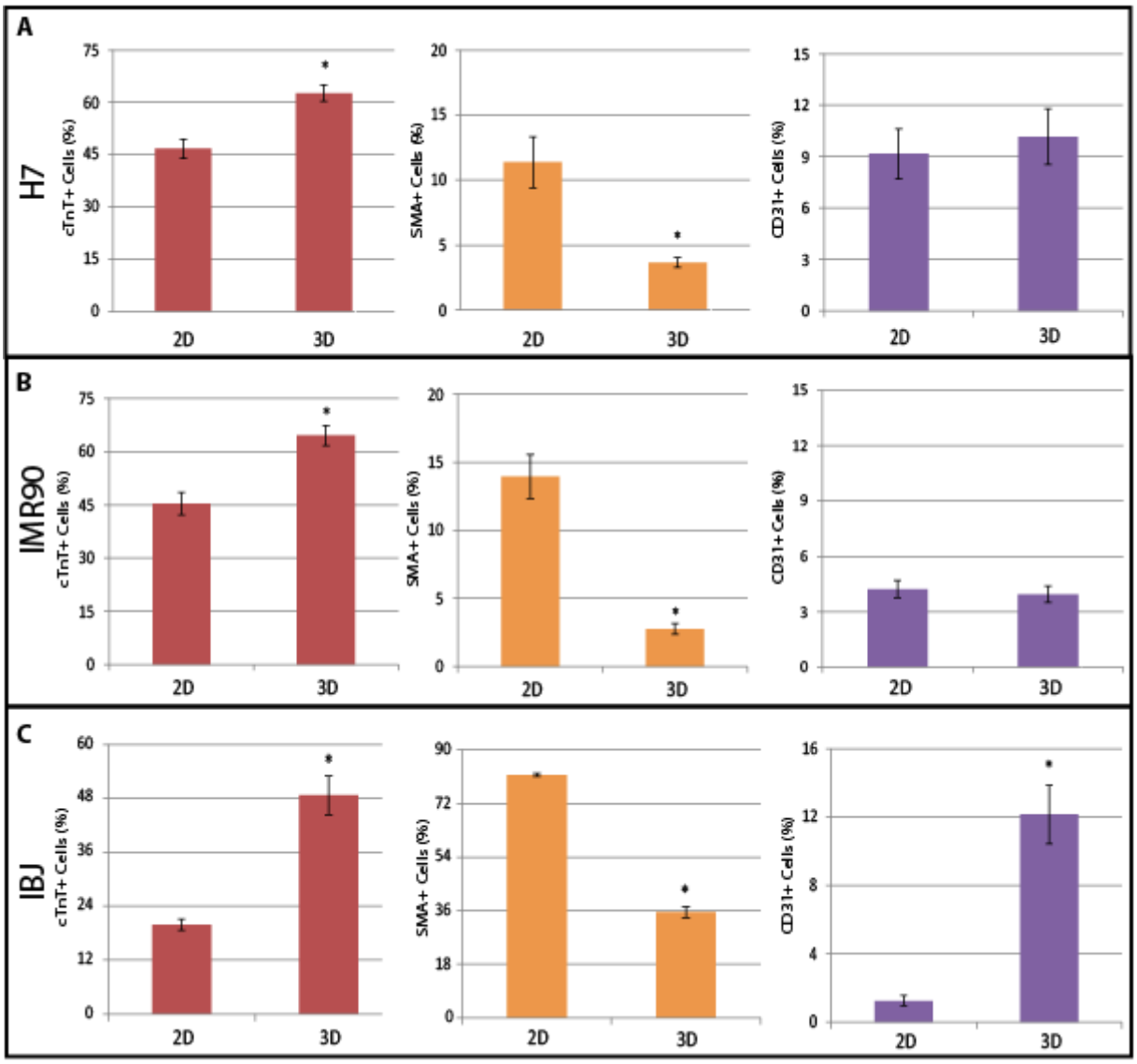

Figure III-5 Quantification of progenitor fate between 2-D and 3-D cultures by flow cytometry.

A, Cardiomyocytes differentiated at 34% higher purity in 3-D ESC-derived CVP constructs versus 2-D plated culture conditions (3-D vs 2-D, 62.6% vs 46.6%, respectively, * $p<0.05$), while smooth muscle cells differentiated at 3-fold lower purity in 3-D constructs (3-D vs 2-D, 3.7% vs 11.4%, respectively, * $p<0.0005$). The differentiation into CD31 positive endothelial cells was not affected by the culturing conditions. B, Similar effect was observed in IMR90-derived CVP constructs, where 3-D culture conditioning induced cardiac differentiation (3-D vs 2-D, 64.5% vs 45.3%, respectively, * $p<0.05$), reduced smooth muscle lineage (3-D vs 2-D, 14.0% vs 2.7%, respectively, * $p<0.005$), and had no effect

on endothelial differentiation. C, Another hiPSC-derived cell line, IBJ line, also showed that the cardiac differentiation was promoted by 3-D conditioning (3-D vs 2-D, 48.7% vs 19.8 %, respectively, * $p<0.05$) and the smooth muscle lineage was promoted by 2-D conditioning (3-D vs 2-D, 35.6 % vs 81.6%, respectively, * $p<0.05$). Interestingly, unlike other two cell lines, IBJ-derived endothelial cells were also promoted under 3-D conditioning (3-D vs 2-D, 1.3% vs 12.2%, respectively, * $p<0.005$).

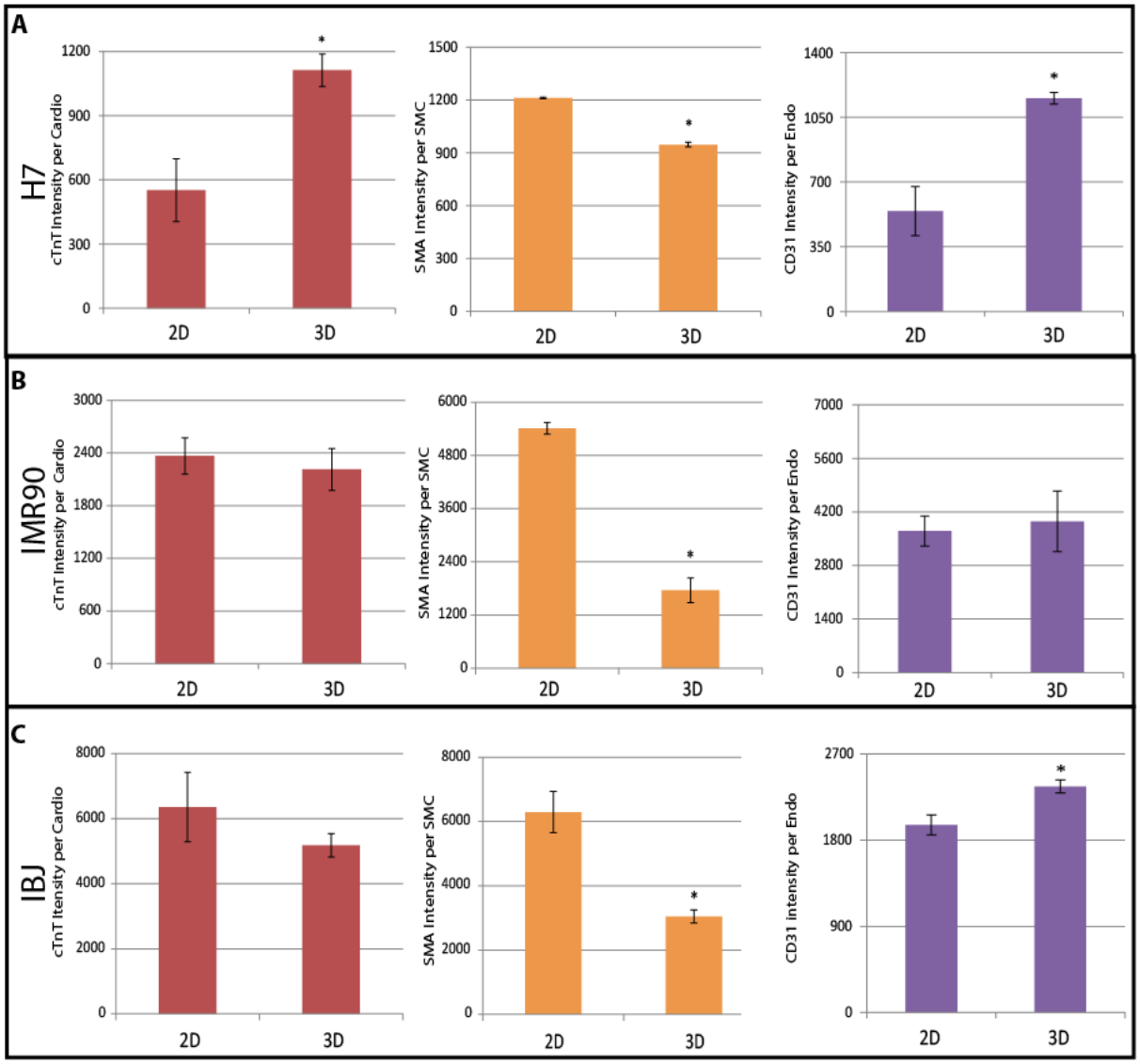

Figure III-6 Quantification of progenitor maturation between 2-D and 3-D cultures by flow cytometry.

A, H7-derived CVP constructs had significantly higher average cTnT intensity per cTnT+ event than plated cells. Conversely, plated smooth muscle cells had a 1.7-fold increased SMA intensity over SMA+ cells derived in 3-D engineered tissue. CD31 was also down-regulated 2-fold in plated CD31+ cells versus those grown in 3-D tissue. B, IMR90-derived CVP constructs did not show similar enhancement in cTnT and CD31 content but demonstrated a reduction in SMA intensity. C, IBJ-derived cardiomyocytes did not differ in cTnT content between 2-D and 3-D culture conditionings. On the other hands, similar to H7- and

IMR90-derived CVPs, the SMA intensity in per smooth muscle cell level was reduced. CD31 was also increased in 3-D culture condition over 2-D condition. * $p < 0.05$

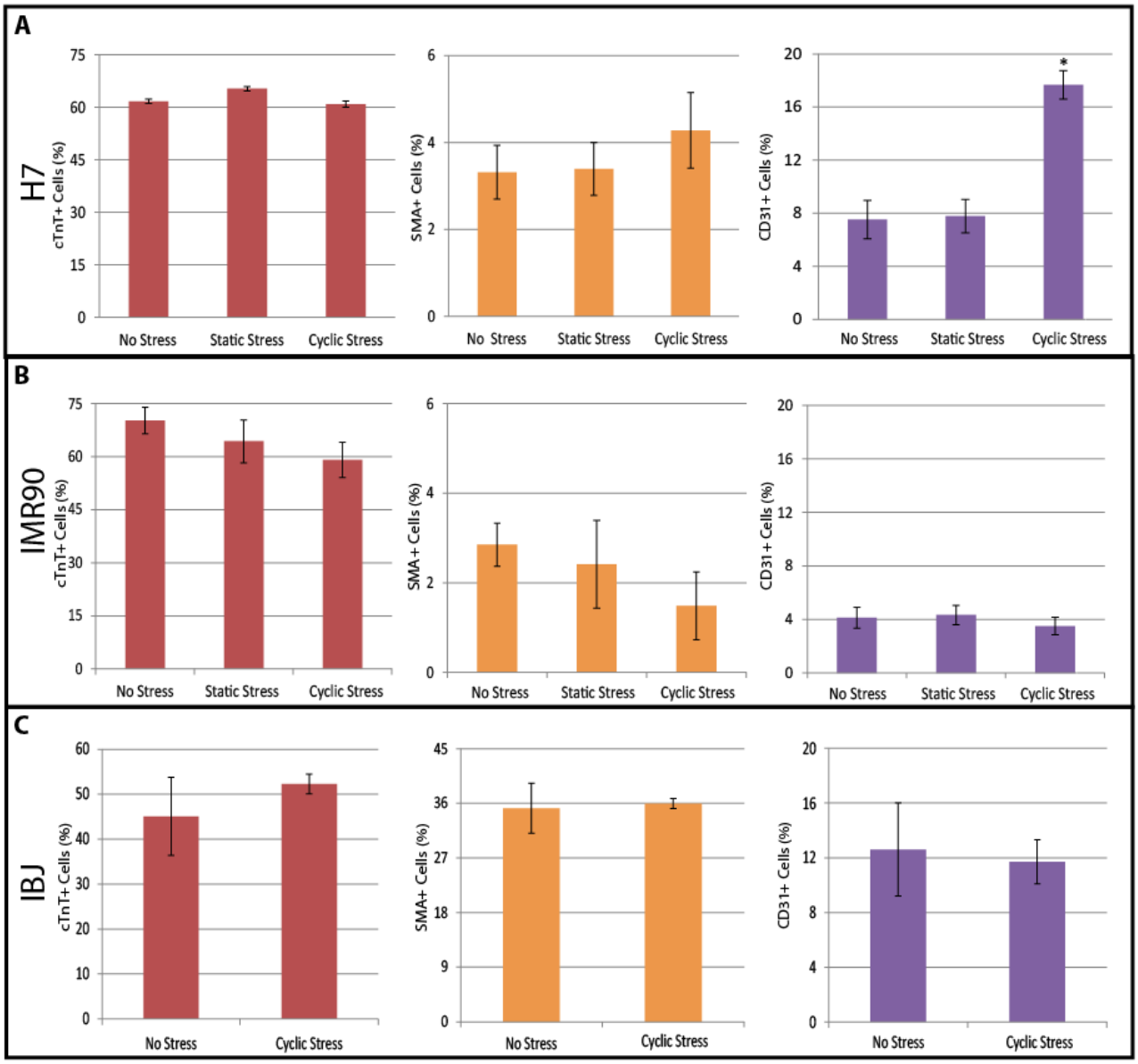

Figure III-7 Quantification of progenitor fate from engineered constructs under different stress regimes.

A, H7-derived CVP differentiation to cardiomyocytes or smooth muscle cells showed no different under three stress conditionings. On the contrary, cyclic stress increased the endothelial cell population over 2-fold (*$p<0.05$). The cardiomyocyte, smooth muscle, and endothelial cell populations from IMR90-derived (B) and IBJ-derived (C) CVPs did not change with different conditionings.

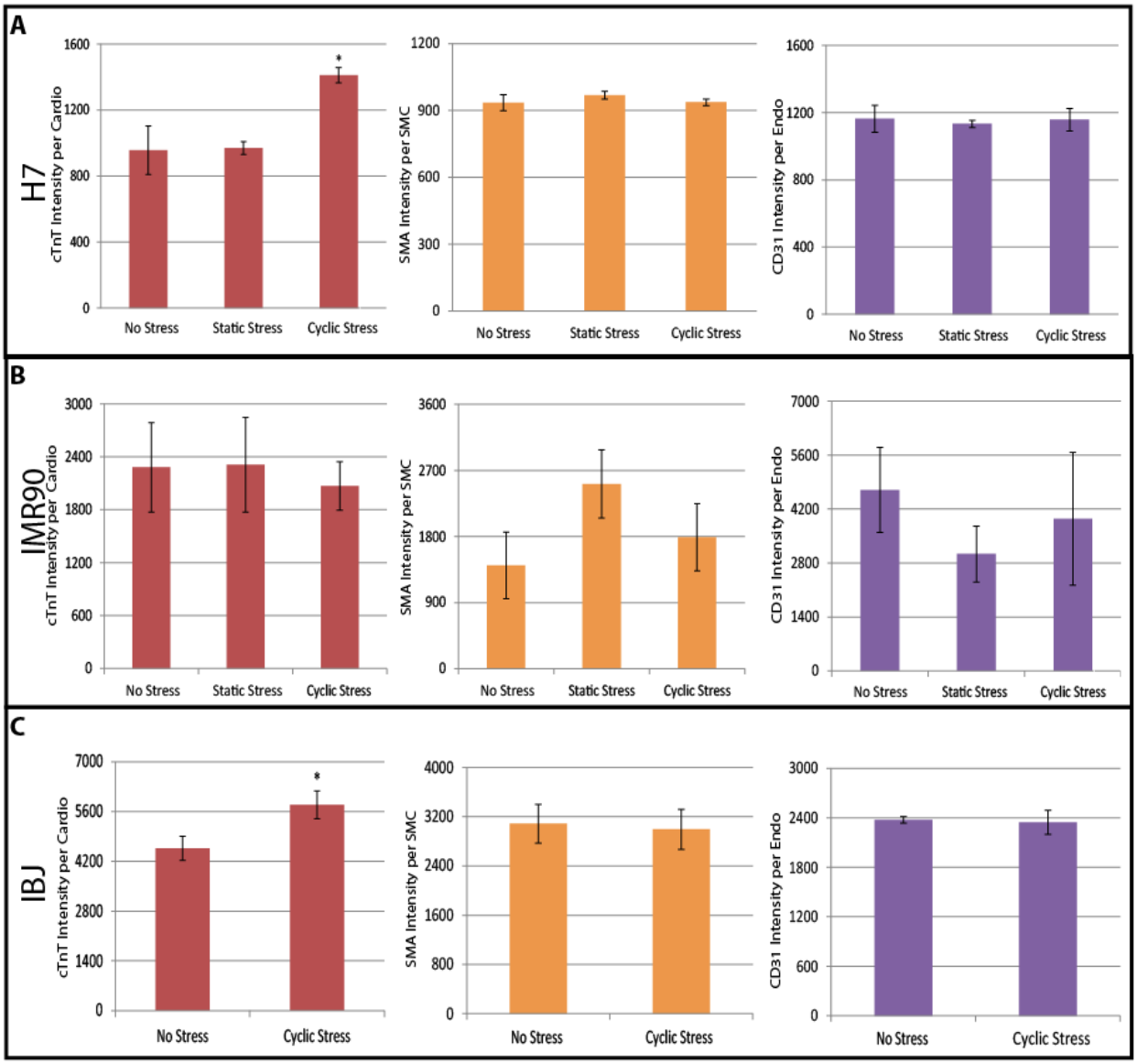

Figure III-8 Quantification of progenitor maturation between three stress conditionings by flow cytometry.

A, H7-derived CVP constructs had significantly higher average cTnT intensity per cTnT+ event under cyclic stress conditioning. However, SMA intensity and CD31 intensity were not affected by different stress conditionings. B, IMR90-derived CVPs did not show any enhancement in cTnT, SMA, or CD31 content under different stress regimes. C, IBJ-derived CVPs showed a similar promoting effect of cTnT intensity under cyclic stress conditioning (*p<0.05).

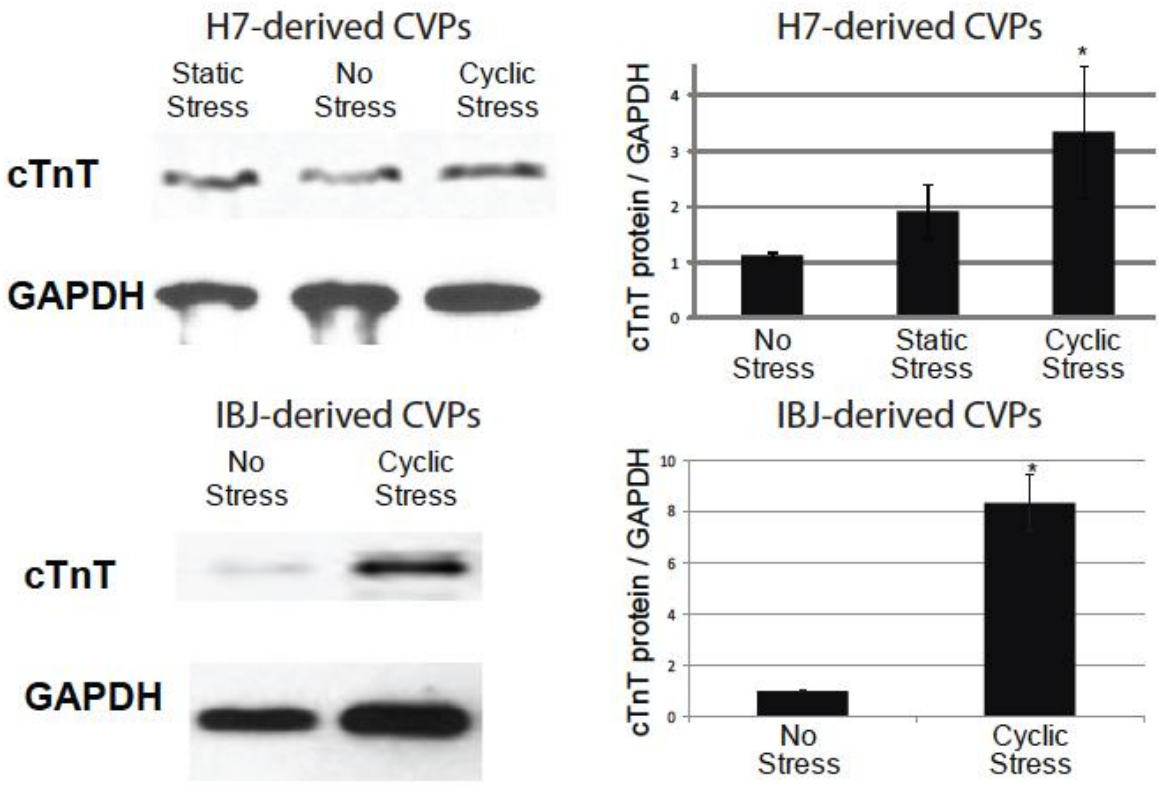

Figure III-9 Cardiac troponin T expression by Western blot.

A and C, Representative Western blot from H7-derived CVP constructs and IBJ-derived CVP constructs. B and D, Quantification of Western blot band intensities of no stress, static stress, and cyclic stress conditioned constructs. cTnT samples were normalized to GAPDH levels and given as fold over no stress constructs probed in the same blot. Error bars represent standard error of the mean; * = $p < 0.05$ with respect to no stress conditioning.

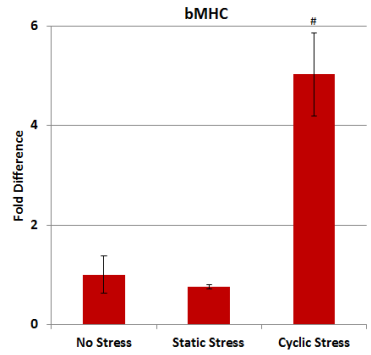

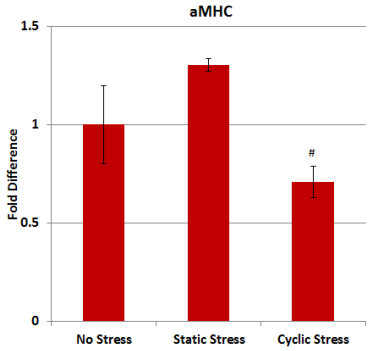

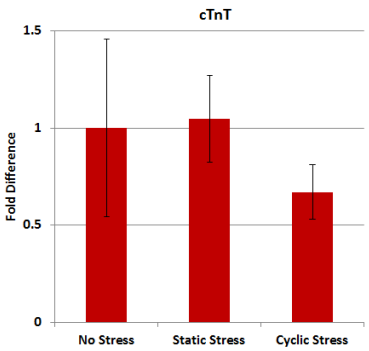

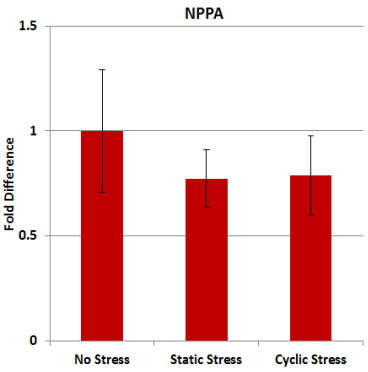

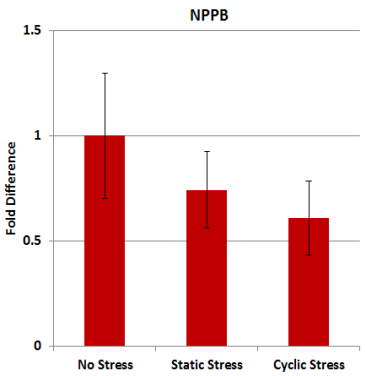

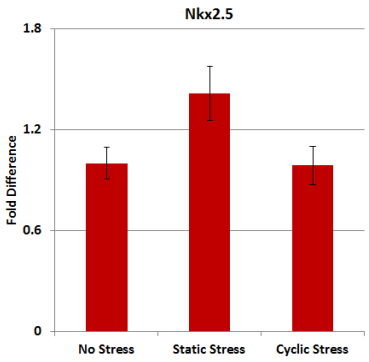

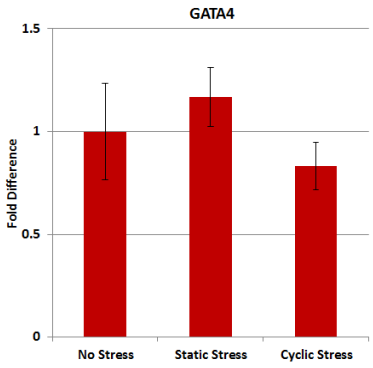

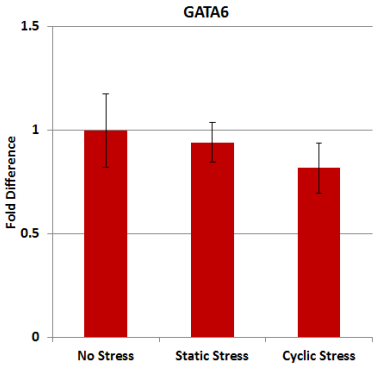

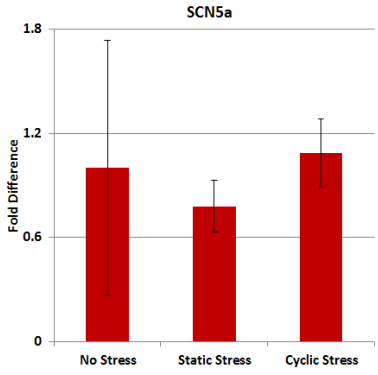

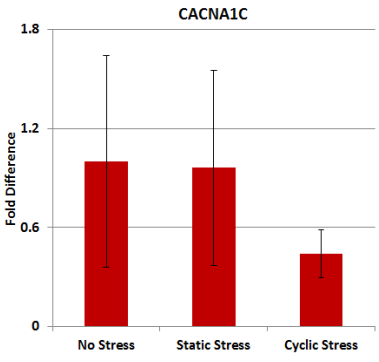

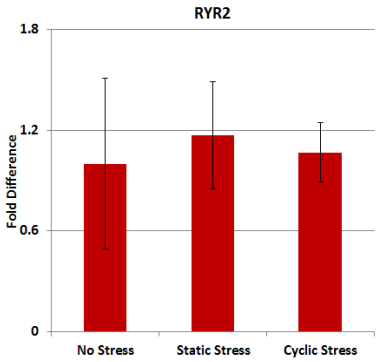

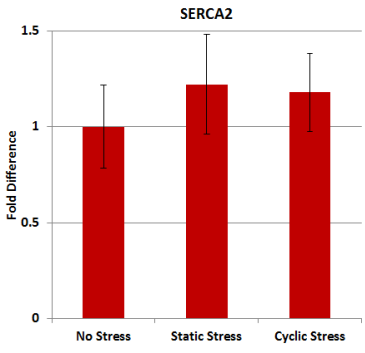

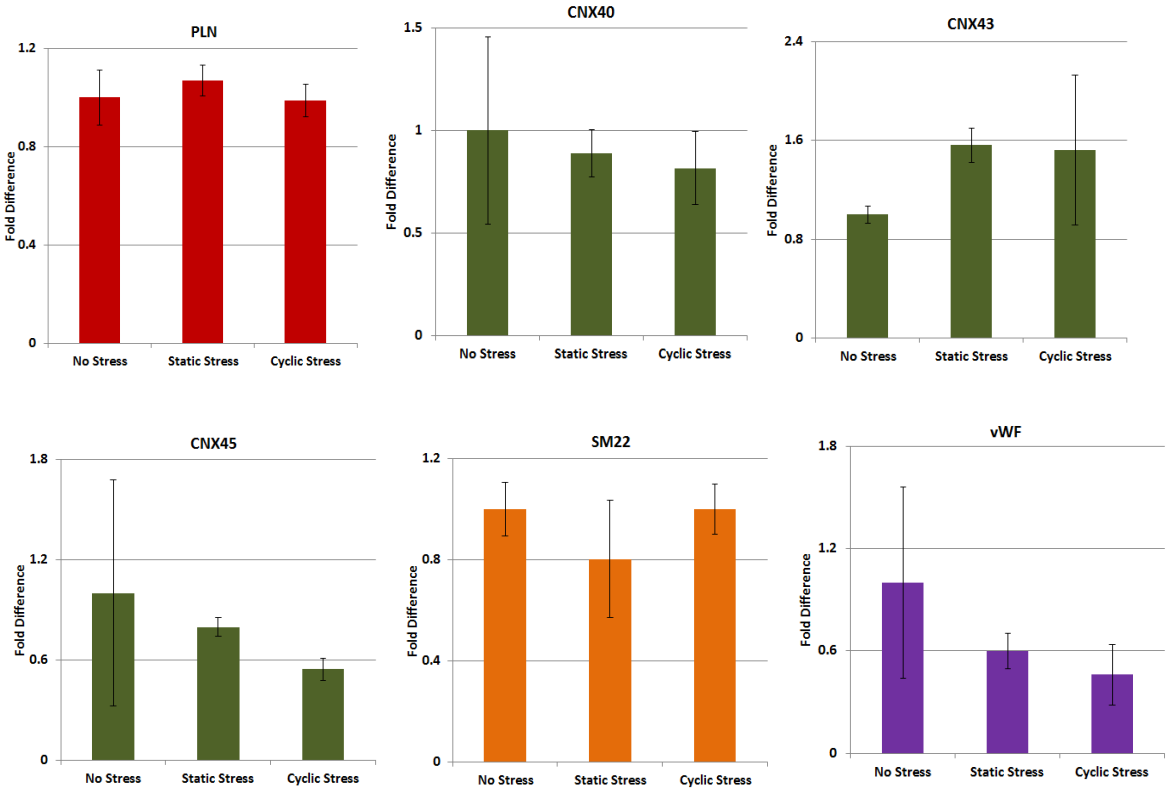

Figure III-10 Transcriptional level response of H7-derived progenitor in 3-D collagen constructs with different stress conditions.

Only βMHC transcript showed enhancement by cyclic stress conditioning ($p < 0.05$) compared to no stress and static stress groups. αMHC transcript from cyclic stress-conditioned constructs was slightly diminished ($p<0.05$ for cyclic stress vs static stress, but $p>0.05$ for cyclic stress vs no stress). All other genes showed no difference in transcript expression level among all three groups.

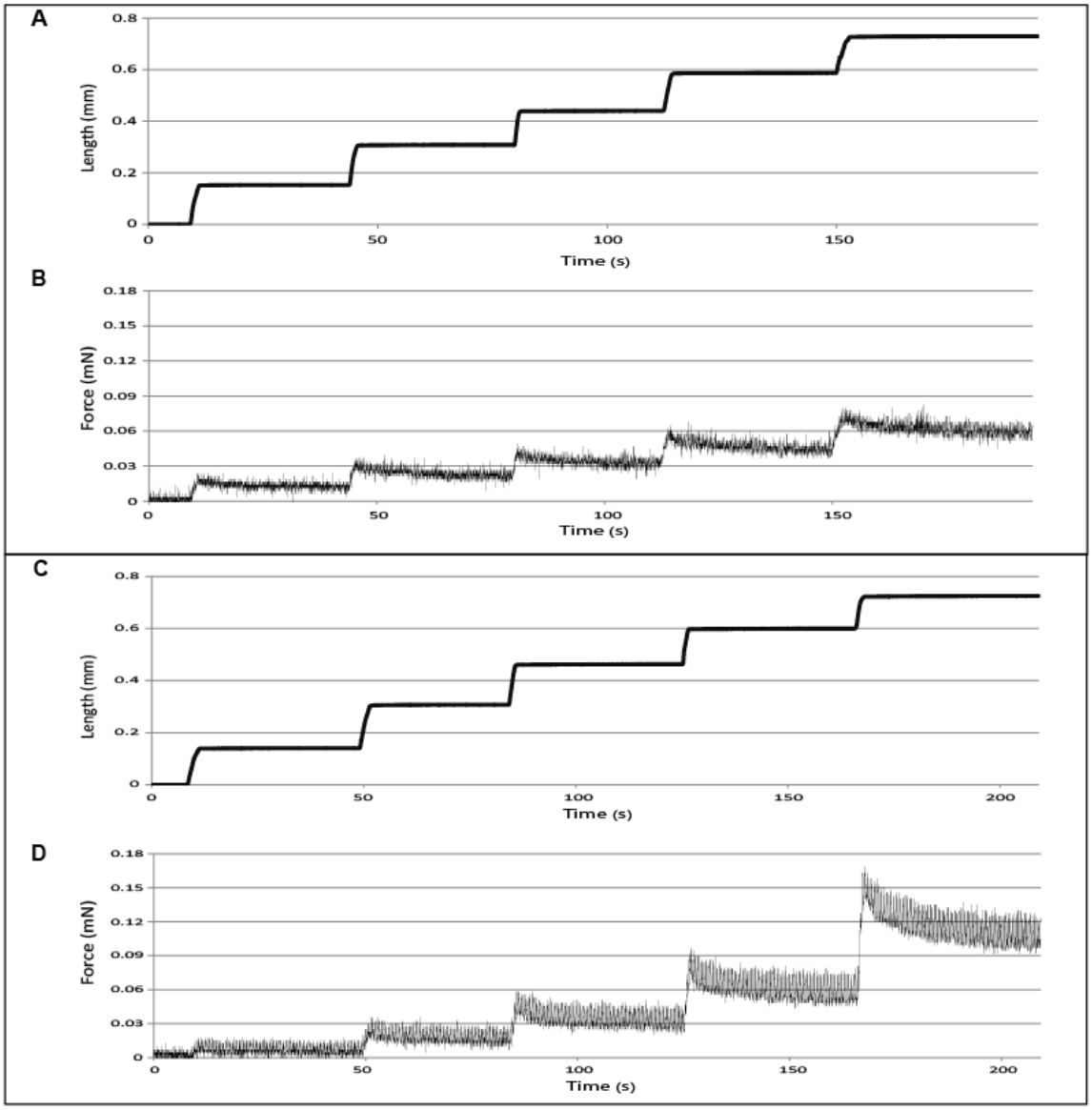

Figure III-11 Frank-Starling effect of engineered cardiovascular constructs.

Increased preload enhance the active force production (showed as the spike in the force trace). A, A non-stressed construct was subject to stepwiase stretch to 125% of its slack length and B, showed the corresponding force trace. C, A cyclic stress-conditioned construct underwent stepwisely incremental stretch to 125% of the slack length and the corresponding force trace was shown as D. Compared to no stress conditioning, a higher force magnitude was observed in cyclic stressed construct at the same stretch step.

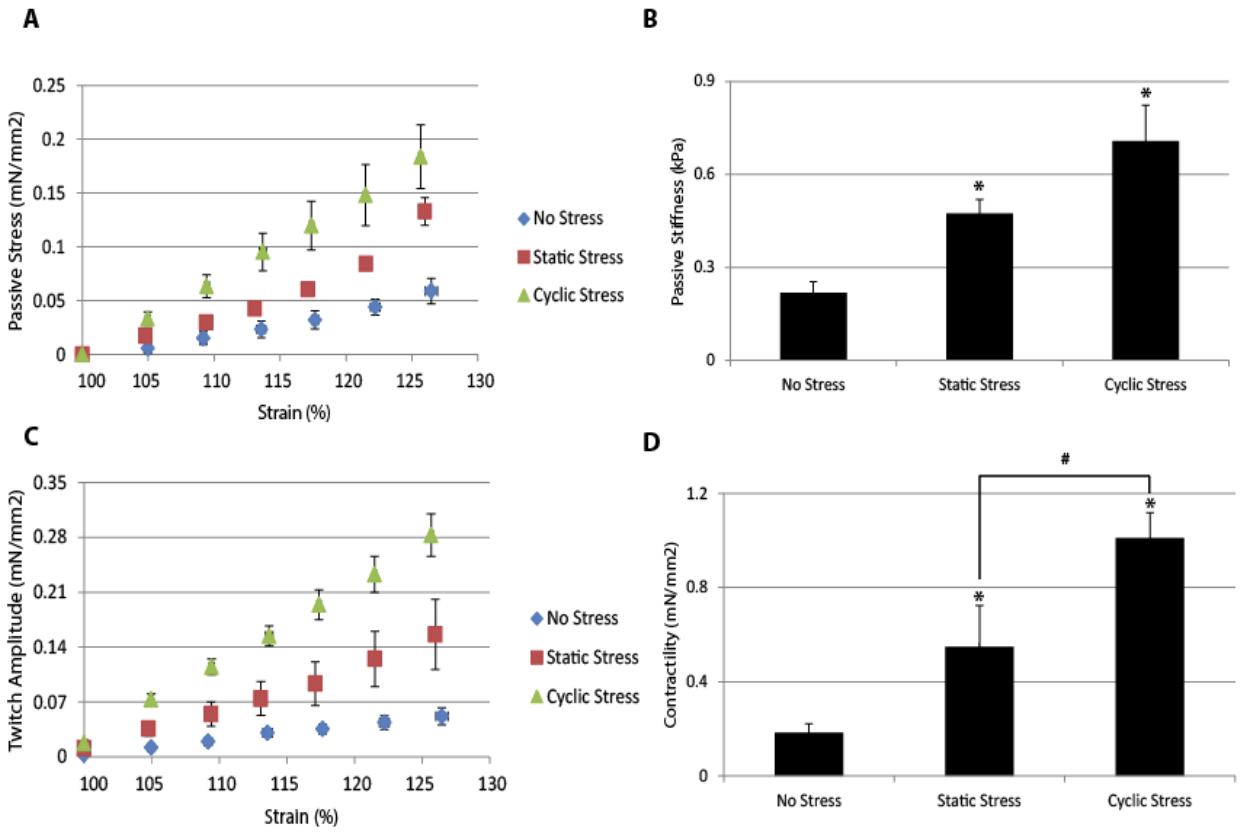

Figure III-12 Cyclic stress conditioning enhanced the passive stiffness and active force production of engineered cardiovascular tissues.

A, Passive stress of construct increased as constructs were stretched. The slope of passive stress vs strain was measured as passive stiffness of the constructs as showed in B. B, Passive stiffness of engineered cardiovascular tissue was increased by both static and cyclic stress conditionings (* $p<0.005$ to no stress conditioning). C, Active force was also increased with increasing strain of the constructs. The slope of the active twitch amplitude and strain was defined as contractility as showed in D. D, Stress conditioning enhanced the contractility of engineered cardiovascular tissues (*$p < 0.05$). Cyclic stress further increase the contractility by 2-fold.

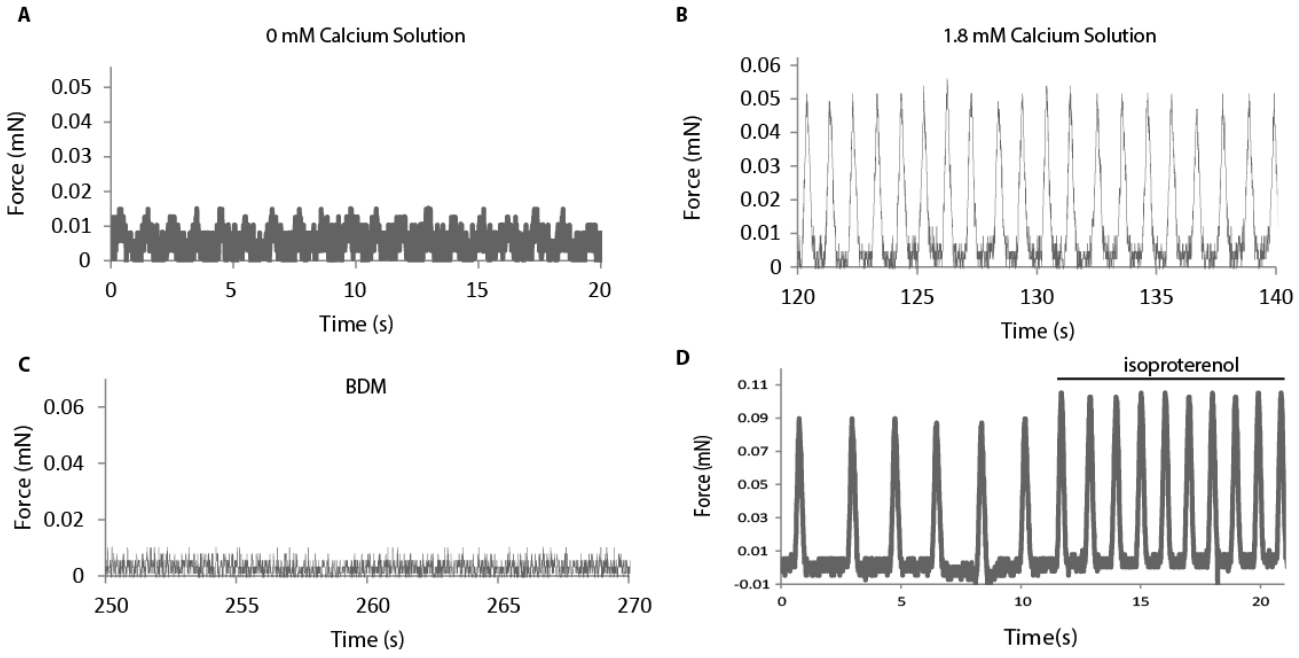

Figure III-13 Force production of engineered cardiovascular tissues.

A, The force production of engineered cardiac tissues was low under calcium free condition. B, High calcium solution (1.8 mM in Tyrode solution) increased the force production. C, The force production was abolished by the myosin ATPase inhibitor, BDM (30 mM). D, Addition of 10 μM isoproterenol increased the contraction rate and force amplitude.

IV. Conclusions and Implications for Future Direction

CVDs have been listed as the leading causes of mortality both in the US and worldwide for years. Billions of cardiomyocytes can be lost during the occurrence of CVDs and the function of heart is irreversibly impaired due to low regeneration capacity of mature cardiomyocytes. *In vitro* culture of large amount of human cardiomyocytes to compensate the cell loss has been made possible with the advancement of stem cell technology. . The rich source of cardiomyocytes provided by hPSCs can be used to generate human myocardium in cardiac tissue engineering, which opens our door to decipher the complexity of cardiac mechanics and physiology. However, stem cell-derived cardiomyocytes generally demonstrate immature or fetal phenotype, which limits their ability to treat adult heart diseases. Since environmental cue is an important factor in mediating the behavior of stem cells and young cardiomyocytes, here we sought to advance the functionality of stem cell-derived engineered cardiac tissues by using mechanical and electrical stimulations.

In Chapter II, we generated human cardiac tissues from hiPSC-derived cardiomyocytes and subjected them to no stress, static stress, or static stress with electrical pacing conditionings for two weeks. We showed that static stress can promote the maturation of engineered cardiac tissues in both structural and functional level. Structurally, static stress was able to promote construct remodeling as shown by cell/collagen alignment, cell volume fraction, and passive stiffness. It also promoted cardiac hypertrophy in cellular level as shown by the increasing cardiomyocyte size. Functionally, stress-conditioned engineered cardiac tissues showed better active force generation and contractility of engineered cardiac tissues. Addition of electrical pacing also further promoted passive stiffness, active force generation, and contractility. The functional improvement was also reflected in calcium handling level. Stress conditioned constructs improved the negative force frequency relationship of stem cell-derived cardiomyocytes, while the addition of electrical pacing made the relationship more newborn-like. The improving trend in force frequency relationship from no stress, static stress, and static stress

with electrical pacing conditionings was also reflected in the expression of SR-related proteins. The expression of SERCA2 was significantly promoted by stress conditionings while the expression of RYR2 was enhanced in electrical pacing. Both proteins may contribute to increase cytosolic calcium concentration by increasing calcium transferring out of SR or increasing SR calcium load.

In Chapter III, we used tri-potential hPSC-derived CVPs to generate engineered human cardiovascular tissues from a single cell source. We showed that CVPs differentiated into cardiomyocytes, smooth muscle cells, and endothelial cells in the 3-D collagen constructs. Similar to our previous study using primary stromal and endothelial cells with stem cell-derive cardiomyocytes,[156] CVPs within the constructs were able to form lumenal structures. 3-D conditionings promoted the cardiac differentiation and repressed the smooth muscle differentiation and maturation. Cardiac maturation was promoted by cyclic stress conditionings of these engineered cardiovascular tissues with increasing in cardiac markers, such as cTnT protein expression and β-MHC transcript, and improving in the contractile functionality. Unlike hiPSC-derived engineered cardiac tissues in Chapter II, stress-conditioned engineered cardiac tissue did not show improvement in collagen alignment. However, the cyclic stress group showed a 3-fold increase in passive stiffness to no stress conditioning, indicating a potential contribution from cardiac maturation in passive mechanical properties. Overall, both stem cell-derived cardiac constructs and stem cell-derived CVP constructs exhibited Frank-Starling curve-type force-length relationships and a positive chronotropic/inotropic response to β-adrenergic agent, isoproterenol. For stem cell-derived cardiac constructs, stress conditioning increased the contractility and stiffness, promoted cell alignment and cardiac hypertrophy, as well as improved the calcium handling dynamics. Addition of electrical pacing further enhanced the force production and passive stiffness, suggesting maturation of excitation-contraction coupling. For stem cell-derived CVPs, 3-D collagen scaffolds modulated their lineage commitment and maturation. While differentiation toward cardiomyocytes was more favorable in 3-D condition, smooth muscle cell population and maturation was promoted under 2-D culture. Cyclic stress

also further promoted the cardiac maturation of CVP-derived engineered tissues in both molecular and functional level. These studies here demonstrate the necessity of environmental stimulations in improving the functionality of stem cell-derived human engineered cardiac tissues. They can be used as a basis for further bioreactor design to enhance and maintain the functionality of stem cell-derived engineered cardiac tissues.

Engineering complex stem cell-derived cardiac tissues for *in vitro* and *in vivo* application provides a promising approach to advance not only the treatment of CVDs but also other practical approaches, like disease modeling and drug testing. Human cardiomyocytes can be generated directly from patient-derived stem cell lines and used to customize the clinical treatment based on personal needs. Moreover, engineered scaffolds provide a platform for cells to survive under the harsh infarct area, and can be modified to incorporate other informative molecules like pro-angiogenic factors to promote the repair of myocardium. Many *in vivo* xenotransplantations of human engineered cardiac graft have been performed in rodent or small animal models. However, so far only limited effects have been observed due to poor coupling between host and engineered tissue interfaces.[100,156] To create engineered cardiac tissues for clinical scale, many parameters such as size, cellularity, matrix composition, and functionality, need to be further optimized and applying external stimulation to engineered cardiac tissues is the first step.

In vitro applications of stem cell-derived engineered cardiac tissues include preclinical cardiac toxicology testing and disease modeling. Various drugs present proarrhythmic side effects such as Torsades de pointes tachycardia and ventricular tachycardia. Currently the toxicology testing panels recommended by FDA and EMA generally include the measurement of hERG channel activity in HEK293 (human embryonic kidney 293 cells), and action potential duration in canine Purkinje fibers.[188] However, the performance of these non-cardiac or non-human cells under 2-D culture conditions is insufficient to

predict the clinical effect. However, studies using 2-D human ESC-derived cardiomyocyte culture display discrepancy to those in hERG channel assay, potentially due to cellular immaturity.[211–213] 3-D engineered human cardiac tissues from stem cells exhibits functional features similar to human fetal myocardium and are able to recapitulate results in cardiac toxicity tests.[188] For disease modeling, iPSCs enable the generation of patient specific cardiomyocytes. 3-D engineered patient specific cardiac tissues may provide novel insights in pathophysiology or drug testing compared to traditional 2-D cardiomyocyte culture.

To justify its *in vitro* and *in vivo* usage, a clear definition of how the engineered cardiac tissue should perform is also required. Therefore, by promoting engineered cardiac tissues maturation to a more advanced stage, we will be able to further investigate the optimal benchmarks for *in vitro* and *in vivo* applications of engineered cardiac tissue. Based on our promising results, there are some advanced questions we can ask. Does synchronized mechanical stress and electrical pacing have a better maturation effect on engineered cardiac tissues? Does the combination of an incremental electrical pacing or an incremental mechanical stress regime with our current settings on engineered cardiac tissues further improve the functional maturation? Can we further promote the maturation by adding other biochemical cues along with these external stimulations? Using different stimulations, can we generate engineered cardiac tissues similar to different stages (fetal, neonatal, and adult) of native myocardium? Answers to these questions not only extend our understanding of cardiac biology but also practically widen the ranges of applications of cardiac tissue engineering.

V. Reference

(1) Braunwrld, E., Zipes, D. P., and Libby, P. (2001) Heart Disease: a textbook of cardiovascular medicine 6th ed., pp 1–17. W. B. Saunders company.

(2) Mathers, C. D., and Loncar, D. (2006) Projections of global mortality and burden of disease from 2002 to 2030. *PLoS Med. 3*, e442.

(3) Heidenreich, P. A., Trogdon, J. G., Khavjou, O. A., Butler, J., Dracup, K., Ezekowitz, M. D., Finkelstein, E. A., Hong, Y., Johnston, S. C., Khera, A., Lloyd-Jones, D. M., Nelson, S. A., Nichol, G., Orenstein, D., Wilson, P. W. F., and Woo, Y. J. (2011) Forecasting the future of cardiovascular disease in the United States: a policy statement from the American Heart Association. *Circulation 123*, 933–44.

(4) WHO. The top 10 causes of death. World Health Organization.

(5) Frieden, T. R. (2012) Use of Selected Clinical Preventive Services Among Adults--United States, 2007–2010. *MMWR. Morb. Mortal. Wkly. Rep. 61 Suppl*, 1–2.

(6) Laflamme, M. A., and Murry, C. E. (2005) Regenerating the heart. *Nat. Biotechnol. 23*, 845–56.

(7) Stehlik, J., Edwards, L. B., Kucheryavaya, A. Y., Benden, C., Christie, J. D., Dobbels, F., Kirk, R., Rahmel, A. O., and Hertz, M. I. (2011) The Registry of the International Society for Heart and Lung Transplantation: Twenty-eighth Adult Heart Transplant Report--2011. *J. Heart Lung Transplant. 30*, 1078–94.

(8) Martin-Rendon, E., Brunskill, S. J., Hyde, C. J., Stanworth, S. J., Mathur, A., and Watt, S. M. (2008) Autologous bone marrow stem cells to treat acute myocardial infarction: a systematic review. *Eur. Heart J. 29*, 1807–18.

(9) Wöhrle, J., Merkle, N., Mailänder, V., Nusser, T., Schauwecker, P., von Scheidt, F., Schwarz, K., Bommer, M., Wiesneth, M., Schrezenmeier, H., and Hombach, V. (2010) Results of intracoronary stem cell therapy after acute myocardial infarction. *Am. J. Cardiol. 105*, 804–12.

(10) Hofmann, M., Wollert, K. C., Meyer, G. P., Menke, A., Arseniev, L., Hertenstein, B., Ganser, A., Knapp, W. H., and Drexler, H. (2005) Monitoring of bone marrow cell homing into the infarcted human myocardium. *Circulation 111*, 2198–202.

(11) Aicher, A., Brenner, W., Zuhayra, M., Badorff, C., Massoudi, S., Assmus, B., Eckey, T., Henze, E., Zeiher, A. M., and Dimmeler, S. (2003) Assessment of the tissue distribution of transplanted human endothelial progenitor cells by radioactive labeling. *Circulation 107*, 2134–9.

(12) Adler, C. P., and Costabel, U. (1975) Cell number in human heart in atrophy, hypertrophy, and under the influence of cytostatics. *Recent Adv. Stud. Cardiac Struct. Metab. 6*, 343–55.

(13) Laflamme, M. A., and Murry, C. E. (2011) Heart regeneration. *Nature 473*, 326–335.

(14) Fujimoto, K. L., Clause, K. C., Liu, L. J., Tinney, J. P., Verma, S., Wagner, W. R., Keller, B. B., and Tobita, K. (2011) Engineered fetal cardiac graft preserves its cardiomyocyte proliferation within postinfarcted myocardium and sustains cardiac function. *Tissue Eng. Part A 17*, 585–96.

(15) Halbach, M., Baumgartner, S., Sahito, R. G. A., Krausgrill, B., Maass, M., Peinkofer, G., Ladage, D., Hescheler, J., and Müller-Ehmsen, J. (2014) Cell persistence and electrical integration of transplanted fetal cardiomyocytes from different developmental stages. *Int. J. Cardiol. 171*, e122–4.

(16) Scorsin, M., Hagège, A., Vilquin, J. T., Fiszman, M., Marotte, F., Samuel, J. L., Rappaport, L., Schwartz, K., and Menasché, P. (2000) Comparison of the effects of fetal cardiomyocyte and skeletal myoblast transplantation on postinfarction left ventricular function. *J. Thorac. Cardiovasc. Surg. 119*, 1169–75.

(17) Dorfman, J., Duong, M., Zibaitis, A., Pelletier, M. P., Shum-Tim, D., Li, C., and Chiu, R. C. (1998) Myocardial tissue engineering with autologous myoblast implantation. *J. Thorac. Cardiovasc. Surg. 116*, 744–51.

(18) Leobon, B., Garcin, I., Menasche, P., Vilquin, J.-T., Audinat, E., and Charpak, S. (2003) Myoblasts transplanted into rat infarcted myocardium are functionally isolated from their host. *Proc. Natl. Acad. Sci. U. S. A. 100*, 7808–11.

(19) Nakanishi, C., Yamagishi, M., Yamahara, K., Hagino, I., Mori, H., Sawa, Y., Yagihara, T., Kitamura, S., and Nagaya, N. (2008) Activation of cardiac progenitor cells through paracrine effects of mesenchymal stem cells. *Biochem. Biophys. Res. Commun. 374*, 11–16.

(20) Mirotsou, M., Zhang, Z., Deb, A., Zhang, L., Gnecchi, M., Noiseux, N., Mu, H., Pachori, A., and Dzau, V. (2007) Secreted frizzled related protein 2 (Sfrp2) is the key Akt-mesenchymal stem cell-released paracrine factor mediating myocardial survival and repair. *Proc. Natl. Acad. Sci. U. S. A. 104*, 1643–8.

(21) Miyahara, Y., Nagaya, N., Kataoka, M., Yanagawa, B., Tanaka, K., Hao, H., Ishino, K., Ishida, H., Shimizu, T., Kangawa, K., Sano, S., Okano, T., Kitamura, S., and Mori, H. (2006) Monolayered mesenchymal stem cells repair scarred myocardium after myocardial infarction. *Nat. Med. 12*, 459–65.

(22) Ramkisoensing, A. A., Pijnappels, D. A., Askar, S. F. A., Passier, R., Swildens, J., Goumans, M. J., Schutte, C. I., de Vries, A. A. F., Scherjon, S., Mummery, C. L., Schalij, M. J., and Atsma, D. E. (2011) Human embryonic and fetal mesenchymal stem cells differentiate toward three different cardiac lineages in contrast to their adult counterparts. *PLoS One 6*, e24164.

(23) Noiseux, N., Gnecchi, M., Lopez-Ilasaca, M., Zhang, L., Solomon, S. D., Deb, A., Dzau, V. J., and Pratt, R. E. (2006) Mesenchymal stem cells overexpressing Akt dramatically repair infarcted myocardium and improve cardiac function despite infrequent cellular fusion or differentiation. *Mol. Ther. 14*, 840–50.

(24) Goumans, M.-J., Maring, J. A., and Smits, A. M. (2014) A straightforward guide to the basic science behind cardiovascular cell-based therapies. *Heart 100*, 1153–7.

(25) Jeevanantham, V., Butler, M., Saad, A., Abdel-Latif, A., Zuba-Surma, E. K., and Dawn, B. (2012) Adult bone marrow cell therapy improves survival and induces long-term improvement in cardiac parameters: a systematic review and meta-analysis. *Circulation 126*, 551–68.

(26) Goumans, M.-J., de Boer, T. P., Smits, A. M., van Laake, L. W., van Vliet, P., Metz, C. H. G., Korfage, T. H., Kats, K. P., Hochstenbach, R., Pasterkamp, G., Verhaar, M. C., van der Heyden, M. A. G., de Kleijn, D., Mummery, C. L., van Veen, T. A. B., Sluijter, J. P. G., and Doevendans, P. A. (2007) TGF-beta1 induces efficient differentiation of human cardiomyocyte progenitor cells into functional cardiomyocytes in vitro. *Stem Cell Res. 1*, 138–49.

(27) Den Haan, M. C., Grauss, R. W., Smits, A. M., Winter, E. M., van Tuyn, J., Pijnappels, D. A., Steendijk, P., Gittenberger-De Groot, A. C., van der Laarse, A., Fibbe, W. E., de Vries, A. A. F., Schalij, M. J., Doevendans, P. A., Goumans, M.-J., and Atsma, D. E. (2012) Cardiomyogenic differentiation-independent improvement of cardiac function by human cardiomyocyte progenitor cell injection in ischaemic mouse hearts. *J. Cell. Mol. Med. 16*, 1508–21.

(28) Bolli, R., Tang, X.-L., Sanganalmath, S. K., Rimoldi, O., Mosna, F., Abdel-Latif, A., Jneid, H., Rota, M., Leri, A., and Kajstura, J. (2013) Intracoronary delivery of autologous cardiac stem cells improves cardiac function in a porcine model of chronic ischemic cardiomyopathy. *Circulation 128*, 122–31.

(29) Chong, J. J. H., Yang, X., Don, C. W., Minami, E., Liu, Y.-W., Weyers, J. J., Mahoney, W. M., Van Biber, B., Cook, S. M., Palpant, N. J., Gantz, J. A., Fugate, J. A., Muskheli, V., Gough, G. M., Vogel, K. W., Astley, C. A., Hotchkiss, C. E., Baldessari, A., Pabon, L., Reinecke, H., Gill, E. A., Nelson, V., Kiem, H.-P., Laflamme, M. A., and Murry, C. E. (2014) Human embryonic-stem-cell-derived cardiomyocytes regenerate non-human primate hearts. *Nature 510*, 273–277.

(30) Fernandes, S., Naumova, A. V, Zhu, W. Z., Laflamme, M. A., Gold, J., and Murry, C. E. (2010) Human embryonic stem cell-derived cardiomyocytes engraft but do not alter cardiac remodeling after chronic infarction in rats. *J. Mol. Cell. Cardiol. 49*, 941–9.

(31) Shiba, Y., Fernandes, S., Zhu, W.-Z., Filice, D., Muskheli, V., Kim, J., Palpant, N. J., Gantz, J., Moyes, K. W., Reinecke, H., Van Biber, B., Dardas, T., Mignone, J. L., Izawa, A., Hanna, R., Viswanathan, M., Gold, J. D., Kotlikoff, M. I., Sarvazyan, N., Kay, M. W., Murry, C. E., and Laflamme, M. A. (2012) Human ES-cell-derived cardiomyocytes electrically couple and suppress arrhythmias in injured hearts. *Nature 489*, 322–5.

(32) Caspi, O., Huber, I., Kehat, I., Habib, M., Arbel, G., Gepstein, A., Yankelson, L., Aronson, D., Beyar, R., and Gepstein, L. (2007) Transplantation of human embryonic stem cell-derived cardiomyocytes improves myocardial performance in infarcted rat hearts. *J. Am. Coll. Cardiol. 50*, 1884–93.

(33) Dai, W., Field, L. J., Rubart, M., Reuter, S., Hale, S. L., Zweigerdt, R., Graichen, R. E., Kay, G. L., Jyrala, A. J., Colman, A., Davidson, B. P., Pera, M., and Kloner, R. A. (2007) Survival and maturation of human embryonic stem cell-derived cardiomyocytes in rat hearts. *J. Mol. Cell. Cardiol. 43*, 504–16.

(34) Gherghiceanu, M., Barad, L., Novak, A., Reiter, I., Itskovitz-Eldor, J., Binah, O., and Popescu, L. M. (2011) Cardiomyocytes derived from human embryonic and induced pluripotent stem cells: comparative ultrastructure. *J. Cell. Mol. Med. 15*, 2539–51.

(35) Chang, D., Wen, Z., Wang, Y., Cai, W., Wani, M., Paul, C., Okano, T., Millard, R. W., and Wang, Y. (2014) Ultrastructural Features of Ischemic Tissue following Application of a Bio-Membrane Based Progenitor Cardiomyocyte Patch for Myocardial Infarction Repair. *PLoS One 9*, e107296.

(36) Sanchez-Freire, V., Lee, A. S., Hu, S., Abilez, O. J., Liang, P., Lan, F., Huber, B. C., Ong, S.-G., Hong, W. X., Huang, M., and Wu, J. C. (2014) Effect of human donor cell source on differentiation and function of cardiac induced pluripotent stem cells. *J. Am. Coll. Cardiol. 64*, 436–48.

(37) Yang, L., Soonpaa, M. H., Adler, E. D., Roepke, T. K., Kattman, S. J., Kennedy, M., Henckaerts, E., Bonham, K., Abbott, G. W., Linden, R. M., Field, L. J., and Keller, G. M. (2008) Human cardiovascular progenitor cells develop from a kdr+ embryonic-stem-cell-derived population. *Nature 453*, 524–528.

(38) Cao, N., Liang, H., Huang, J., Wang, J., Chen, Y., Chen, Z., and Yang, H.-T. (2013) Highly efficient induction and long-term maintenance of multipotent cardiovascular progenitors from human pluripotent stem cells under defined conditions. *Cell Res.* 1–14.

(39) Lu, T.-Y., Lin, B., Kim, J., Sullivan, M., Tobita, K., Salama, G., and Yang, L. (2013) Repopulation of decellularized mouse heart with human induced pluripotent stem cell-derived cardiovascular progenitor cells. *Nat. Commun. 4*, 2307.

(40) Ardehali, R., Ali, S. R., Inlay, M. a, Abilez, O. J., Chen, M. Q., Blauwkamp, T. a, Yazawa, M., Gong, Y., Nusse, R., Drukker, M., and Weissman, I. L. (2013) Prospective isolation of human embryonic stem cell-derived cardiovascular progenitors that integrate into human fetal heart tissue. *Proc. Natl. Acad. Sci. U. S. A. 110*, 3405–10.

(41) Tomescot, A., Leschik, J., Bellamy, V., Dubois, G., Messas, E., Bruneval, P., Desnos, M., Hagège, A. A., Amit, M., Itskovitz, J., Menasché, P., and Pucéat, M. (2007) Differentiation in vivo of cardiac committed human embryonic stem cells in postmyocardial infarcted rats. *Stem Cells 25*, 2200–5.

(42) Danoviz, M. E., and Yablonka-Reuveni, Z. (2012) Skeletal muscle satellite cells: background and methods for isolation and analysis in a primary culture system. *Methods Mol. Biol. 798*, 21–52.

(43) Neef, K., Choi, Y.-H., Perumal Srinivasan, S., Treskes, P., Cowan, D. B., Stamm, C., Rubach, M., Adelmann, R., Wittwer, T., and Wahlers, T. (2012) Mechanical preconditioning enables electrophysiologic coupling of skeletal myoblast cells to myocardium. *J. Thorac. Cardiovasc. Surg. 144*, 1176–1184.e1.

(44) Tolmachov, O., Ma, Y.-L., Themis, M., Patel, P., Spohr, H., Macleod, K. T., Ullrich, N. D., Kienast, Y., Coutelle, C., and Peters, N. S. (2006) Overexpression of connexin 43 using a retroviral vector improves electrical coupling of skeletal myoblasts with cardiac myocytes in vitro. *BMC Cardiovasc. Disord. 6*, 25.

(45) Narita, T., Shintani, Y., Ikebe, C., Kaneko, M., Harada, N., Tshuma, N., Takahashi, K., Campbell, N. G., Coppen, S. R., Yashiro, K., Sawa, Y., and Suzuki, K. (2013) The use of cell-sheet technique eliminates arrhythmogenicity of skeletal myoblast-based therapy to the heart with enhanced therapeutic effects. *Int. J. Cardiol. 168*, 261–9.

(46) Blumenthal, B., Poppe, A., Golsong, P., Blanke, P., Rylski, B., Beyersdorf, F., Schlensak, C., and Siepe, M. (2011) Functional regeneration of ischemic myocardium by transplanted cells overexpressing stromal cell-derived factor-1 (SDF-1): intramyocardial injection versus scaffold-based application. *Eur. J. Cardiothorac. Surg. 40*, e135–41.

(47) Siepe, M., Golsong, P., Poppe, A., Blumenthal, B., von Wattenwyl, R., Heilmann, C., Förster, K., Schlensak, C., and Beyersdorf, F. (2011) Scaffold-based transplantation of akt1-overexpressing skeletal myoblasts: functional regeneration is associated with angiogenesis and reduced infarction size. *Tissue Eng. Part A 17*, 205–12.

(48) Hinds, S., Bian, W., Dennis, R. G., and Bursac, N. (2011) The role of extracellular matrix composition in structure and function of bioengineered skeletal muscle. *Biomaterials 32*, 3575–83.

(49) Cheng, C. S., Davis, B. N., Madden, L., Bursac, N., and Truskey, G. a. (2014) Physiology and metabolism of tissue-engineered skeletal muscle. *Exp. Biol. Med. (Maywood). 239*, 1203–14.

(50) Freed, L., and Vunjak-Novakovic, G. (1997) Microgravity tissue engineering. *Vitr. Cell. Dev. Biol. 33*, 381–385.

(51) Carrier, R. L., Papadaki, M., Rupnick, M., Schoen, F. J., Bursac, N., Langer, R., Freed, L. E., and Vunjak-Novakovic, G. (1999) Cardiac tissue engineering: cell seeding, cultivation parameters, and tissue construct characterization. *Biotechnol. Bioeng. 64*, 580–9.

(52) Bursac, N., Papadaki, M., Cohen, R. J., Schoen, F. J., Eisenberg, S. R., Carrier, R., Vunjak-Novakovic, G., and Freed, L. E. (1999) Cardiac muscle tissue engineering: toward an in vitro model for electrophysiological studies. *Am. J. Physiol. 277*, H433–44.

(53) Eschenhagen, T., Fink, C., Remmers, U., Scholz, H., Wattchow, J., Weil, J., Zimmermann, W., Dohmen, H., Schafer, H., Bishopric, N., Wakatsuki, T., and Elson, E. (1997) Three-dimensional reconstitution of embryonic cardiomyocytes in a collagen matrix: a new heart muscle model system. *FASEB J 11*, 683–694.

(54) Zimmermann, W. H., Fink, C., Kralisch, D., Remmers, U., Weil, J., and Eschenhagen, T. (2000) Three-dimensional engineered heart tissue from neonatal rat cardiac myocytes. *Biotechnol. Bioeng. 68*, 106–14.

(55) Zhang, D., Shadrin, I. Y., Lam, J., Xian, H.-Q., Snodgrass, H. R., and Bursac, N. (2013) Tissue-engineered cardiac patch for advanced functional maturation of human ESC-derived cardiomyocytes. *Biomaterials 34*, 5813–5820.

(56) Fink, C., Ergün, S., Kralisch, D., Remmers, U., Weil, J., and Eschenhagen, T. (2000) Chronic stretch of engineered heart tissue induces hypertrophy and functional improvement. *FASEB J. 14*, 669–679.

(57) Zimmermann, W., Schneiderbanger, K., Schubert, P., Didié, M., Münzel, F., Heubach, J., Kostin, S., Neuhuber, W., and Eschenhagen, T. (2001) Tissue Engineering of a Differentiated Cardiac Muscle Construct. *Circ. Res. 90*, 223–230.

(58) Lasher, R. a, Pahnke, A. Q., Johnson, J. M., Sachse, F. B., and Hitchcock, R. W. (2012) Electrical stimulation directs engineered cardiac tissue to an age-matched native phenotype. *J. Tissue Eng. 3*, 2041731412455354.

(59) Cheng, M., Park, H., Engelmayr, G. C., Moretti, M., and Freed, L. E. (2007) Effects of regulatory factors on engineered cardiac tissue in vitro. *Tissue Eng. 13*, 2709–19.

(60) Bondue, A., Tännler, S., Chiapparo, G., Chabab, S., Ramialison, M., Paulissen, C., Beck, B., Harvey, R., and Blanpain, C. (2011) Defining the earliest step of cardiovascular progenitor specification during embryonic stem cell differentiation. *J. Cell Biol. 192*, 751–65.

(61) Evseenko, D., Zhu, Y., Schenke-Layland, K., Kuo, J., Latour, B., Ge, S., Scholes, J., Dravid, G., Li, X., MacLellan, W. R., and Crooks, G. M. (2010) Mapping the first stages of mesoderm commitment during differentiation of human embryonic stem cells. *Proc. Natl. Acad. Sci. U. S. A. 107*, 13742–7.

(62) Kattman, S. J., Adler, E. D., and Keller, G. M. (2007) Specification of multipotential cardiovascular progenitor cells during embryonic stem cell differentiation and embryonic development. *Trends Cardiovasc. Med. 17*, 240–6.

(63) Kattman, S. J., Huber, T. L., and Keller, G. M. Multipotent flk-1+ cardiovascular progenitor cells give rise to the cardiomyocyte, endothelial, and vascular smooth muscle lineages. *Dev. Cell 11*, 723–732.

(64) Chimenti, I., Rizzitelli, G., Gaetani, R., Angelini, F., Ionta, V., Forte, E., Frati, G., Schussler, O., Barbetta, A., Messina, E., Dentini, M., and Giacomello, A. (2011) Human cardiosphere-seeded gelatin and collagen scaffolds as cardiogenic engineered bioconstructs. *Biomaterials 32*, 9271–81.

(65) Gaetani, R., Doevendans, P. A., Metz, C. H. G., Alblas, J., Messina, E., Giacomello, A., and Sluijter, J. P. G. (2012) Cardiac tissue engineering using tissue printing technology and human cardiac progenitor cells. *Biomaterials 33*, 1782–90.

(66) Hosseinkhani, H., Hosseinkhani, M., Hattori, S., Matsuoka, R., and Kawaguchi, N. (2010) Micro and nano-scale in vitro 3D culture system for cardiac stem cells. *J. Biomed. Mater. Res. A 94*, 1–8.

(67) Di Felice, V., De Luca, A., Serradifalco, C., Di Marco, P., Verin, L., Motta, A., Guercio, A., and Zummo, G. (2010) Adult stem cells, scaffolds for in vivo and in vitro myocardial tissue engineering. *Ital. J. Anat. Embryol. 115*, 65–9.

(68) Chang, C. Y., Chan, A. T., Armstrong, P. A., Luo, H.-C., Higuchi, T., Strehin, I. A., Vakrou, S., Lin, X., Brown, S. N., O'Rourke, B., Abraham, T. P., Wahl, R. L., Steenbergen, C. J., Elisseeff, J. H., and Abraham, M. R. (2012) Hyaluronic acid-human blood hydrogels for stem cell transplantation. *Biomaterials 33*, 8026–33.

(69) Xu, Y., Patnaik, S., Guo, X., Li, Z., Lo, W., Butler, R., Claude, A., Liu, Z., Zhang, G., Liao, J., Anderson, P. M., and Guan, J. (2014) Cardiac differentiation of cardiosphere-derived cells in scaffolds mimicking morphology of the cardiac extracellular matrix. *Acta Biomater. 10*, 3449–62.

(70) Seif-Naraghi, S. B., Salvatore, M. A., Schup-Magoffin, P. J., Hu, D. P., and Christman, K. L. (2010) Design and characterization of an injectable pericardial matrix gel: a potentially autologous scaffold for cardiac tissue engineering. *Tissue Eng. Part A 16*, 2017–27.

(71) Zhang, J., Klos, M., Wilson, G. F., Herman, A. M., Lian, X., Raval, K. K., Barron, M. R., Hou, L., Soerens, A. G., Yu, J., Palecek, S. P., Lyons, G. E., Thomson, J. a, Herron, T. J., Jalife, J., and Kamp, T. J. (2012) Extracellular matrix promotes highly efficient cardiac differentiation of human pluripotent stem cells: the matrix sandwich method. *Circ. Res. 111*, 1125–36.

(72) Minami, I., Yamada, K., Otsuji, T. G., Yamamoto, T., Shen, Y., Otsuka, S., Kadota, S., Morone, N., Barve, M., Asai, Y., Tenkova-Heuser, T., Heuser, J. E., Uesugi, M., Aiba, K., and Nakatsuji, N. (2012) A small molecule that promotes cardiac differentiation of human pluripotent stem cells under defined, cytokine- and xeno-free conditions. *Cell Rep. 2*, 1448–60.

(73) Tohyama, S., Hattori, F., Sano, M., Hishiki, T., Nagahata, Y., Matsuura, T., Hashimoto, H., Suzuki, T., Yamashita, H., Satoh, Y., Egashira, T., Seki, T., Muraoka, N., Yamakawa, H., Ohgino, Y., Tanaka, T., Yoichi, M., Yuasa, S., Murata, M., Suematsu, M., and Fukuda, K. (2013) Distinct metabolic flow enables large-scale purification of mouse and human pluripotent stem cell-derived cardiomyocytes. *Cell Stem Cell 12*, 127–37.

(74) Xi, J., Khalil, M., Shishechian, N., Hannes, T., Pfannkuche, K., Liang, H., Fatima, A., Haustein, M., Suhr, F., Bloch, W., Reppel, M., Sarić, T., Wernig, M., Jänisch, R., Brockmeier, K., Hescheler, J., and Pillekamp, F. (2010) Comparison of contractile behavior of native murine ventricular tissue and cardiomyocytes derived from embryonic or induced pluripotent stem cells. *FASEB J. 24*, 2739–51.

(75) Fijnvandraat, A. C., van Ginneken, A. C. G., de Boer, P. A. J., Ruijter, J. M., Christoffels, V. M., Moorman, A. F. M., and Lekanne Deprez, R. H. (2003) Cardiomyocytes derived from embryonic stem cells resemble cardiomyocytes of the embryonic heart tube. *Cardiovasc. Res. 58*, 399–409.

(76) Guo, X.-M., Zhao, Y.-S., Chang, H.-X., Wang, C.-Y., E, L.-L., Zhang, X.-A., Duan, C.-M., Dong, L.-Z., Jiang, H., Li, J., Song, Y., and Yang, X. J. (2006) Creation of engineered cardiac tissue in vitro from mouse embryonic stem cells. *Circulation 113*, 2229–37.

(77) Caspi, O., Lesman, A., Basevitch, Y., Gepstein, A., Arbel, G., Habib, I. H. M., Gepstein, L., and Levenberg, S. (2007) Tissue engineering of vascularized cardiac muscle from human embryonic stem cells. *Circ. Res. 100*, 263–272.

(78) Ulery, B. D., Nair, L. S., and Laurencin, C. T. (2011) Biomedical Applications of Biodegradable Polymers. *J. Polym. Sci. B. Polym. Phys. 49*, 832–864.

(79) Ceonzo, K., Gaynor, A., Shaffer, L., Kojima, K., Vacanti, C. A., and Stahl, G. L. (2006) Polyglycolic acid-induced inflammation: role of hydrolysis and resulting complement activation. *Tissue Eng. 12*, 301–8.

(80) Duong, H., Wu, B., and Tawil, B. (2009) Modulation of 3D fibrin matrix stiffness by intrinsic fibrinogen-thrombin compositions and by extrinsic cellular activity. *Tissue Eng. Part A 15*, 1865–76.

(81) Thomson, K. S., Korte, F. S., Giachelli, C. M., Ratner, B. D., Regnier, M., and Scatena, M. (2013) Prevascularized microtemplated fibrin scaffolds for cardiac tissue engineering applications. *Tissue Eng. Part A 19*, 967–977.

(82) Bashey, R. I., Martinez-Hernandez, a., and Jimenez, S. a. (1992) Isolation, characterization, and localization of cardiac collagen type VI. Associations with other extracellular matrix components. *Circ. Res. 70*, 1006–1017.

(83) Marijianowski, M. (1994) The neonatal heart has a relatively high content of total collagen and type I collagen, a condition that may explain the less compliant state. *J Am Coll Cardiol. 23*, 1204–8.

(84) Gross, J., and Kirk, D. (1958) The heat precipitation of collagen from neutral salt solutions: some rate-regulating factors. *J. Biol. Chem. 233*, 355–60.

(85) GRILLO, H. C., and GROSS, J. (1962) Thermal reconstitution of collagen from solution and the response to its heterologous implantation. *J. Surg. Res. 2*, 69–82.

(86) O'Leary, L., Fallas, J., and Bakota, E. (2011) Multi-hierarchical self-assembly of a collagen mimetic peptide from triple helix to nanofibre and hydrogel. *Nat. Chem. 3*, 821–28.

(87) Buehler, M. J. (2006) Nature designs tough collagen: explaining the nanostructure of collagen fibrils. *Proc. Natl. Acad. Sci. U. S. A. 103*, 12285–90.

(88) Kadler, K. E., Holmes, D. F., Trotter, J. a, and Chapman, J. a. (1996) Collagen fibril formation. *Biochem. J. 316*, 1–11.

(89) Serpooshan, V. (2010) Control of dense collagen gel scaffolds for tissue engineering through measurement and modeling of hydraulic permeability. McGill University.

(90) Sung, K. E., Su, G., Pehlke, C., Trier, S. M., Eliceiri, K. W., Keely, P. J., Friedl, A., and Beebe, D. J. (2009) Control of 3-dimensional collagen matrix polymerization for reproducible human mammary fibroblast cell culture in microfluidic devices. *Biomaterials 30*, 4833–41.

(91) Yang, Y., Motte, S., and Kaufman, L. J. (2010) Pore size variable type I collagen gels and their interaction with glioma cells. *Biomaterials 31*, 5678–5688.

(92) Tulloch, N. L. (2012) Conditioning Controls Differentiation, Organization, and Maturation of Functional Bioengineered Human Cardiovascular Tissue. University of Washington.

(93) Raeber, G. P., Lutolf, M. P., and Hubbell, J. a. (2005) Molecularly engineered PEG hydrogels: a novel model system for proteolytically mediated cell migration. *Biophys. J. 89*, 1374–88.

(94) Raub, C. B., Putnam, A. J., Tromberg, B. J., and George, S. C. (2010) Predicting bulk mechanical properties of cellularized collagen gels using multiphoton microscopy. *Acta Biomater. 6*, 4657–65.

(95) Moreno-Gonzalez, A., Korte, F. S., Dai, J., Chen, K., Ho, B., Reinecke, H., Murry, C. E., and Regnier, M. (2009) Cell therapy enhances function of remote non-infarcted myocardium. *J. Mol. Cell. Cardiol. 47*, 603–613.

(96) Kim, H., Yoon, C. S., and Rah, B. (1999) Expression of extracellular matrix components fibronectin and laminin in the human fetal heart. *Cell Struct. Funct. 24*, 19–26.

(97) Ott, H. C., Matthiesen, T. S., Goh, S.-K., Black, L. D., Kren, S. M., Netoff, T. I., and Taylor, D. A. (2008) Perfusion-decellularized matrix: using nature's platform to engineer a bioartificial heart. *Nat. Med. 14*, 213–21.

(98) Masumoto, H., Matsuo, T., Yamamizu, K., Uosaki, H., Narazaki, G., Katayama, S., Marui, A., Shimizu, T., Ikeda, T., Okano, T., Sakata, R., and Yamashita, J. K. (2012) Pluripotent stem cell-engineered cell

sheets reassembled with defined cardiovascular populations ameliorate reduction in infarct heart function through cardiomyocyte-mediated neovascularization. *Stem Cells 30*, 1196–205.

(99) Stevens, K. R., Pabon, L., Muskheli, V., and Murry, C. E. (2009) Scaffold-free human cardiac tissue patch created from embryonic stem cells. *Tissue Eng. Part A 15*, 1211–22.

(100) Lesman, A., Habib, M., Caspi, O., Gepstein, A., Arbel, G., Levenberg, S., and Gepstein, L. (2010) Transplantation of a tissue-engineered human vascularized cardiac muscle. *Tissue Eng. Part A 16*, 115–25.

(101) Abu-Issa, R., and Kirby, M. L. (2007) Heart field: from mesoderm to heart tube. *Annu. Rev. Cell Dev. Biol. 23*, 45–68.

(102) Murry, C. E., and Keller, G. (2008) Differentiation of embryonic stem cells to clinically relevant populations: lessons from embryonic development. *Cell 132*, 661–80.

(103) Burridge, P. W., Keller, G., Gold, J. D., and Wu, J. C. (2012) Production of de novo cardiomyocytes: human pluripotent stem cell differentiation and direct reprogramming. *Cell Stem Cell 10*, 16–28.

(104) Kattman, S. J., Witty, A. D., Gagliardi, M., Dubois, N. C., Niapour, M., Hotta, A., Ellis, J., and Keller, G. (2011) Stage-specific optimization of activin/nodal and BMP signaling promotes cardiac differentiation of mouse and human pluripotent stem cell lines. *Cell Stem Cell 8*, 228–40.

(105) Yang, L., Soonpaa, M. H., Adler, E. D., Roepke, T. K., Kattman, S. J., Kennedy, M., Henckaerts, E., Bonham, K., Abbott, G. W., Linden, R. M., Field, L. J., and Keller, G. M. (2008) Human cardiovascular progenitor cells develop from a KDR+ embryonic-stem-cell-derived population. *Nature 453*, 524–8.

(106) Hirata, H., Kawamata, S., Murakami, Y., Inoue, K., Nagahashi, A., Tosaka, M., Yoshimura, N., Miyamoto, Y., Iwasaki, H., Asahara, T., and Sawa, Y. (2007) Coexpression of platelet-derived growth factor receptor alpha and fetal liver kinase 1 enhances cardiogenic potential in embryonic stem cell differentiation in vitro. *J. Biosci. Bioeng. 103*, 412–9.

(107) Chong, J. J. H., Reinecke, H., Iwata, M., Torok-Storb, B., Stempien-Otero, A., and Murry, C. E. (2013) Progenitor cells identified by PDGFR-alpha expression in the developing and diseased human heart. *Stem Cells Dev. 22*, 1932–43.

(108) Laflamme, M. a, Chen, K. Y., Naumova, A. V, Muskheli, V., Fugate, J. a, Dupras, S. K., Reinecke, H., Xu, C., Hassanipour, M., Police, S., O'Sullivan, C., Collins, L., Chen, Y., Minami, E., Gill, E. a, Ueno, S., Yuan, C., Gold, J., and Murry, C. E. (2007) Cardiomyocytes derived from human embryonic stem cells in pro-survival factors enhance function of infarcted rat hearts. *Nat. Biotechnol. 25*, 1015–24.

(109) Lian, X., Hsiao, C., Wilson, G., Zhu, K., Hazeltine, L. B., Azarin, S. M., Raval, K. K., Zhang, J., Kamp, T. J., and Palecek, S. P. (2012) Robust cardiomyocyte differentiation from human pluripotent stem cells via temporal modulation of canonical Wnt signaling. *Proc. Natl. Acad. Sci.* 1–10.

(110) Ueno, S., Weidinger, G., Osugi, T., Kohn, A. D., Golob, J. L., Pabon, L., Reinecke, H., Moon, R. T., and Murry, C. E. (2007) Biphasic role for Wnt/beta-catenin signaling in cardiac specification in zebrafish and embryonic stem cells. *Proc. Natl. Acad. Sci. U. S. A. 104*, 9685–90.

(111) Zhu, W.-Z., Xie, Y., Moyes, K. W., Gold, J. D., Askari, B., and Laflamme, M. a. (2010) Neuregulin/ErbB signaling regulates cardiac subtype specification in differentiating human embryonic stem cells. *Circ. Res. 107*, 776–86.

(112) Gupta, M. K., Illich, D. J., Gaarz, A., Matzkies, M., Nguemo, F., Pfannkuche, K., Liang, H., Classen, S., Reppel, M., Schultze, J. L., Hescheler, J., and Sarić, T. (2010) Global transcriptional profiles of beating clusters derived from human induced pluripotent stem cells and embryonic stem cells are highly similar. *BMC Dev. Biol. 10*, 98.

(113) Bilic, J., and Izpisua Belmonte, J. C. (2012) Concise review: Induced pluripotent stem cells versus embryonic stem cells: close enough or yet too far apart? *Stem Cells 30*, 33–41.

(114) Snir, M., Kehat, I., Gepstein, A., Coleman, R., Itskovitz-Eldor, J., Livne, E., and Gepstein, L. (2003) Assessment of the ultrastructural and proliferative properties of human embryonic stem cell-derived cardiomyocytes. *Am. J. Physiol. Heart Circ. Physiol. 285*, H2355–63.

(115) Bergmann, O., Bhardwaj, R. D., Bernard, S., Zdunek, S., Barnabé-Heider, F., Walsh, S., Zupicich, J., Alkass, K., Buchholz, B. A., Druid, H., Jovinge, S., and Frisén, J. (2009) Evidence for cardiomyocyte renewal in humans. *Science 324*, 98–102.

(116) Lieu, D. K., Liu, J., Siu, C.-W., McNerney, G. P., Tse, H.-F., Abu-Khalil, A., Huser, T., and Li, R. A. (2009) Absence of transverse tubules contributes to non-uniform Ca(2+) wavefronts in mouse and human embryonic stem cell-derived cardiomyocytes. *Stem Cells Dev. 18*, 1493–500.

(117) Barth, E., Stämmler, G., Speiser, B., and Schaper, J. (1992) Ultrastructural quantitation of mitochondria and myofilaments in cardiac muscle from 10 different animal species including man. *J. Mol. Cell Cardiol. 681*, 669–681.

(118) Keung, W., Boheler, K. R., and Li, R. a. (2014) Developmental cues for the maturation of metabolic, electrophysiological and calcium handling properties of human pluripotent stem cell-derived cardiomyocytes. *Stem Cell Res. Ther. 5*, 17.

(119) Pillekamp, F., Haustein, M., Khalil, M., Emmelheinz, M., Nazzal, R., Adelmann, R., Nguemo, F., Rubenchyk, O., Pfannkuche, K., Matzkies, M., Reppel, M., Bloch, W., Brockmeier, K., and Hescheler, J. (2012) Contractile properties of early human embryonic stem cell-derived cardiomyocytes: beta-adrenergic stimulation induces positive chronotropy and lusitropy but not inotropy. *Stem Cells Dev. 21*, 2111–21.

(120) Kim, H., Kim, D., Lee, I., and Rah, B. (1992) Human fetal heart development after mid-term: morphometry and ultrastructural study. *J. Mol. Cell. Cardiol. 965*, 949–965.

(121) Synnergren, J., Akesson, K., Dahlenborg, K., Vidarsson, H., Améen, C., Steel, D., Lindahl, A., Olsson, B., and Sartipy, P. (2008) Molecular signature of cardiomyocyte clusters derived from human embryonic stem cells. *Stem Cells 26*, 1831–40.

(122) Poon, E., Yan, B., Zhang, S., Rushing, S., Keung, W., Ren, L., Lieu, D. K., Geng, L., Kong, C.-W., Wang, J., Wong, H. S., Boheler, K. R., and Li, R. A. (2013) Transcriptome-guided functional analyses reveal novel biological properties and regulatory hierarchy of human embryonic stem cell-derived ventricular cardiomyocytes crucial for maturation. *PLoS One 8*, e77784.

(123) Durrer, D., van Dam, R. T., Freud, G. E., Janse, M. J., Meijler, F. L., and Arzbaecher, R. C. (1970) Total excitation of the isolated human heart. *Circulation 41*, 899–912.

(124) Dolnikov, K., Shilkrut, M., Zeevi-Levin, N., Gerecht-Nir, S., Amit, M., Danon, A., Itskovitz-Eldor, J., and Binah, O. (2006) Functional properties of human embryonic stem cell-derived cardiomyocytes: intracellular Ca2+ handling and the role of sarcoplasmic reticulum in the contraction. *Stem Cells 24*, 236–45.

(125) Qu, Y., Ghatpande, A., El-Sherif, N., and Boutjdir, M. (2000) Gene expression of Na+/Ca2+ exchanger during development in human heart. *Cardiovasc. Res. 45*, 866–73.

(126) Fu, J.-D., Jiang, P., Rushing, S., Liu, J., Chiamvimonvat, N., and Li, R. a. (2010) Na+/Ca2+ exchanger is a determinant of excitation-contraction coupling in human embryonic stem cell-derived ventricular cardiomyocytes. *Stem Cells Dev. 19*, 773–82.

(127) Liu, J., Fu, J. D., Siu, C. W., and Li, R. a. (2007) Functional sarcoplasmic reticulum for calcium handling of human embryonic stem cell-derived cardiomyocytes: insights for driven maturation. *Stem Cells 25*, 3038–44.

(128) Lynch, J., Chilibeck, K., Qui, Y., and Michalak, M. (2006) Assembling pieces of the cardiac puzzle; calreticulin and calcium-dependent pathways in cardiac development, health, and disease. *Trends Cardiovasc. Med. 16*, 65–69.

(129) Liu, J., Lieu, D. K., Siu, C. W., Fu, J., Tse, H., and Li, R. A. (2009) Facilitated maturation of Ca 2 ε handling properties of human embryonic stem cell-derived cardiomyocytes by calsequestrin expression 152–159.

(130) Itzhaki, I., Rapoport, S., Huber, I., Mizrahi, I., Zwi-Dantsis, L., Arbel, G., Schiller, J., and Gepstein, L. (2011) Calcium handling in human induced pluripotent stem cell derived cardiomyocytes. *PLoS One 6*, e18037.

(131) Bedada, F. B., Chan, S. S.-K., Metzger, S. K., Zhang, L., Zhang, J., Garry, D. J., Kamp, T. J., Kyba, M., and Metzger, J. M. (2014) Acquisition of a Quantitative, Stoichiometrically Conserved Ratiometric Marker of Maturation Status in Stem Cell-Derived Cardiac Myocytes. *Stem Cell Reports 3*, 594–605.

(132) Krüger, M., Kohl, T., and Linke, W. a. (2006) Developmental changes in passive stiffness and myofilament Ca2+ sensitivity due to titin and troponin-I isoform switching are not critically triggered by birth. *Am. J. Physiol. Heart Circ. Physiol. 291*, H496–506.

(133) Lundy, S. D., Zhu, W.-Z., Regnier, M., and Laflamme, M. A. (2013) Structural and functional maturation of cardiomyocytes derived from human pluripotent stem cells. *Stem Cells Dev. 22*, 1991–2002.

(134) Kamakura, T., Makiyama, T., Sasaki, K., Yoshida, Y., Wuriyanghai, Y., Chen, J., Hattori, T., Ohno, S., Kita, T., Horie, M., Yamanaka, S., and Kimura, T. (2013) Ultrastructural Maturation of Human-Induced Pluripotent Stem Cell-Derived Cardiomyocytes in a Long-Term Culture. *Circ. J. 77*, 1307–1314.

(135) Otsuji, T. G., Minami, I., Kurose, Y., Yamauchi, K., Tada, M., and Nakatsuji, N. (2010) Progressive maturation in contracting cardiomyocytes derived from human embryonic stem cells: Qualitative effects on electrophysiological responses to drugs. *Stem Cell Res. 4*, 201–13.

(136) Yang, X., Rodriguez, M., Pabon, L., Fischer, K. a, Reinecke, H., Regnier, M., Sniadecki, N. J., Ruohola-Baker, H., and Murry, C. E. (2014) Tri-iodo-l-thyronine promotes the maturation of human cardiomyocytes-derived from induced pluripotent stem cells. *J. Mol. Cell. Cardiol. 72*, 296–304.

(137) Fu, J.-D., Rushing, S. N., Lieu, D. K., Chan, C. W., Kong, C.-W., Geng, L., Wilson, K. D., Chiamvimonvat, N., Boheler, K. R., Wu, J. C., Keller, G., Hajjar, R. J., and Li, R. A. (2011) Distinct roles of microRNA-1 and -499 in ventricular specification and functional maturation of human embryonic stem cell-derived cardiomyocytes. *PLoS One 6*, e27417.

(138) Lieu, D., and Fu, J. (2013) Mechanism-Based Facilitated Maturation of Human Pluripotent Stem Cell–Derived Cardiomyocytes. *Circ. … 6*, 191–201.

(139) Liu, J., Lieu, D. K., Siu, C. W., Fu, J.-D., Tse, H.-F., and Li, R. A. (2009) Facilitated maturation of Ca2+ handling properties of human embryonic stem cell-derived cardiomyocytes by calsequestrin expression. *Am. J. Physiol. Cell Physiol. 297*, C152–9.

(140) Ruwhof, C., and van der Laarse, a. (2000) Mechanical stress-induced cardiac hypertrophy: mechanisms and signal transduction pathways. *Cardiovasc. Res. 47*, 23–37.

(141) Granados-Riveron, J. T., and Brook, J. D. (2012) The impact of mechanical forces in heart morphogenesis. *Circ. Cardiovasc. Genet. 5*, 132–42.

(142) Yu, J., Vodyanik, M. a, Smuga-Otto, K., Antosiewicz-Bourget, J., Frane, J. L., Tian, S., Nie, J., Jonsdottir, G. a, Ruotti, V., Stewart, R., Slukvin, I. I., and Thomson, J. a. (2007) Induced pluripotent stem cell lines derived from human somatic cells. *Science 318*, 1917–1920.

(143) McCain, M. L., and Parker, K. K. (2011) Mechanotransduction: the role of mechanical stress, myocyte shape, and cytoskeletal architecture on cardiac function. *Pflugers Arch. 462*, 89–104.

(144) Bartman, T., and Hove, J. (2005) Mechanics and function in heart morphogenesis. *Dev. Dyn. 233*, 373–81.

(145) Mills, R. W., Cornelussen, R. N., Mulligan, L. J., Strik, M., Rademakers, L. M., Skadsberg, N. D., van Hunnik, A., Kuiper, M., Lampert, A., Delhaas, T., and Prinzen, F. W. (2009) Left ventricular septal and left

ventricular apical pacing chronically maintain cardiac contractile coordination, pump function and efficiency. *Circ. Arrhythm. Electrophysiol. 2*, 571–9.

(146) Prinzen, F. W., Vernooy, K., De Boeck, B. W. L., DeBoeck, B. W. L., and Delhaas, T. (2011) Mechano-energetics of the asynchronous and resynchronized heart. *Heart Fail. Rev. 16*, 215–24.

(147) Feng, Z., Ishibashi, M., Nomura, Y., Kitajima, T., and Nakamura, T. (2006) Constraint stress, microstructural characteristics, and enhanced mechanical properties of a special fibroblast-embedded collagen construct. *Artif. Organs 30*, 870–7.

(148) Cooke, M. E., Sakai, T., and Mosher, D. F. (2000) Contraction of collagen matrices mediated by alpha2beta1A and alpha(v)beta3 integrins. *J. Cell Sci. 113*, 2375–83.

(149) Feng, Z., Tateishi, Y., Nomura, Y., Kitajima, T., and Nakamura, T. (2006) Construction of fibroblast-collagen gels with orientated fibrils induced by static or dynamic stress: toward the fabrication of small tendon grafts. *J. Artif. Organs 9*, 220–5.

(150) Krishnan, L., Weiss, J. a, Wessman, M. D., and Hoying, J. B. (2004) Design and application of a test system for viscoelastic characterization of collagen gels. *Tissue Eng. 10*, 241–52.

(151) Van den Hoff, M. J. B., Deprez, R. H. L., Ruijter, J. M., de Boer, P. a J., Tesink-Taekema, S., Buffing, A. a, Lamers, W. H., and Moorman, A. F. M. (2004) Increased cardiac workload by closure of the ductus arteriosus leads to hypertrophy and apoptosis rather than to hyperplasia in the late fetal period. *Naunyn. Schmiedebergs. Arch. Pharmacol. 370*, 193–202.

(152) Barbera, a, Giraud, G. D., Reller, M. D., Maylie, J., Morton, M. J., and Thornburg, K. L. (2000) Right ventricular systolic pressure load alters myocyte maturation in fetal sheep. *Am. J. Physiol. Regul. Integr. Comp. Physiol. 279*, R1157–64.

(153) Hirt, M. N., Sörensen, N. A., Bartholdt, L. M., Boeddinghaus, J., Schaaf, S., Eder, A., Vollert, I., Stöhr, A., Schulze, T., Witten, A., Stoll, M., Hansen, A., and Eschenhagen, T. (2012) Increased afterload induces pathological cardiac hypertrophy: a new in vitro model. *Basic Res. Cardiol. 107*, 307.

(154) Oparil, S., Bishop, S. P., and Clubb, F. J. Myocardial cell hypertrophy or hyperplasia. *Hypertension 6*, III38–43.

(155) Zimmermann, W.-H., Melnychenko, I., Wasmeier, G., Didié, M., Naito, H., Nixdorff, U., Hess, A., Budinsky, L., Brune, K., Michaelis, B., Dhein, S., Schwoerer, A., Ehmke, H., and Eschenhagen, T. (2006) Engineered heart tissue grafts improve systolic and diastolic function in infarcted rat hearts. *Nat. Med. 12*, 452–458.

(156) Tulloch, N. L., Muskheli, V., Razumova, M. V, Korte, F. S., Regnier, M., Hauch, K. D., Pabon, L., Reinecke, H., and Murry, C. E. (2011) Growth of Engineered Human Myocardium With Mechanical Loading and Vascular Coculture. *Circ. Res. 109*, 47–59.

(157) Kensah, G., Roa Lara, A., Dahlmann, J., Zweigerdt, R., Schwanke, K., Hegermann, J., Skvorc, D., Gawol, A., Azizian, A., Wagner, S., Maier, L. S., Krause, A., Dräger, G., Ochs, M., Haverich, A., Gruh, I., and

Martin, U. (2013) Murine and human pluripotent stem cell-derived cardiac bodies form contractile myocardial tissue in vitro. *Eur. Heart J. 34*, 1134–1146.

(158) Mihic, A., Li, J., Miyagi, Y., Gagliardi, M., Li, S.-H., Zu, J., Weisel, R. D., Keller, G., and Li, R.-K. (2014) The effect of cyclic stretch on maturation and 3D tissue formation of human embryonic stem cell-derived cardiomyocytes. *Biomaterials 35*, 2798–2808.

(159) Shimko, V., and Claycomb, W. (2008) Effect of mechanical loading on three-dimensional cultures of embryonic stem cell-derived cardiomyocytes. *Tissue Eng. Part A 14*, 49–58.

(160) Clause, K., Tinney, J., Liu, L., Keller, B., and Tobita, K. (2009) Engineered early embryonic cardiac tissue increases cardiomyocyte proliferation by cyclic mechanical stretch via p38-MAP kinase phosphorylation. *Tissue Eng. Part A 15*, 1373–80.

(161) Battista, S., Guarnieri, D., Borselli, C., Zeppetelli, S., Borzacchiello, A., Mayol, L., Gerbasio, D., Keene, D. R., Ambrosio, L., and Netti, P. A. (2006) The effect of cyclic strain on embryonic stem cell-derived cardiomyocytes. *Biomaterials 27*, 4409–4418.

(162) Földes, G., Mioulane, M., Wright, J. S., Liu, A. Q., Novak, P., Merkely, B., Gorelik, J., Schneider, M. D., Ali, N. N., and Harding, S. E. (2011) Modulation of human embryonic stem cell-derived cardiomyocyte growth: a testbed for studying human cardiac hypertrophy? *J. Mol. Cell. Cardiol. 50*, 367–376.

(163) Heo, J. S., and Lee, J.-C. (2011) β-Catenin mediates cyclic strain-stimulated cardiomyogenesis in mouse embryonic stem cells through ROS-dependent and integrin-mediated PI3K/Akt pathways. *J. Cell. Biochem. 112*, 1880–9.

(164) Prosser, B. L., Ward, C. W., and Lederer, W. J. (2013) X-ROS signalling is enhanced and graded by cyclic cardiomyocyte stretch. *Cardiovasc. Res. 98*, 307–14.

(165) Komuros, I., Katoh, Y., Kaida, T., Shibazaki, Y., Kurabayashi, M., Hoh, E., Takaku, F., and Yazaki, Y. (1991) Mechanical Loading Stimulates Cell Hypertrophy and Specific Gene Expression in Cultured Rat Cardiac Myocytes. *J. Biol. Chem. 266*, 1265–1268.

(166) Yamazaki, T., Komuro, I., Kudoh, S., Zou, Y., Shiojima, I., Mizuno, T., Takano, H., Hiroi, Y., Ueki, K., and Tobe, K. (1995) Mechanical stress activates protein kinase cascade of phosphorylation in neonatal rat cardiac myocytes. *J. Clin. Invest. 96*, 438–46.

(167) Sadoshima, J., and Izumo, S. (1993) Mechanical stretch rapidly activates multiple signal transduction pathways in cardiac myocytes: potential involvement of an autocrine/paracrine mechanism. *EMBO J. 12*, 1681–92.

(168) Salameh, A., Wustmann, A., Karl, S., Blanke, K., Apel, D., Rojas-Gomez, D., Franke, H., Mohr, F. W., Janousek, J., and Dhein, S. (2010) Cyclic mechanical stretch induces cardiomyocyte orientation and polarization of the gap junction protein connexin43. *Circ. Res. 106*, 1592–602.

(169) Schats, R., Jansen, C. A., and Wladimiroff, J. W. (1990) Embryonic heart activity: appearance and development in early human pregnancy. *Br. J. Obstet. Gynaecol. 97*, 989–94.

(170) Gilbert, R. D. (1980) Control of fetal cardiac output during changes in blood volume. *Am. J. Physiol. 238*, H80–6.

(171) Rudolph, A. M., and Heyman, M. A. (1974) Fetal and neonatal circulation and respiration. *Annu. Rev. Physiol. 36*, 187–207.

(172) Sartiani, L., Bettiol, E., Stillitano, F., Mugelli, A., Cerbai, E., and Jaconi, M. E. (2007) Developmental changes in cardiomyocytes differentiated from human embryonic stem cells: a molecular and electrophysiological approach. *Stem Cells 25*, 1136–44.

(173) Satin, J., Kehat, I., Caspi, O., Huber, I., Arbel, G., Itzhaki, I., Magyar, J., Schroder, E. a, Perlman, I., and Gepstein, L. (2004) Mechanism of spontaneous excitability in human embryonic stem cell derived cardiomyocytes. *J. Physiol. 559*, 479–96.

(174) McDonough, P., and Glembotski, C. (1992) Induction of atrial natriuretic factor and myosin light chain-2 gene expression in cultured ventricular myocytes by electrical stimulation of contraction. *J. Biol. Chem. 267*, 11665–11668.

(175) Xia, Y., McMillin, J. B., Lewis, A., Moore, M., Zhu, W. G., Williams, R. S., and Kellems, R. E. (2000) Electrical Stimulation of Neonatal Cardiac Myocytes Activates the NFAT3 and GATA4 Pathways and Up-regulates the Adenylosuccinate Synthetase 1 Gene. *J. Biol. Chem. 275*, 1855–1863.

(176) Xia, Y., Buja, L. M., Scarpulla, R. C., and McMillin, J. B. (1997) Electrical stimulation of neonatal cardiomyocytes results in the sequential activation of nuclear genes governing mitochondrial proliferation and differentiation. *Proc. Natl. Acad. Sci. 94*, 11399–11404.

(177) Burstein, B., Qi, X.-Y., Calderone, A., and Nattel, S. (2007) Rapid electrical pacing of cardiomyocytes alters the behavior of cardiac fibroblasts: Implications for atrial fibrillations. *Clin. Investig. Med. 30*, S75–S76.

(178) Holt, E., Lunde, P. K., Sejersted, O. M., and Christensen, G. (1997) Electrical stimulation of adult rat cardiomyocytes in culture improves contractile properties and is associated with altered calcium handling. *Basic Res. Cardiol. 92*, 289–98.

(179) Radisic, M., Park, H., Shing, H., Consi, T., Schoen, F. J., Langer, R., Freed, L. E., and Vunjak-Novakovic, G. (2004) Functional assembly of engineered myocardium by electrical stimulation of cardiac myocytes cultured on scaffolds. *Proc. Natl. Acad. Sci. U. S. A. 101*, 18129–34.

(180) Nunes, S. S., Miklas, J. W., Liu, J., Aschar-Sobbi, R., Xiao, Y., Zhang, B., Jiang, J., Massé, S., Gagliardi, M., Hsieh, A., Thavandiran, N., Laflamme, M. a, Nanthakumar, K., Gross, G. J., Backx, P. H., Keller, G., and Radisic, M. (2013) Biowire: a platform for maturation of human pluripotent stem cell-derived cardiomyocytes. *Nat. Methods 10*, 781–787.

(181) Long, M. (Ed.). (2013) World Congress on Medical Physics and Biomedical Engineering May 26-31, 2012, Beijing, China. Springer Berlin Heidelberg, Berlin, Heidelberg.

(182) Laflamme, M. A., Chen, K. Y., Naumova, A. V, Muskheli, V., Fugate, J. A., Dupras, S. K., Reinecke, H., Xu, C., Hassanipour, M., Police, S., O'Sullivan, C., Collins, L., Chen, Y., Minami, E., Gill, E. A., Ueno, S., Yuan, C., Gold, J., and Murry, C. E. (2007) Cardiomyocytes derived from human embryonic stem cells in pro-survival factors enhance function of infarcted rat hearts. *Nat. Biotechnol. 25*, 1015–1024.

(183) Ruifrok, a C., and Johnston, D. a. (2001) Quantification of histochemical staining by color deconvolution. *Anal. Quant. Cytol. Histol. 23*, 291–299.

(184) Willems, E., Leyns, L., and Vandesompele, J. (2008) Standardization of real-time PCR gene expression data from independent biological replicates. *Anal. Biochem. 379*, 127–129.

(185) Wiegerinck, R., Cojoc, A., and Zeidenweber, C. (2009) Force frequency relationship of the human ventricle increases during early postnatal development. *Pediatr. Res. 65*, 414–419.

(186) Germanguz, I., Sedan, O., Zeevi-Levin, N., Shtrichman, R., Barak, E., Ziskind, A., Eliyahu, S., Meiry, G., Amit, M., Itskovitz-Eldor, J., and Binah, O. (2011) Molecular characterization and functional properties of cardiomyocytes derived from human inducible pluripotent stem cells. *J. Cell. Mol. Med. 15*, 38–51.

(187) Dolnikov, K., Shilkrut, M., Zeevi-Levin, N., Danon, A., Gerecht-Nir, S., Itskovitz-Eldor, J., and Binah, O. (2005) Functional properties of human embryonic stem cell-derived cardiomyocytes. *Ann. N. Y. Acad. Sci. 1047*, 66–75.

(188) Schaaf, S., Shibamiya, A., Mewe, M., Eder, A., Stöhr, A., Hirt, M. N., Rau, T., Zimmermann, W.-H., Conradi, L., Eschenhagen, T., and Hansen, A. (2011) Human engineered heart tissue as a versatile tool in basic research and preclinical toxicology. *PLoS One 6*, e26397.

(189) Turnbull, I. C., Karakikes, I., Serrao, G. W., Backeris, P., Lee, J.-J., Xie, C., Senyei, G., Gordon, R. E., Li, R. a, Akar, F. G., Hajjar, R. J., Hulot, J.-S., and Costa, K. D. (2014) Advancing functional engineered cardiac tissues toward a preclinical model of human myocardium. *FASEB J. 28*, 644–654.

(190) Zhou, J., Shu, Y., Lü, S.-H., Li, J.-J., Sun, H.-Y., Tang, R.-Y., Duan, C.-M., Wang, Y., Lin, Q.-X., Mou, Y.-C., Li, X., and Wang, C.-Y. (2013) The spatiotemporal development of intercalated disk in three-dimensional engineered heart tissues based on collagen/matrigel matrix. *PLoS One 8*, e81420.

(191) Hirt, M. N., Boeddinghaus, J., Mitchell, A., Schaaf, S., Börnchen, C., Müller, C., Schulz, H., Hubner, N., Stenzig, J., Stoehr, A., Neuber, C., Eder, A., Luther, P. K., Hansen, A., and Eschenhagen, T. (2014) Functional Improvement and Maturation of Rat and Human Engineered Heart Tissue by Chronic Electrical Stimulation. *J. Mol. Cell. Cardiol. 74*, 151–161.

(192) Lahmers, S., Wu, Y., Call, D. R., Labeit, S., and Granzier, H. (2004) Developmental control of titin isoform expression and passive stiffness in fetal and neonatal myocardium. *Circ. Res. 94*, 505–513.

(193) Mulieri, L. A., Hasenfuss, G., Leavitt, B., Allen, P. D., and Alpert, N. R. (1992) Altered myocardial force-frequency relation in human heart failure. *Circulation 85*, 1743–1750.

(194) Holubarsch, C., Lüdemann, J., Wiessner, S., Ruf, T., Schulte-Baukloh, H., Schmidt-Schweda, S., Pieske, B., Posival, H., and Just, H. (1998) Shortening versus isometric contractions in isolated human failing and non-failing left ventricular myocardium: dependency of external work and force on muscle length, heart rate and inotropic stimulation. *Cardiovasc. Res. 37*, 46–57.

(195) Leontyev, S., Schlegel, F., Spath, C., Schmiedel, R., Nichtitz, M., Boldt, A., Rübsamen, R., Salameh, A., Kostelka, M., Mohr, F.-W., and Dhein, S. (2013) Transplantation of engineered heart tissue as a biological cardiac assist device for treatment of dilated cardiomyopathy. *Eur. J. Heart Fail. 15*, 23–35.

(196) Kensah, G., Gruh, I., Viering, J., Schumann, H., Dahlmann, J., Meyer, H., Skvorc, D., Bär, A., Akhyari, P., Heisterkamp, A., Haverich, A., and Martin, U. (2011) A novel miniaturized multimodal bioreactor for continuous in situ assessment of bioartificial cardiac tissue during stimulation and maturation. *Tissue Eng. Part C. Methods 17*, 463–73.

(197) Wiegerinck, R. F., Cojoc, A., Zeidenweber, C. M., Ding, G., Shen, M., Joyner, R. W., Fernandez, J. D., Kanter, K. R., Kirshbom, P. M., Kogon, B. E., and Wagner, M. B. (2009) Force frequency relationship of the human ventricle increases during early postnatal development. *Pediatr. Res. 65*, 414–419.

(198) Li, S., Chen, G., and Li, R. (2013) Calcium signalling of human pluripotent stem cell-derived cardiomyocytes. *J. Physiol. 591*, 5279–90.

(199) Kattman, S. J., Huber, T. L., and Keller, G. M. (2006) Multipotent flk-1+ cardiovascular progenitor cells give rise to the cardiomyocyte, endothelial, and vascular smooth muscle lineages. *Dev. Cell 11*, 723–32.

(200) Ema, M., Takahashi, S., and Rossant, J. (2006) Deletion of the selection cassette, but not cis-acting elements, in targeted Flk1-lacZ allele reveals Flk1 expression in multipotent mesodermal progenitors. *Blood 107*, 111–7.

(201) Motoike, T., Markham, D. W., Rossant, J., and Sato, T. N. (2003) Evidence for novel fate of Flk1+ progenitor: contribution to muscle lineage. *Genesis 35*, 153–9.

(202) Kataoka, H., Takakura, N., Nishikawa, S., Tsuchida, K., Kodama, H., Kunisada, T., Risau, W., Kita, T., and Nishikawa, S. I. (1997) Expressions of PDGF receptor alpha, c-Kit and Flk1 genes clustering in mouse chromosome 5 define distinct subsets of nascent mesodermal cells. *Dev. Growth Differ. 39*, 729–40.

(203) Paige, S. L., Thomas, S., Stoick-Cooper, C. L., Wang, H., Maves, L., Sandstrom, R., Pabon, L., Reinecke, H., Pratt, G., Keller, G., Moon, R. T., Stamatoyannopoulos, J., and Murry, C. E. A temporal chromatin signature in human embryonic stem cells identifies regulators of cardiac development. *Cell 151*, 221–232.

(204) Paige, S. L., Osugi, T., Afanasiev, O. K., Pabon, L., Reinecke, H., and Murry, C. E. (2010) Endogenous Wnt/beta-catenin signaling is required for cardiac differentiation in human embryonic stem cells. *PLoS One 5*, e11134.

(205) Kennedy, M., D'Souza, S. L., Lynch-Kattman, M., Schwantz, S., and Keller, G. (2007) Development of the hemangioblast defines the onset of hematopoiesis in human ES cell differentiation cultures. *Blood 109*, 2679–87.

(206) Haddad, F., Qin, A. X., Bodell, P. W., Jiang, W., Giger, J. M., and Baldwin, K. M. (2008) Intergenic transcription and developmental regulation of cardiac myosin heavy chain genes. *Am. J. Physiol. Heart Circ. Physiol. 294*, H29–40.

(207) Reiser, P., and Portman, M. (2001) Human cardiac myosin heavy chain isoforms in fetal and failing adult atria and ventricles. *Am. J. …*.

(208) Cadre, B. M., Qi, M., Eble, D. M., Shannon, T. R., Bers, D. M., and Samarel, A. M. (1998) Cyclic stretch down-regulates calcium transporter gene expression in neonatal rat ventricular myocytes. *J. Mol. Cell. Cardiol. 30*, 2247–59.

(209) Nourse, M. B., Halpin, D. E., Scatena, M., Mortisen, D. J., Tulloch, N. L., Hauch, K. D., Torok-Storb, B., Ratner, B. D., Pabon, L., and Murry, C. E. (2010) VEGF induces differentiation of functional endothelium from human embryonic stem cells: implications for tissue engineering. *Arterioscler. Thromb. Vasc. Biol. 30*, 80–9.

(210) Kim, C., Majdi, M., Xia, P., Wei, K. a, Talantova, M., Spiering, S., Nelson, B., Mercola, M., and Chen, H.-S. V. (2010) Non-cardiomyocytes influence the electrophysiological maturation of human embryonic stem cell-derived cardiomyocytes during differentiation. *Stem Cells Dev. 19*, 783–95.

(211) Braam, S. R., Tertoolen, L., van de Stolpe, A., Meyer, T., Passier, R., and Mummery, C. L. (2010) Prediction of drug-induced cardiotoxicity using human embryonic stem cell-derived cardiomyocytes. *Stem Cell Res. 4*, 107–16.

(212) Caspi, O., Itzhaki, I., Kehat, I., Gepstein, A., Arbel, G., Huber, I., Satin, J., and Gepstein, L. (2009) In vitro electrophysiological drug testing using human embryonic stem cell derived cardiomyocytes. *Stem Cells Dev. 18*, 161–72.

(213) Jonsson, M. K. B., Vos, M. a, Mirams, G. R., Duker, G., Sartipy, P., de Boer, T. P., and van Veen, T. a B. (2012) Application of human stem cell-derived cardiomyocytes in safety pharmacology requires caution beyond hERG. *J. Mol. Cell. Cardiol. 52*, 998–1008.